AALBORG UNIVERSITY
STUDENT REPORT

Department of Energy Technology - Pontoppidanstræde 101
Aalborg University, Denmark

Control of Grid Connected PV Systems with Grid Support Functions

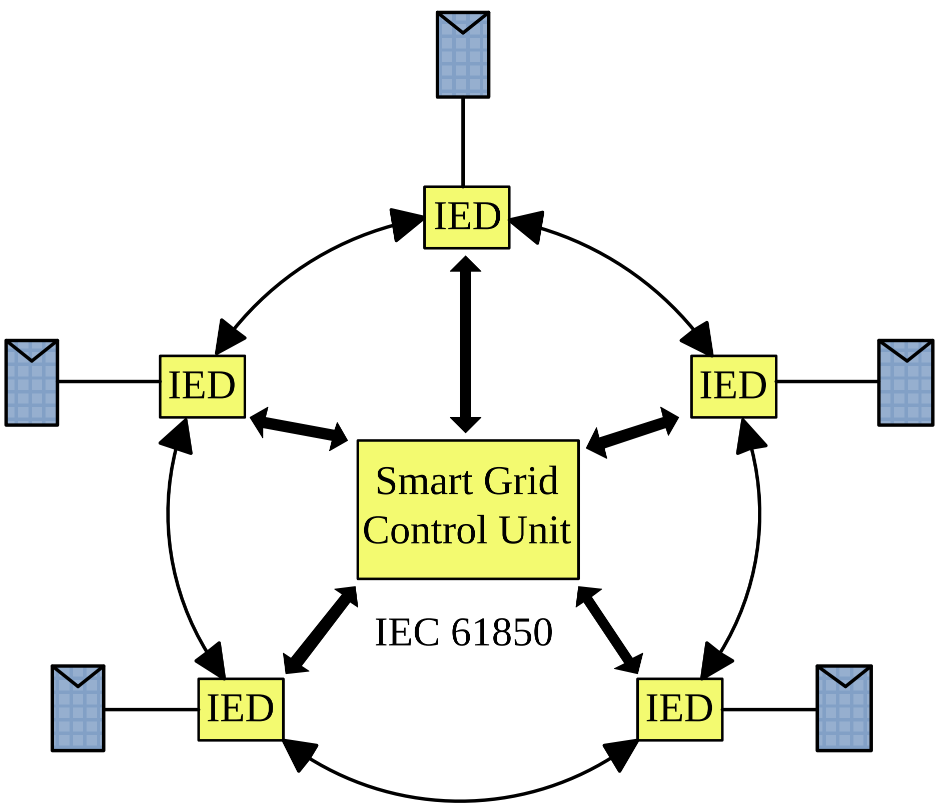

Conducted by group PED4 - 1043
-Autumn/ Spring Semester, 2011-2012-

Title:	**Control of Grid Connected PV Systems with Grid Support Functions**
Semester:	**9-10th Semester 2011/2012**
Semester theme:	**Master Thesis**
Project period:	**15/09/2011 – 31/08/2012**
ECTS:	**50 ECTS**
Supervisor:	**Bogdan Craciun, Tamás Kerekes, Dezső Séra, Remus Teodorescu**
Project group:	**PED4 / 1043**

Vlad Alexandru Muresan

Copies:	[5]
Pages, total:	[151]
Appendix:	[51]
Supplements:	[1CD]

SYNOPSIS:

The increased active power generation due to increased photovoltaic (PV) installations leads to voltage rise especially in the low voltage networks (LV) and can exceed the limits imposed by the grid codes (GCs). Therefore, the PV capacity is limited and further investments in the network are needed.

The project goal is to analyze and improve the voltage regulation methods for grid connected PV inverters proposed by the new German grid code. The support strategies based on reactive power (cosφ(P) and Q(U)) were modeled and simulated by performing load flow analysis on a typical LV distribution network.

An optimized voltage regulation method has been developed which minimizes the reactive power consumption using coordinated control. The Ethernet communication IEC 61850 based on server/ client architecture was used to exchange information between PVs and master controller. A laboratory setup has been developed for the experimental validation of IEC 61850.

By signing this document, each member of the group confirms that all participated in the project work and thereby that all members are collectively liable for the content of the report.

Preface

This report has been written by the group PED4 1043 during 9^{th}–10^{th}semester at the Department of Energy Technology, Aalborg University. The project has been carried out between the 15^{th} of September 2011 – 31^{st} August 2012.

The first 4 chapters have been written by both students from the group PED4 1043, while the Chapter 5 of the report was written only by the student Vlad Alexandru Muresan. Due to unexpected circumstances, the student Vlad Alexandru Muresan could not continue the project work being involved in re-examinations for course modules and therefore the project has been divided in 2 different parts. The first project version was submitted by the student Elena Anamaria Man in 31.05.2012 while the second project version is submitted by the student Vlad Alexandru Muresan in 31.08.2012 with different Chapter 5 (Experimental Work).

Reading Instructions

The main report can be read as an independent piece, from which the appendices derive including mathematical calculations, simulations and other details in order to make the main report more understandable. In this project, the chapters are arranged numerically, whereas appendixes are sorted alphabetically.

Frequently used constants and abbreviations are described in the report nomenclature list, which can be found after the table of contents. Sources are inserted using the IEEE method, with a [number], which refers to the bibliography in the back of the report. Additionally, a CD is included, which features the report and other source files in digital format.

Acknowledgement

First of all I would like to express my gratitude to my colleague and friend Elena Anamaria Man for her important contribution to this project.

I gratefully appreciate all the support and guidance received during the carried work from my supervisors Remus Teodorescu, Tamás Kerekes, Dezső Séra and especially Bogdan Crăciun.

Special thanks go to Danfoss Solar Department for their financial support during my studies.

Summary

This current report is divided in six chapters and investigates different voltage regulation strategies proposed by the new German GC which are applied to the grid connected PV inverters in LV networks.

In the first chapter, a short description concerning the background of the solar energy is given with focus on the current status of PV technology and grid connected PV systems. The project motivation is represented by the problems (voltage rise, frequency variations, power quality) appeared as a cause of continuous PV installments especially in the lower parts of the grid. One of the measures taken to improve grid stability and achieve further installments was to equip the PV inverters with support functions. This refers especially to the capability of provide grid voltage support by means of reactive power.

The new grid codes (GCs) which contain the requirements for PV inverters have been changed also in order to suppress the above mentioned problems. Chapter 2 gives a short description of the requirements for LV grid connected systems, by comparing the previous and the actual German GC with focus on grid interface requirements, power quality issues and anti-islanding. The known faults that may appear in the utility grid are also discussed.

Due to the fact that the PV installments are especially in the LV part, a European benchmark network was selected to investigate the voltage rise problem. In Chapter 3, load flow studies using the Newton-Raphson method have been performed in order to observe the voltage rise problem. The regulation methods proposed by the German GC (cosφ(P) and Q(U)) have been investigated and implemented using real power generation profiles. The strategies were then compared and discussed in terms of performance to keep the voltage inside boundaries and absorb minimum reactive power.

The aim of Chapter 4 is to improve the voltage regulation strategy studied in Chapter 3. An optimized voltage regulation method was developed using optimal power flow calculations which minimizes the losses and achieves better distribution of reactive power between the PV inverters. The optimized algorithm is using the communication concept for information exchange IEC 61850 to share information. The improvements brought by the coordinated control are highlighted in comparison with the classical Q(U) method.

Chapter 5 describes the experimental implementation of the IEC 61850 communication concept. The structure and description of the information model is explained along with the configuration of IEDs and the necessary functions for server/client application. The laboratory setup is composed by three 3-phase inverters connected to the utility grid. Each inverter is sending its voltage magnitude and active power reference to the master controller (Client) which decides the new reactive power reference and transmits the information back to the inverters. To access any parameter or signal from the inverter, the dSPACE processor board was used together with the C Library (CLIB). The information exchange between server and client is bi-directional;

therefore data can be read from the dSPACE processor by the server and transmitted to the client. To validate the experimental results, screen captures of the console applications for client and server have been presented and explained.

In Chapter 6, the general conclusions of the carried work are presented together with the future work that can be done.

Contributions

An article was published during the period of the research. The focus of the article is on the results of the developed optimized Q(U) algorithm compared with the ones of the best candidate from the German GC VDE-AR-N 4105. The method was implemented on the chosen European LV benchmark network and the complete publication can be found in Appendix I.

- B.I. Craciun, E.A. Man, D. Sera, V.A. Muresan, T. Kerekes, and R. Teodorescu, *Improved Voltage Regulation Strategies by PV Inverters in LV Rural Networks*, published in *The 3rd International Symposium on Power Electronics for Distributed Generation Systems (PEDG), Aalborg June 2012, Denmark, ISBN 978-1-4673-2022-1*

Table of contents

Nomenclature

List of abbreviations

API	Application Programming Interface
CDC	Common Data Classes
CLIB	C Library
CP	Connection Point
DA	Data Attribute
DER	Distributed Energy Resources
DER-Lab	Distributed Energy Resources Laboratories
DG	Distributed Generation
DO	Data Object
DS	Distribution System
DSO	Distribution System Operator
DR	Distributed Resources
EPIA	European Photovoltaic Industry Association
EPS	Electric Power System
GC	Grid Code
GOOSE	Generic Object Oriented Substation Events
GUI	Graphical User Interface
IEA	International Energy Agency
IED	Intelligent Electronic Device
IP	Internet Protocol
IPC2	Interface and Protection Card
LD	Logical Device
LN	Logical Node
LVRT	Low-Voltage Ride Through
MMS	Manufacturing Message Specification
MPPT	Maximum Power Point Tracking
OLTC	On-Load Tap-Changing Transformer
PD	Physical Device
PIS	Protocol Integration Stack
PLL	Phase Locked Loop
PV	Photovoltaic
SAS	Substation Automation System
SCL	System Configuration description Language
SCM	Specific Communication Mapping
SV	Sample Value

TCP	Transmission Control Protocol
THD	Total Harmonic Distortion
VU	Voltage Unbalance
VUF	Voltage Unbalance Factor

List of symbols

ς	voltage variation
δ_i	voltage angle at bus i
θ_{ij}	voltage angle difference between bus i and j
$\Delta\delta_i$	corrections for voltage angle at bus i
ΔV_i	corrections for voltage magnitude at bus i
ΔP_i	active power mismatches at node i
ΔQ_i	reactive power mismatches at node i
B_{ii}	self susceptance of bus i
B_{ij}	mutual susceptance between bus i and j
G_{ii}	self conductance of bus i
G_{ij}	mutual conductance between bus i and j
P_i	active power injected in node i
P_i^{ref}	active power reference at node i
P_n	rated active power of the PV inverters
Q_i	reactive power injected in node i
Q_i^{ref}	reactive power reference at node i
Q_{max}	maximum reactive power reference of the PV inverters
S_i	rated power of PV inverters
V_i	voltage magnitude at bus i
Y_{ii}	self-admittance
Y_{ij}	mutual admittance
Y_{bus}	admittance matrix
Z_{bus}	impedance matrix

Chapter 1 Introduction

This chapter presents a background of the solar energy followed by a short description of the current status of photovoltaic (PV) technology and grid connected PV systems. Afterwards, the motivation, objectives and limitations of the report are stated.

1.1 Background of solar energy

The growth of world energy demand and the environmental concerns lead to an increase of the renewable energy production over the last decade. Energy sources such as solar, wind or hydro became more and more popular mainly because they produce no emissions and are inexhaustible. PV energy is the fastest growing renewable source with a history dating since it has been first used as power supply for space satellites. The increased efforts in the semiconductor material technology resulted in the appearance of commercial PV cells and consequently made the PVs an important alternative energy source [1].

One of the major advantage of PV technology is the lack of moving parts which offers the possibility to obtain a long operating time (>20 years) and low maintenance cost. The main drawbacks are the high manufacturing cost and low efficiency (15-20 %). As one of the most promising renewable and clean energy resources, PV power development has been also boosted by the favorable governmental support [2, 3].

According to European Photovoltaic Industry Association (EPIA), at the end of 2011 the total installed PV capacity in the world has reached over 67.4 GW, with an increase of 68.5 % compared to 2010. Europe still leads the market with over 50 GW of cumulative power installed with a70 % increase in 2011. Italy became for the first time the top PV market in 2011 with 9 GW of newly connected capacity, with an impressive 290% increase from 2010. This increase was a consequence of advantageous tariffs if the systems were installed by the end of 2010 and connected until mid 2011. Germany was the second big player on the PV market in 2011 with 7.5 GW of new connected systems with a 44% increase from 2010 where more than 80% of the installed systems were located in the LV network [4].

In Figure 1-1, the total PV power installed in Europe at the end of 2010 is presented. The figure shows an unbalanced market, where Germany is leading with 24.7 GW of total installed capacity. Italy has increased its PV capacity at a total of 12.5 GW and holds the second place on the market. On the other side, Spain is third in 2011 after a low development of PV power. The rest of EU countries are still far behind, but progresses are expected in the future [4].

The high penetration of the PV technology was induced by the continuous increase of energy price generated in traditional coal and gas power plants. PV power systems have been required to reduce costs in order to compete on the energy market, but on the same time to provide a good reliability.

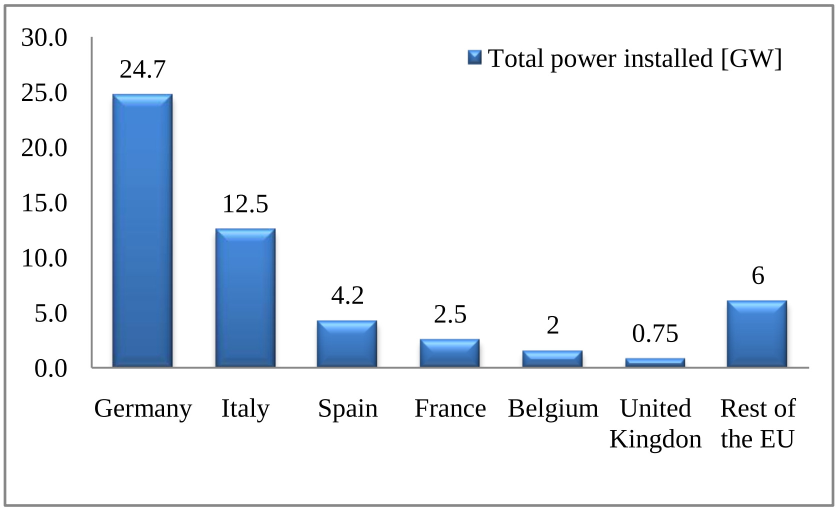

Figure 1-1 European total PV power installed at the end of 2010 [4]

Usually the reliability of a PV system is associated with the inverter topology and the main components (switching devices, capacitors).The lifetime of a system regarding the PV panels has been approximated to be around 25 year, while in the inverter sector, future improvements are expected [5].

In Figure 1-2 the electricity generation costs for large PV systems are exposed.

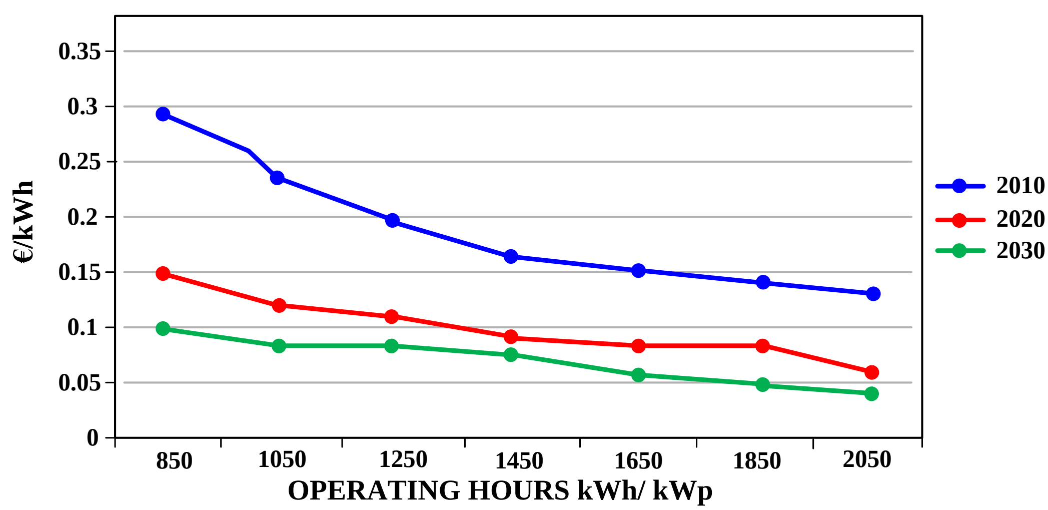

Figure 1-2 Levelised cost of electricity for large PV ground-mounted systems [6]

The energy generation costs in 2010 varied from €0.15/kWh in the north of Europe to €0.12/kWh in south of Europe and Asia. By 2020, the expected generation costs for large PV systems will vary between €0.07/kWh to €0.17/kWh. Also, the prices for the residential PV systems are expected to drop significantly in the next 20 years [6].

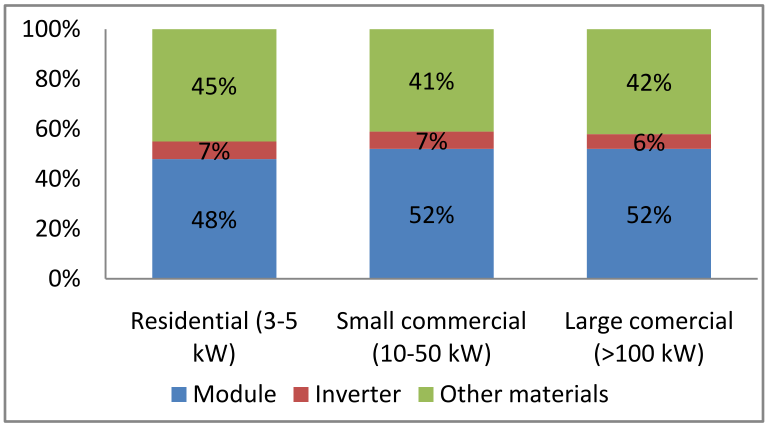

Figure 1-3 System percent share of each component for different power ratings [7]

In Figure 1-3, the typical percentage contribution to total cost for a variety of specific cost components (e.g. modules, inverters, installation labour, etc.) are shown. Typically, PV module costs are about 50% of total installed ones, while inverters represented approximately 6-7%. Other costs such as installation labour, materials, and regulatory compliance represent an important part from the total price [7].

The fast expansion of PV system into the lower parts of the grid raised several concerns for grid reinforcement. In consequence, grid operators had to impose strict operational rules in order to keep the LV grid under control and to harmonize the behavior of all distributed generators connected to it in terms of reliability, efficiency and costs [8, 9].

The first cost-effective measure, which brought a major improvement to the grid stability, was for the grid operators to suggest PV systems manufacturers to equip their products with grid support functions [10]. It is expected that until the end of 2015, the shipments of smart inverters in terms of MW will have a market share of 60 %, overtaking the standard inverter (Figure 1-4). Still, most of them will have only reactive power capabilities [11].

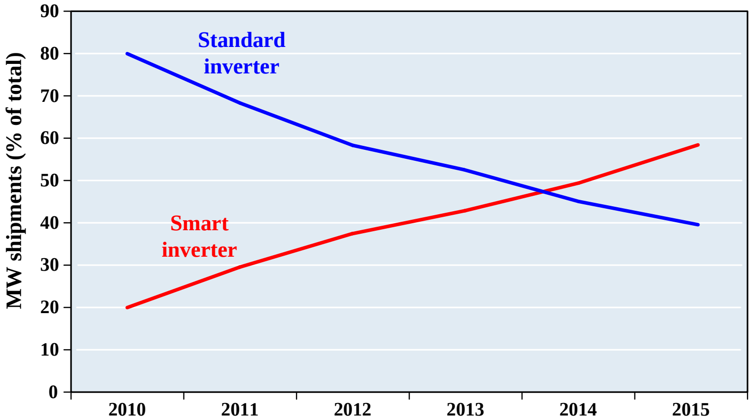

Figure 1-4 Total world market share for standard and smart PV inverters [11]

1.1.1 Grid connected PV systems

Grid connected PV systems represent around 92 % of the total PV installed power. Thyristor-based central inverters connected to the utility grid emerged on the market in the mid-1980s. Later, in the 1990s, SMA produced the first transistor-based inverters. Figure 1-5 briefly presents the evolution of grid connected PV systems together with off-grid systems up to the year 2010 [12].

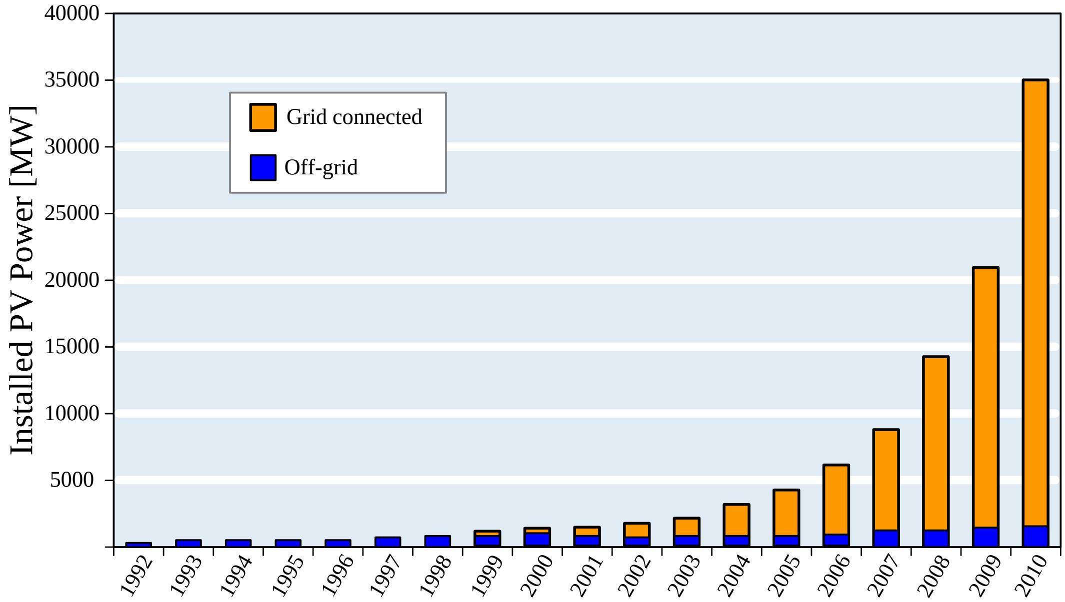

Figure 1-5 Cumulative installed grid connected and off-grid PV power in the reporting countries between 1992-2009 [12]

It can be observed that the off-grid development has slightly changed since 1999, whereas the installed power of grid connected systems increased significantly since 2006.

According to International Energy Agency (IEA), the PV systems can be divided into two main categories: off-grid and grid connected, depending on their connection with the utility grid. Further, a short description of the configurations is presented [12].

The standalone systems are used in places where there is no connection to the utility grid. They provide electricity to small rural areas and are usually used for low power loads (refrigeration, lightning). Their power ratings are around 1 kW and they offer a good alternative to meet the energy demands of off-grid communities [12]. Grid connected distributed systems gained popularity in the last years, as they can be used as power generators for grid connected customers or directly for the grid. Different sizes are possible since they can be mounted on public or commercial buildings [12].

Grid connected centralized systems are specific for power plants. They produce and transform the power directly to the utility grid. The configuration is usually ground mounted and the power rating is above kW order [12].

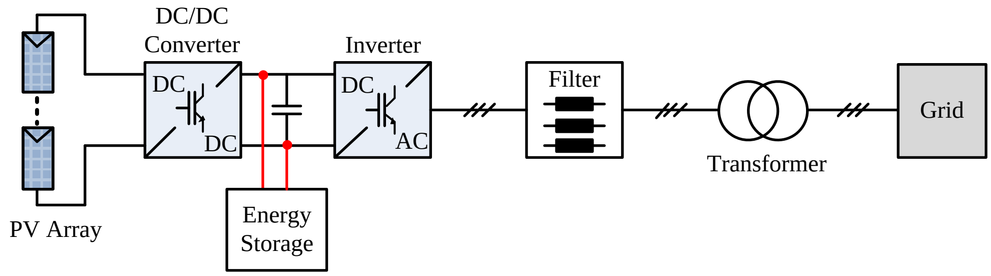

Figure 1-6 Components of a grid connected PV systems [13]

The typical configuration of a PV system can be observed in Figure 1-6. Depending on the number of the modules, the PV array converts the solar irradiation into specific DC current and voltage. A DC/DC boost converter is used to meet the voltage level required by the inverter. Energy storage devices can be included in order to store the energy produced in case of grid support connection. The power conversion is realized by a three-phase inverter which delivers the energy to the grid. High frequency harmonics that appear due to power semiconductors switching are reduced by the filter. The power transformer is used only for galvanic isolation between the PV system and the utility grid [13].

1.1.2 Topologies of grid connected PV systems

In PV plants applications, various technological concepts are used for connecting the PV array to the utility grid. Further, the existing configurations will be explained [3, 14-17].

Central Inverters

For this architecture, presented in Figure 1-7a, the PV arrays are connected in parallel to one central inverter. The configuration is used for three-phase power plants, with power ranges between 10-1000 kW. The main advantage of central inverters is the high efficiency (low losses in the power conversion stage) and low cost due to usage of only one inverter. The drawbacks of this topology are the long DC cables required to connect the PV modules to the inverter and the losses caused by string diodes, mismatches between PV modules, and centralized maximum power point tracking (MPPT) [3, 14-17].

String Inverters

The configuration presented in Figure 1-7b emerged on the PV market in 1995 with the purpose of improving the drawbacks of central inverters. Compared to central inverters, in this topology the PV strings are connected to separate inverters. If the voltage level before the inverter is too low, a DC-DC converter can be used to boost it. For this topology, each string has its own inverter and therefore the need for string diodes is eliminated leading to total loss reduction of the system. The configuration allows individual MPPT for each string; hence the reliability of the system is improved due to the fact that the system is no longer dependent on only one inverter compared to the central inverter topology [3, 14-17].

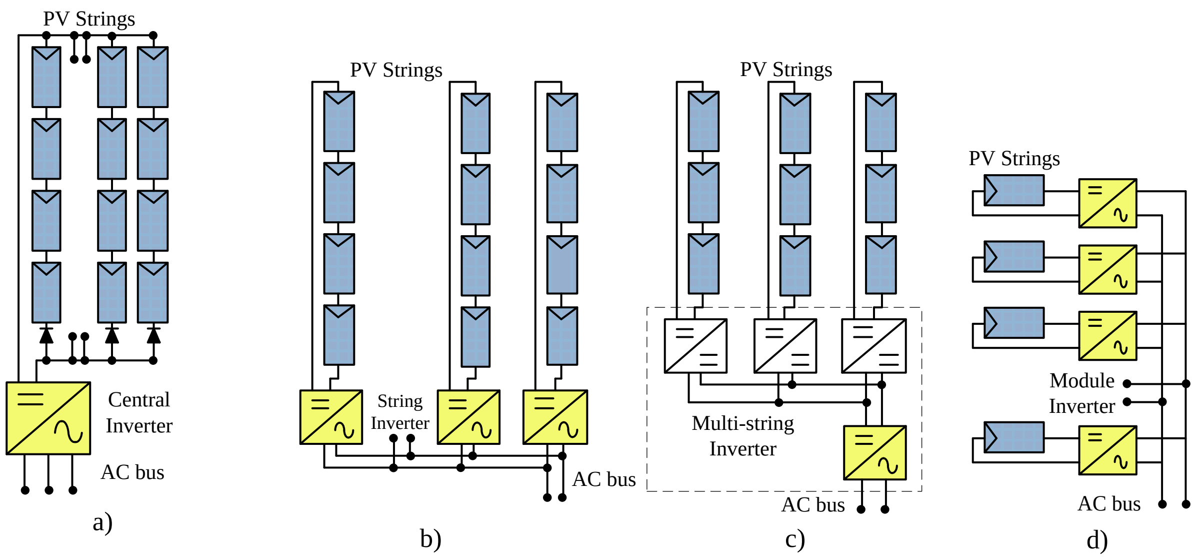

Figure 1-7 PV grid connected systems configurations a).Central Inverters; b). String Inverters; c).Multi-String Inverters; d). Module inverters [3]

Multi-String Inverters

The multi-string inverter configuration presented in Figure 1-7c became available on the PV market in 2002 being a mixture of the string and module inverters. The power ranges of this configuration are maximum 5 kW and the strings use an individual DC-DC converter before the connection to a common inverter. The topology allows the connection of inverters with different power ratings and PV modules with different current-voltage (I-V) characteristics. MPPT is implemented for each string, thus an improved power efficiency can be obtained [3, 14-17].

Module Inverters

Module Inverters shown in Figure 1-7d consists of single solar panels connected to the grid through an inverter. A better efficiency is obtained compared to string inverters as MPPT is implemented for every each panel. Still, voltage amplification might be needed with the drawback of reducing the overall efficiency of the topology (losses in DC/DC converter). The price per watt achieved is still high compared to the previous configurations [3, 14-17].

1.2 Motivation

Over the last decade various reasons have determined a continuous increase of the PV power systems. Some of them are the price drop of the PV modules manufacturing, better social acceptance of PV parks or government support for renewable energy. At the same time, the grid connected systems development requires better understanding, evaluation and performance of the PV inverters in case of normal and abnormal conditions in the grid, as well as the quality of the energy generated by the PV systems.

The increased number of grid connected PV inverters gave rise to problems concerning the stability and safety of the utility grid, as well as power quality issues. The main problems are:

- **Voltage rise problem**

The integration of large amounts of PV systems mostly in the low voltage (LV) networks increases the generation of active power leading to voltage rise along the feeders. At the moment the voltage rise does not exceed the 2% limit imposed by the old GC [18], but it is expected in the future; therefore, the admissible voltage increase after the connection of PV generators at their connection point(CP) has been increased in the new GC to 3% (absolute value) [19].

- **50.2 Hz problem**

According to VDE 0126-1-1 [18], when the grid frequency reaches and exceeds 50.2 Hz an immediate shutdown is required from the grid connected generators to avoid risks which can appear in the operation of the network. It is possible that the shutdown occurs while high power infeed, therefore the resulting sudden deviation can cause the primary control to malfunction. In other words, if the power deviation is higher than the predefined power of the primary control, the system will not be able to stabilize the grid frequency. The solution to prevent system-critical states proposed by the new GC VDE-AN-R 4105 is a frequency-dependent active power control [19].

- **Increased harmonics**

Researches carried out show that the high penetration of PV systems lead also to an increase in harmonic content at the CP. Each PV system connected to the grid injects harmonics, therefore the more PV systems are connected the more harmonic content will increase. Furthermore, if one or more non-linear loads are present, the total harmonic distortion (THD) can increase above the allowable limit [19]. This increase can be noticed in both current and voltage [20].

- **Increased voltage unbalance**

Studies have shown that features of the installed PV systems such as their location and power generation capacity can lead to an increase in the voltage unbalance (VU). This affects most the power quality in the LV residential networks, due to the random location of the PV installations and their single-phase grid connection. In other words, the voltage profile of the three phases is different because the PV systems are installed randomly along the feeders and with various ratings. When the difference in amplitude between the phases is high, the VU increases [21]. According to the study described in [22] the VU will have the most significant impact at the end of the feeder where it could exceed the allowed limit [19]. Furthermore, a PV installation along a feeder will create a voltage unbalance that will be modified on all the feeders of the network.

- **Anti-islanding**

Islanding occurs when the PV generator is disconnected from the grid, but continues to power locally. The islanding problem is dominant in LV networks, therefore it is recommended for the generation units to disconnect within a narrow frequency band such as 49-51 Hz [23].

Taking into consideration the previously presented problems which are a high concern for the utility grid in the present and expected in the future, new and more restrictive GCs have been issued.

In the past there were no requirements for the PV inverters to contribute to the grid stability. German standard VDE 0126.1.1 from 2005 specifies that inverters connected to LV network must disconnect in the following cases [18]:

When voltage changes exceed the limits $80\%V_n < V_{pcc} < 115\%V_n$, disconnection is necessary within 200 ms. In case the upper limit is exceeded, according to DIN EN 50160:2000-03, inverter must shut down.

- Frequency limits are $47.5Hz < f < 50.2Hz$. If these values are exceeded, the inverter must disconnect in 200 ms.
- If the DC current exceeds the limit of 1A due to abnormal operation, inverter must shut down in 200 ms

Nowadays, the concept of smart inverter raised new challenges in terms of converter control. At the moment, the PV inverters are required to contribute to the grid stability and provide support functions during normal and abnormal operation of utility grid such as [10]:

- *Grid Voltage Support:* - it involves trade-off between active and reactive power production in order to maintain the voltage between specific limits
- *Grid Frequency Support:* - implies active power supply to the grid to reduce sudden unbalance and keep frequency between specific limits
- *Grid Angular (Transient) Stability:* - oscillations reduction when sudden events occur by means of real power transfer
- *Load Leveling/Peak Shaving:* - loads management during peak periods
- *Power Quality Improvement:* - mitigation of problems (harmonics, power factor, flicker, etc.) that affect the magnitude and shape of voltage/current
- *Power Reliability:* - ratio of interruptions in power delivery versus a period of time
- *Fault Ride Through Support:* - ability of the electric devices to stay connected and provide energy during system disturbances

The specific behavior of the inverters under grid faults is very important, since it is desired that the system avoids as much as possible disconnection. The services delivered by the inverters are based on grid monitoring and have to follow the demands from the Distribution System Operator (DSO). Is it very important also that the quality and services delivered to meet the new grid codes requirements [19] for interconnection of PV systems, where certain limits are stated (in terms of voltage rise, harmonics, unbalance, etc).

1.3 Problem Formulation

More than 80% of the PV installations in Germany were on LV network. The main problem which arises due to massive PV penetration is the voltage variation caused by the injection of active power and reverse power flow (see Figure 1-8). Usually, over voltages affect the network in case of high irradiation and light load. In consequence, the inverters can trip, the operation of the loads can be affected and the lines and/or transformers can become overloaded.

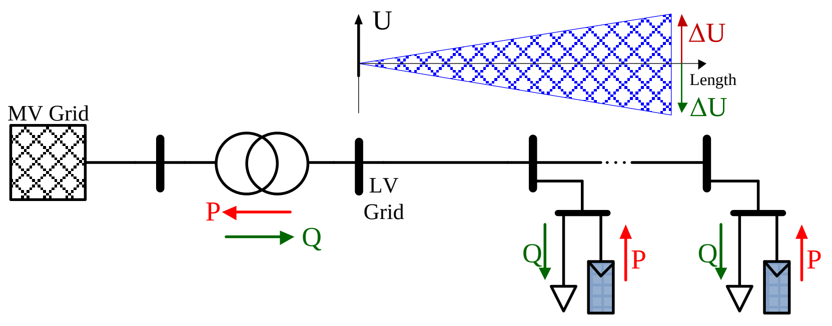

Figure 1-8 Reverse power flow and voltage variations in LV networks with PVs [24]

To achieve further PV capacity of the network and to overcome the voltage variation problem with minimum reinforcement of the grid, the system operators recently adopted new GCs [19] which require PV inverters to be more flexible and to participate with ancillary functions to the grid stability. For LV networks, the main requirement refers to voltage regulation techniques and different methods are proposed with the focus on fixed reference or static droop characteristics. The fixed reference values for reactive power provision or the droop curve will be specified by the network operators.

Due to high amount of space for the PV arrays to be connected in the rural area, the chance of violating voltage limitations is higher than in suburban networks. Therefore, the project will analyze a typical European LV rural network where high PV penetration can be achieved and consequently the risk for voltage variations outside the prescribed limits is higher.

1.4 Objectives

The main objectives of this project are the following:

- Classical voltage regulation strategies:
  - ❖ Study the German GCs and the requirements for LV networks (VDE 0126-1-1 and VDE-AR-N 4105)

- Choose and model a LV benchmark network to analyze the voltage variations and test the voltage regulation methods to maintain the voltage variations between the imposed limits
- Model and implement the voltage regulation strategies encouraged by German GC
- Asses the performance of the control strategies and choose the best candidate

- Improved voltage regulation strategies using coordinated control:
  - Design and simulate an optimized voltage regulation method to improve the best candidate from the German GC with focus on reducing the reactive power consumption and increase PV capacity in the LV network. The optimized algorithm should use the communication approach.
  - Asses the performance of the optimized control algorithm and demonstrate the improvements brought using the communication concept.
- Voltage regulation strategies using the communication concept:
  - Study the communication standard IEC 61850 with focus on 7th series called "Basic communication structure for substation and feeder equipment".
  - Design and simulate the IEC 61850 communication protocol, using the client/server architecture to exchange information between intelligent electronic devices (IEDs).
  - Experimentally validate the best candidate of voltage regulation strategies as well as the optimized algorithm on a laboratory setup, using coordinated control of inverters with information exchange IEC 61850.

1.5 Limitations

This project will consider the following limitations:

- The simulations will consider the inverter as an average model, therefore the switching is neglected.
- Overall response of the system will be considered, with no focus on power quality or anti-islanding.
- No meshed networks for analysis are considered (only radial).
- The study carried assumes that all PVs are grid connected units and no energy storage is considered.
- For simulating the worst case scenario, in terms of voltage variation, no load consumption is assumed.
- The inverters used for the experimental validation of IEC 61850 have no smart capabilities, therefore dSPACE and PC has been used to access and write the data.

Chapter 2 Grid codes and regulations

The chapter describes the new regulations for the connection of PV systems to the LV grid. A parallel between the old and new GC is presented with the focus on the main requirements in terms of grid interface, power quality and anti islanding. The main faults and disturbances which appear in the utility grid are as well briefly discussed.

2.1 Introduction

In the last years, an important amount of distributed generation (DG) systems were connected to the grid with the main purpose of increasing renewable power production. The utility grid is not ideal; therefore the grid voltage and frequency may exceed the prescribed limits, which is undesirable and unacceptable [5].

The electrical power systems require ancillary services such as voltage and frequency regulation, power quality improvement and energy balancing to operate efficient and reliable. In a power system, the DSO is responsible to maintain the correct operations and can purchase ancillary services directly from the PV generators. Until recently, the inverter requirements in case of abnormal grid conditions and faults were to disconnect and wait for fault clearance. The massive development in the PV sector faced new challenges for the inverter which is now required to contribute to grid stability by providing support functions [25-27].

In Figure 2-1, the main challenges which inverters face are presented.

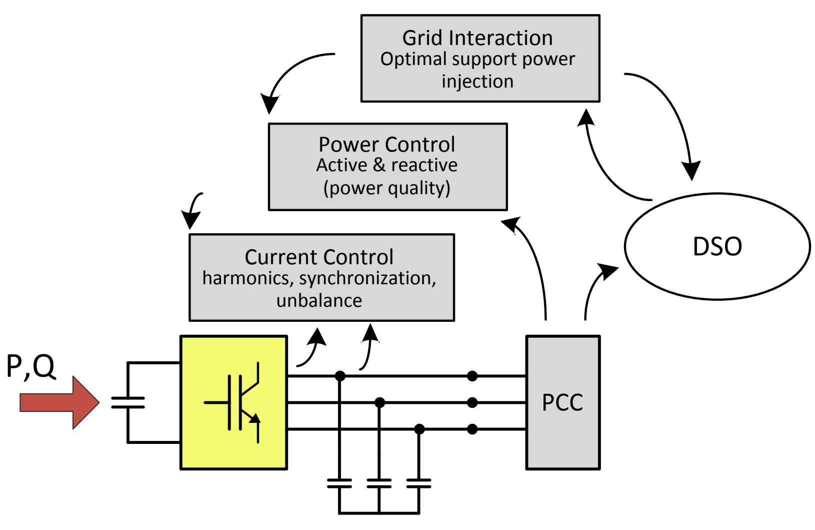

Figure 2-1 PV Inverter control functions [28]

As shown in Figure 2-1, the control functions can be divided in three separate levels: current control, power control and grid interaction. The first part deals with the current control which can be considered to be the basic one as it decides the performance of the entire system.

The second part is in charge with the generation of current control references for the first control level having a time response 10 times slower compared to the current control part [28]. The third level is in charge with the requirements specified by the DSO and also provides the reference values for active and reactive power.

Increasing PV penetration into the grid leads to elaboration of specific technical requirements for grid integration. The wide variety of regulations and norms are a major barrier for the PV industry. Interconnection requirements in certain European countries are available with the main focus on reducing the cost of PV systems by achieving further growth in the future market [29].

In order to diminish the diversity of requirements and standards, the ongoing activities of Distributed Energy Resources Laboratories (DER-Lab) are focused on developing and implementing a coordinated European standard [29].

There are two main steps for developing jointly grid codes: structural and technical harmonization. The aim of the structural process is to set a common grid code template while the technical one is more of a long-term implementation. The process aims to expand PV systems which would lead to an increasing propagation of renewable energies [29, 30].

Further in this chapter, the requirements for the grid connected PV systems will be presented in form of a parallel between the previous (VDE 0126-1-1) and the new (VDE-AR-N 4105) German GC for LV networks [18, 19]. The most relevant requirements concern the grid interface, power quality and anti-islanding [14].

2.2 Grid interface requirements

a) Voltage variations

- **Undervoltage**

This particular fault is also known as voltage ‘dip’ or ‘sag’. It is characterized by sudden a reduction in voltage amplitude to less than 90 % from nominal value with a duration time from 10 ms to several seconds, depending on the location of the fault which occurs in the network. The common cause for these types of failures are short circuits, faults to ground, transformer energizing inrush currents and connection of large induction motors. The consequences of voltage sags are the disconnection of power electronic devices from the grid with fault clearance in the range of 0.1- 0.2 s [14, 31].

- **Overvoltage**

These faults are less frequent than sags and appear usually due to lightning on transmission cables, with voltage magnitude of several kV introduced in overhead LV networks. Overvoltages can be caused also by the switching of LV appliances (pumps, fans, electric boilers etc), large loads which are switched off, capacitor bank energizing or voltage increase on the unfaulted phases during a single line to ground fault. In this case, the voltage magnitude increase is between 1.1 and 1.8 p.u. and accepted time duration is up to 1 minute [32] .

Under normal operating conditions, the voltage variations should not exceed the standard limits from Table 2-1.

Table 2-1 Supply voltage variation limits from German GCs [18, 19]

VDE 0126-1-1		VDE-AR-N 4105	
Voltage range [Hz]	Disconnection time [s]	Voltage range [Hz]	Disconnection time [s]
V < 85 V ≥ 110	0.20	V < 80 V ≥ 110	0.10

In Table 2-1, the disconnection time for voltage variations is also available. The voltage deviations are detected by voltage measurements made at the CP, which is the default according to the standards [33].

- **Low-Voltage Ride Through (LVRT)**

According to VDE-AR-N 4105, there are no requirements for LVRT.

b) Frequency variations

Frequency variations are a common problem that affects the power systems being caused by the unbalanced power ratio between energy production and consumption. The frequency variation is defined by the following relation [34]:

$$\Delta f = f - f_r \tag{2.1}$$

Where: f - real frequency;
f_r - rated frequency;

The nominal frequency of the supply voltage in Europe is 50 Hz. The value of the fundamental frequency measured over 10 s should be in range of:

Table 2-2 Frequency variation limits from German GCs [18, 19]

VDE 0126-1-1		VDE-AR-N 4105	
Frequency range [Hz]	Disconnection time [s]	Frequency range [Hz]	Disconnection time [s]
47.5 < f < 50.2	0.20	47.5 < f < 51.5	0.10

In case of abnormal grid conditions, PV inverters need to disconnect from the grid to ensure safety of humans and equipment. In Table 2-2, disconnection time for frequency variations is also available.

c) Frequency requirements

An important issue in a power system is balancing power production and consumption because changes in power supply or demand can lead to temporary unbalance; hence the operating conditions of the power plants and consumer loads can be affected. To avoid unbalanced conditions, power plants must be capable to adjust power production by means of frequency regulation [35].The requirements regarding active power control aim to ensure a stable frequency in the power system [36].

The frequency requirements for active power reduction in LV networks were added for the first time in the VDE-AR-N 4105 (Figure 2-2). According to this standard, the generating plants with the capacity over 100 kW have to reduce their real power in steps of at most 10% of the maximum active power $P_{\max}$. Systems with power lower than 30 kW are allowed to participate in frequency regulation with a rate limit specified by the DSO. This power reduction must be possible in any operating condition and from any operating point to a target value imposed by the DSOs. The plant has to accept any set point in active power reduction. In the present, the set points are: 100% / 60% / 30% / 0% if technical feasible, otherwise shutdown of the generating plant must be performed.

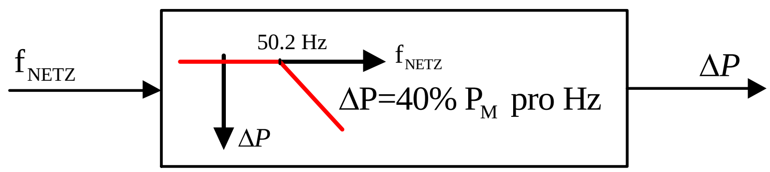

Figure 2-2 Active power reduction in case of over frequency [19]

The gradient for active power reduction can be calculated using the following formula:

$$\Delta P = 20 P_M \frac{50.2Hz - f_{Netz}}{50Hz} \quad \text{when } 50.2Hz < f_{Netz} < 51.5Hz \tag{2.2}$$

Where:

ΔP - active power reduction gradient

P_M - power generated after exceeding the 50.2 Hz limit

f_{Netz} - network frequency

Generating units have to reduce with a gradient of 40%/ Hz their power output when a certain frequency limit is surpassed (50.2 Hz for Germany). The output power is allowed to increase again when the frequency is below a specific limit (50.05 Hz for Germany). Outside the frequency limits imposed by the GC, the plant has to disconnect from the grid [36].

Controllable power plants have to reduce the power output to the target value within a maximum period of time of 1 minute. If the set point is not reached in the mentioned period of time, the generating plant must be shutdown.

d) Reconnection after trip

The inverter allows reconnection after fault as soon as the conditions from Table 2-3 are satisfied. The purpose of the allowed time delay is to ride-through short-term disturbances.

Table 2-3 Conditions for reconnection after trip [19]

VDE 0126-1-1	VDE-AR-N 4105
90 < V < 115 [%] AND 47.5 < f < 50.2 [Hz] AND Min. Delay of 30 seconds	85 < V < 110 [%] AND 47.5 < f < 50.05 [Hz] AND Min. Delay of 5 seconds

e) Voltage rise

- **Admissible voltage changes**

During normal operation, the magnitude of the voltage change caused by the generating plants must not exceed, in any CP, a value of 3% compared with the voltage when the generating plants were not connected. The preferred method to calculate the voltage changes is using complex load-flow calculations [19].

$$\Delta u_a \leq 3\% \tag{2.3}$$

- **Sudden voltage changes**

The voltage change at CPs when the generators are connected or disconnected is limited at 3% per generating unit and should not occur more frequently than once every 10 minutes. In this case the disturbances caused by the switching operation remain between admissible limits.

The maximum allowed voltage rise is calculated in terms of short circuit power at CP [19]:

$$\Delta u_{\max} = \frac{I_a}{I_{rE}} \cdot \frac{S_{E\max}}{S_{kV}} \tag{2.4}$$

Where:

S_{kV} - network short circuit power at CP

$S_{E\max}$ - maximum generating power at CP

I_a - starting current

I_{rE} - rated current

f) *Reactive Power Control and Real Power Curtailment*

Under normal operation, when required by the DSO, the generating plants have to supply static grid support functions, meaning voltage stability by means of reactive power control. The working point for reactive power exchange should be determined in accordance with the need of the grid.

The reactive power provision must be available in any operating point. The operation of the generating plant must be possible with a reactive power output corresponding to the power factor (PF) values and depending also on the rated power of the generating unit.

- if $\sum S_{E\max} < 3.68kVA$ - the generating plant should operate in: *cosφ=0.95 (under excited)* to *cosφ=0.95 (over excited)*, according with EN 50438
- if $3.68kVA < \sum S_{E\max} < 13.8kVA$ - the generating plant shall accept any set point from the DSO: *cosφ=0.95 (under excited)* to *cosφ=0.95 (over excited)*
- if $\sum S_{E\max} > 13.8kVA$ - the generating plant have to accept any set point from the DSO: *cosφ=0.90 (under excited)* to *cosφ=0.90 (over excited)*

When the active power output is fluctuating, the reactive power has to be adjusted according to the specified power factor; hence the name of the method: cosφ(P). The type of the regulation method and the nominal values of the reactive power adjustment are dependent on the network conditions and can therefore be determined individually by the DSO. Each generating unit has to automatically adjust their set point according to the characteristic curve received from the DSO within 10 seconds (Figure 2-3) [19].

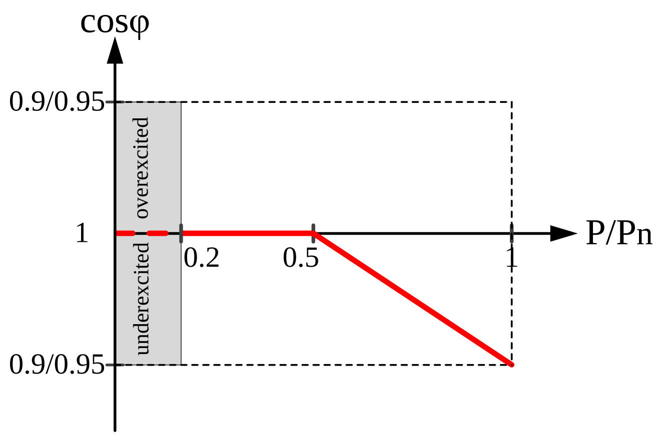

Figure 2-3 cosφ(P) droop characteristic for LV networks [19]

In case the generators can supply a constant active power output, the fixed PF control method is more suitable. The generating units directly connected to the power grid have a transition time to reach the reactive power set point of 10 minutes.

The future requirements, in terms of voltage stability, are to use the voltage-dependent Q(U) method, which calculates the reactive power reference according to the droop characteristic Q-U set by the DSO.

2.3 Power quality

Power quality is an important aspect in grid connected PV systems, as the utility grid can be affected by reliability problems. In Figure 2-4, an overview of the power quality aspects can be observed.

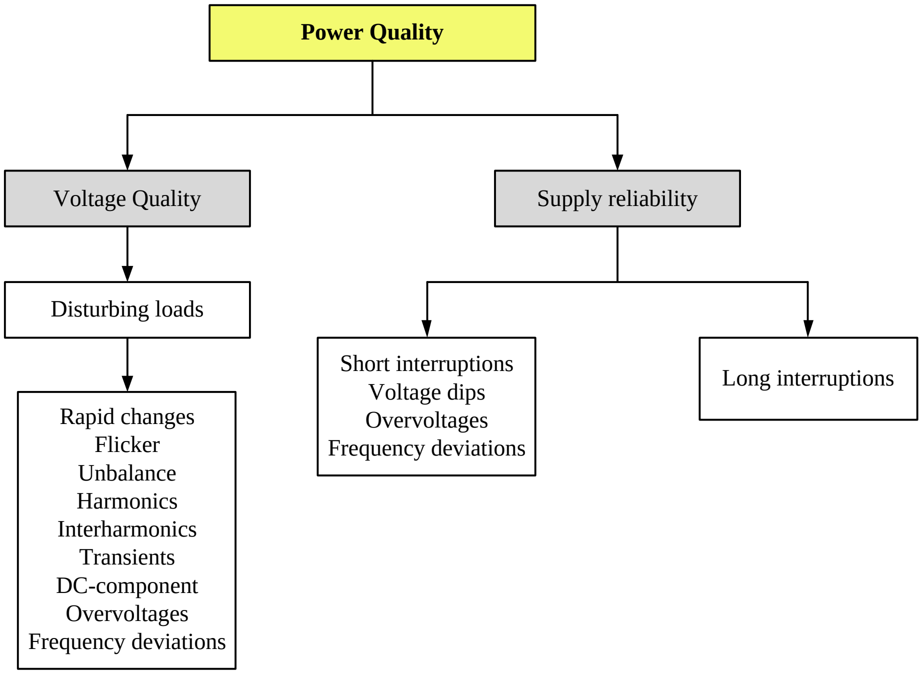

Figure 2-4 Power quality aspects classification, depending on the disturbances that can appear in the grid [31]

Voltage quality is regulated in Europe according to EN 50160 [37]. The following requirements are general:

- Voltage unbalance for three-phase inverters: max. 3%
- Voltage amplitude variations: max. ±10%
- Frequency variations: max. ±1%
- Voltage dips: duration <1s, deep <60%

a) Harmonic requirements

Harmonics are sinusoidal components of voltage or current signals with the frequency equal to an integer multiple of the fundamental frequency. The main source of harmonics currents in DS are non-linear loads.

Harmonic currents are transferred into harmonic voltages through the grid impedance. The harmonics present in the grid appear most likely as a consequence of high harmonics in the customer load, saturation of transformers caused by higher voltage during light load demand conditions and amplified by resonance in the utility system. Excessive harmonic current leads to voltage stress which reduces the reliability of equipment due to temperature increase [38]. The current harmonic requirements present in VDE-AR-N 4105 are outlined in Table 2-4.

Table 2-4 Allowable harmonic limits based on network short circuit power at CP [19]

Harmonic number	**Allowable, Ssc based harmonic current $i_{\nu,\mu\ zul}$ in A/MVA**
3	3
5	1,5
7	1
9	0,7
11	0,5
13	0,4
17	0,3
19	0,25
23	0,2
25	0,15
$25 < \nu < 40$	0,15 x 25/ν
even	1,5/ν
$\mu < 40$	1,5/ν
$\mu,\nu > 40$	4,5/ν

b) Voltage Unbalance

Voltage unbalance occurs when the three-phase voltages differ in amplitude or they are displaced from their normal 120° phase relationship or both. The voltage unbalance of a DS is defined by the Voltage Unbalance Factor (VUF), which can be expressed as the ratio between the negative (V_-) and the positive (V_+) sequence voltage component or between the negative (I_-) and the positive (I_+) sequence currents.

$$VUF = \frac{V_-}{V_+} = \frac{I_-}{I_+} \tag{2.5}$$

The limit for the %VUF allowed in European networks according to EN 50160 is 3% [39].

Voltage unbalance is caused by:

- Impedance asymmetry of the LV network
- Single-phase connection of the generators
- Uneven distribution of loads across each phase of the LV network

However, according to [40], LV networks are affected predominantly by the voltage rise problem than voltage unbalance. Furthermore, control of generation and controllable load could bring benefits in terms of equalizing the load distribution and generation across the three-phases.

According to VDE-AR-N 4105, the maximum allowed unbalance for three phases connection is 4.6 kVA and 10 kVA for single-phase connection. If the rated power of the systems is bigger than 30 kVA, only a three-phase connection is allowed. Table 2-5 presents some examples of unbalance in systems.

Table 2-5 Example of unbalance for different systems

L1	**L2**	**L3**	**Unsymmetric**	**Allowed?**
4,6 kVA	0	0	4,6 kVA	**Yes**
4,6 kVA	2,5 kVA	0	4,6 kVA	**Yes**
10 kVA	6 kVA	8 kVA	4 kVA	**Yes**
10 kVA	5 kVA	3 kVA	**7 kVA**	**No**
10 kVA	7 kVA	**11 kVA**	4 kVA	**No**
10 kVA	**10 kVA**	**11 kVA**	1 kVA	**No**
50 kVA (3-phase ac)			0	**Yes**

c) DC current injection

DC current injection introduced by the PV inverter generates a DC offset in voltage waveform which can cause significant malfunctions to the distribution transformers. Saturation of transformers results in harmonic current injection into the power system. In addition, DC current injection can cause increased heating of magnetic components, audible noise and reactive power demand [17]. Standards limit the maximum allowable amount of injected DC current into the grid and according to [41], Germany follows VDE 0126-1-1 standard [18] which is the most restrictive in terms of DC current injection. The limit set by the previously mentioned GC is presented in Table 2-6.

Table 2-6 Limit for injected DC current [18, 19]

VDE 0126-1-1	VDE AR-N 4015
Idc < 1A Max Trip Time 0.2 s	No specifications

d) Flicker

Flicker phenomena are produced by the system loads which are experiencing rapid changes in power demand and they can cause voltage variations in the electrical system [33]. Usually, the amplitude of voltage fluctuation does not exceed 10 % from the nominal value.

Although the flicker is harmful for electrical systems, the majority are designed to be insensitive to voltage fluctuations within some limits (maximum 3%). According to VDE-AR-N 4105, the generating unit should not create objectionable flicker for other customers. The standard for all grid connected system in terms of flicker regulations is IEC 61000-3-3 [42].

2.4 Anti-islanding requirements

Islanding condition occur when a part of the grid is disconnected and PV inverter continues to operate with local load. For safety reasons, islanding is a major concern, especially for personnel who attempt to work on lines which they believe to be disconnected. If the reconnection is established, the voltage at the point where island occurred is not synchronized with the grid voltage causing disturbances in the system. In order to avoid these consequences, anti-islanding measures were issued in standards [43].

Anti-islanding methods are divided into [14]:

1. Passive methods:
   - Based on grid parameter monitoring
   - Do not affect the overall system, unless limits are strict and the inverter trips without being island mode:
     - Frequency limitations (magnitude change, rate of change, phase shift)
     - Voltage limitations
     - Power (change of active/reactive power, power factor)
     - Harmonic content changes
2. Active methods:
   - Disturbances are injected into the supply to detect from their behavior if the grid is still present:
     - Impedance measurement
     - Voltage variation
     - Frequency variation
     - Output power variation

Requirements for grid connected PV inverters involve using any passive or active method to detect islanding condition. If significant parameter changes are detected which could lead to transition from normal operation to islanding, the inverter will be shut down and shall not reconnect before voltage and frequency have been maintained within specified limits for at least 5 minutes. Afterwards, the inverter will automatically reconnect to the utility grid.

According to IEEE 1547, when unintentional islanding occurs, the DR interconnection system must detect the island and stop energizing the area Electric Power System (EPS) within 2s [33].

According to VDE-AR-N 4105, the method proposed for anti-islanding is the "Impedance measurement" method. The required disconnection time for the inverter is 5 seconds.

Chapter 3 Voltage regulation strategies

The chapter describes the voltage regulation methods proposed by the German GC and the LV network chosen for their study. Further on, cosφ(P) and Q(U) strategies are modeled and simulated. Their results are discussed and compared in order to find the best candidate of voltage regulation strategy for the LV network.

3.1 Introduction

The voltage and frequency levels in the utility system represent a fundamental criterion to determine the quality of the power delivered to customers. The voltage has to be controlled to remain within the prescribed limits; therefore devices such as on-load tap transformers, shunt capacitors and compensators are responsible with the voltage regulation process [25].

The massive integration of DG systems into distribution networks raises stability problems. It is expected that DGs will take part in the regulation process, as it has been revealed that operating with active and reactive power simultaneously result in benefit for the utilities as well as for customers. The purpose of controlling the reactive power consumption in the network is to support the voltage level in the grid during normal operation [44].

To give a precise view of how the voltage at the CP is changing depending on the load, we consider the circuit from Figure 3-1 represented by a Thevenin equivalent bus system. The grid is seen by a voltage source E and the line equivalent impedance $Z = R + jX$ [38].

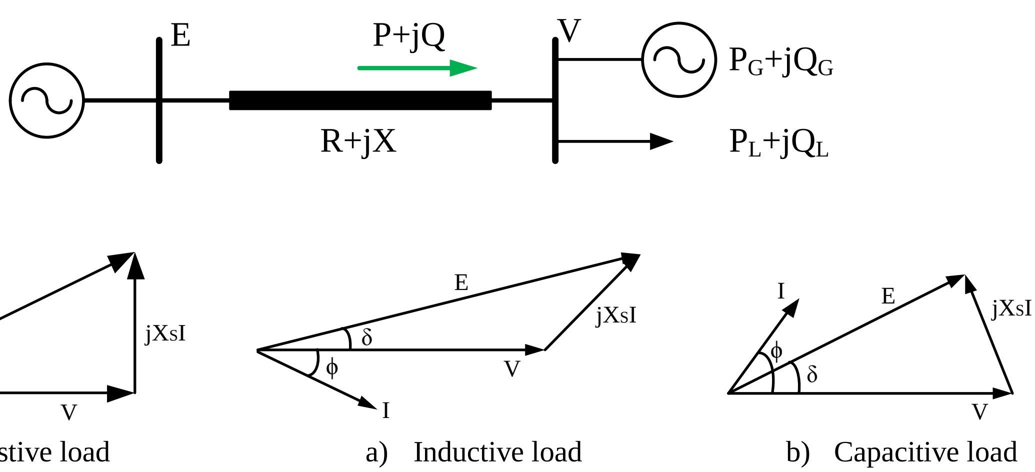

Figure 3-1 Phasor diagrams at point of common connection depending on the connected load
a) Resistive load b) Inductive load c) Capacitive load

In case of a resistive load as presented in Figure 3-1a, the voltage and current are in phase and no reactive power is consumed or generated by the load. When the current is lagging the voltage (current vector rotating negatively), the load draws reactive power from the grid and in consequence the supply voltage (E) has to be higher to maintain the terminal voltage (V) at the same value. The last case presented in Figure 3-1c occurs when the current is leading the voltage (capacitive load). The terminal voltage (V) can be kept at the same value even with lower supply source voltage (E) due to the injection of reactive power [38].

3.2 Conventional voltage regulation methods

When the DG systems connection effect is not considered, the voltage is maintained within prescribed limits based on the power flow from substation towards loads. The current flow in the conductors and lines, transformer and load impedance causes voltage drop and therefore voltage regulation devices are needed to keep the deviations in the acceptable range. The conventional voltage regulation methods are discussed in more detail in what follows [45].

The on-load tap-changing transformer (OLTC) represents the mostly used voltage regulation method in distribution networks. The working principle is similar to an autotransformer with automatically tap changes. The control variables are the voltage and current and based on that, the tap change is triggered until the voltage returns within the desired bounds. A range of ±10% of transformer rated voltage is normally provided by the tap positions and the total number of steps equals 32 [45].

Another technique to regulate the voltage along the feeder is by means of capacitor banks which are designed to supply reactive power and consequently compensate the lagging (inductive) power factor of the loads. The capacitor banks connection can be fixed (permanently connected) or switched. In order to avoid the overcompensation of reactive power and voltage rise along the feeder which will trigger unwanted tap changes of the transformers, control algorithms are used. The reactive power demand is usually determined based on: time of the day (loads connected during certain hours), temperature (appliances as air-conditioning dependant on ambient temperature) and voltage (decrease of the voltage along the feeder as consequence of reactive power consumption) [45].

Static Synchronous Compensator (STATCOM) is a Voltage Source Inverter (VSI) connected to the grid for reactive power compensation and power factor improvement purposes [46]. The most common configuration (see Figure 3-2) consists of VSI, DC-link capacitor, line filter and coupling transformer [47]. Due to the shunt connection, STATCOM can be seen as a current source; therefore, active and reactive power exchange between DS and STATCOM is possible by controlling the magnitude and the phase angle of the output voltage of the VSI.

STATCOM device has the capability to sustain reactive current when the system experience voltage variations. It also provides various additional advantages such as: voltage sag mitigation, voltage stabilization, flicker suppression, power factor correction and harmonic control. The voltage dip compensation is limited by the equivalent impedance of the power system seen by the device, which is connected in parallel with the load impedance. In order to minimize the losses, the STATCOM should be installed as close as possible to the load [46].

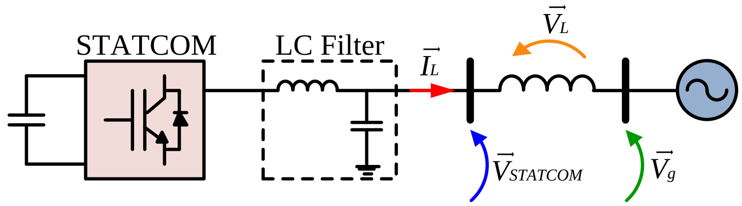

Figure 3-2 STATCOM connection to the utility grid [47]

3.3 Voltage regulation methods proposed by German GC VDE-AR-N 4105

Reverse power flow in the electrical power grids limit the DG absorption capacity and bring additional problems such as voltage rise and limited PV penetration. The problems can be overcome by generation/absorption of reactive power by each PV inverter. The set power values for each strategy are decided depending on the active power generation, voltage rise or consumption profiles.[3, 48]

According to the new German GC, the voltage regulation methods for the PV generators are the following:

- Fixed power factor: cosφ method
- Power factor characteristic: cosφ(P) method
- Fixed Q reactive power method
- Reactive power / voltage characteristic: Q(U) method

Both cosφ(P) and Q(U) strategies are based on droop characteristic. The fixed cosφ method is suitable for systems where the active output generation is kept constant, otherwise, if the active output is fluctuating, it is recommended to use one of the droop-based regulation strategies. The fixed Q method assigns a reactive power reference for the PV generators based on the network power flow investigation. Load power profile information and PV power production are needed in order to in order to assign a reasonable fixed reactive power set values to the inverters [49]. Furthermore, GCs encourage the use of load-flow calculations when determining the voltage change values.

This project will further focus only on the droop-based regulations strategies because the active generating output of the PV generators is fluctuating depending on the level of irradiation. In all the cases, the voltage changes will be determined using load-flow analysis.

3.4 LV network analysis

The increased active power generation due to high PV penetration leads to voltage rise in the network and can exceed the limit imposed by the GCs or can cause unexpected tripping of other grid connected PV systems. Therefore, the PV capacity is limited and further investments of transformer and lines upgrade are needed [49-54].

3.4.1 PV Inverter reactive power capability

The new regulations as German GC require from the PV inverters to inject or absorb reactive power, depending on the grid status. The maximum and minimum value of reactive power that an inverter can deliver is determined by its rated power (S) and active power from the PV array P_{PV}. When the active power produced equals with zero, the inverter can deliver maximum reactive power and consequently, when $P_{PV} = S$, there is no reserve for reactive power. Usually by over sizing the inverter with a 10 % it is enough to operate at power factor equal with 0.9 (inductive or capacitive). Therefore, for future investigations, it is assumed that all inverters have this capability [45].

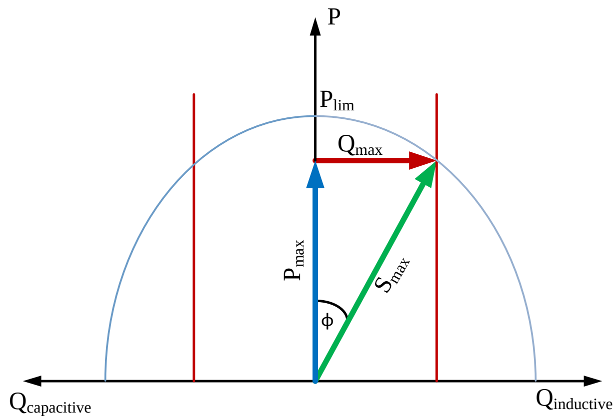

Figure 3-3 Inverter capability of providing reactive power [25]

When operating at 0.9 power factor, the phase displacement between real and apparent power will be:

$$\varphi = a\cos(0.90) \cdot \frac{180}{\pi} = 25.84° \tag{3.1}$$

Maximum reactive power that the inverter is able to supply at rated power is:

$$Q_{max} = S_{max} \cdot 45.2\% \tag{3.2}$$

In Figure 3-4, the inverter oversizing and reactive power supply capacity dependency is illustrated.

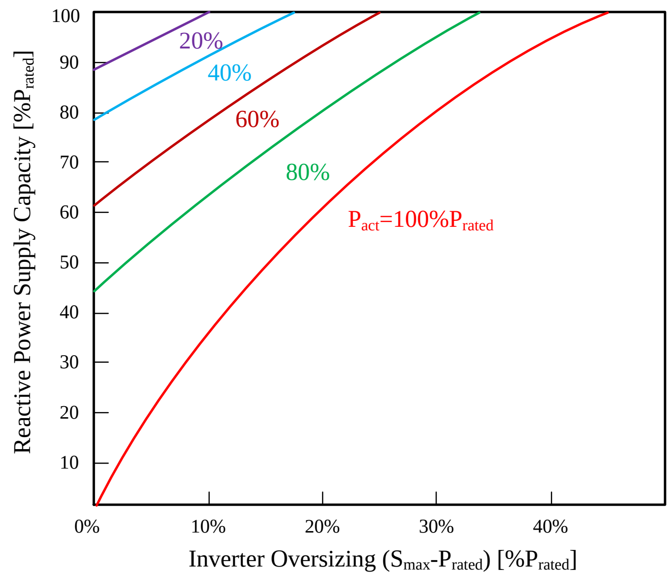

Figure 3-4 Reactive power supply capacity [$\%P_{rated}$] depending on the inverter oversizing ($S_{\max}P_{rated}$)[48]

3.4.2 European Network Benchmark Analysis

The focus of this project is on the voltage rise problem and, according to the new German GC VDE-AR-N 4105, the maximum voltage variation at CP after the connection of a distributed generator is maximum 3%. Therefore the PV capacity is limited by [19]:

$$V_{CP} \leq 1.03V_n \tag{3.3}$$

$$\text{Transf.loading}_{\max} = 100\% \tag{3.4}$$

Where V_n is the voltage at the CP before the connection of the PV systems.

Besides the above mentioned limitations, rural LV network are characterized by long distances between distribution transformer and cables having large R/X ratios which are usually bigger than 1. This drawback results in limited impact of reactive power over the grid voltage magnitude [53-56].

The network configuration chosen to be analyzed is a European LV benchmark and it can be observed in Figure 3-5 [57, 58]. The network is composed of a 100 kVA 20/0.4 kV transformer, one main feeder and two sub-feeders. For simplification purposes the impedances of the cables used to connect the PV system to the LV grid were assumed to be negligible in the calculation process. For simulation purposes, to observe the impact of PV generators over the LV network, 18 PV systems were analyzed, each having a peak installed power of 5 kW. The PV generators are three-phase connected and they operate with reactive power output corresponding to a minimum power factor of 0.9. The distance between the PV generators was chosen to be between 30m and 35m, depending on the LV topology.

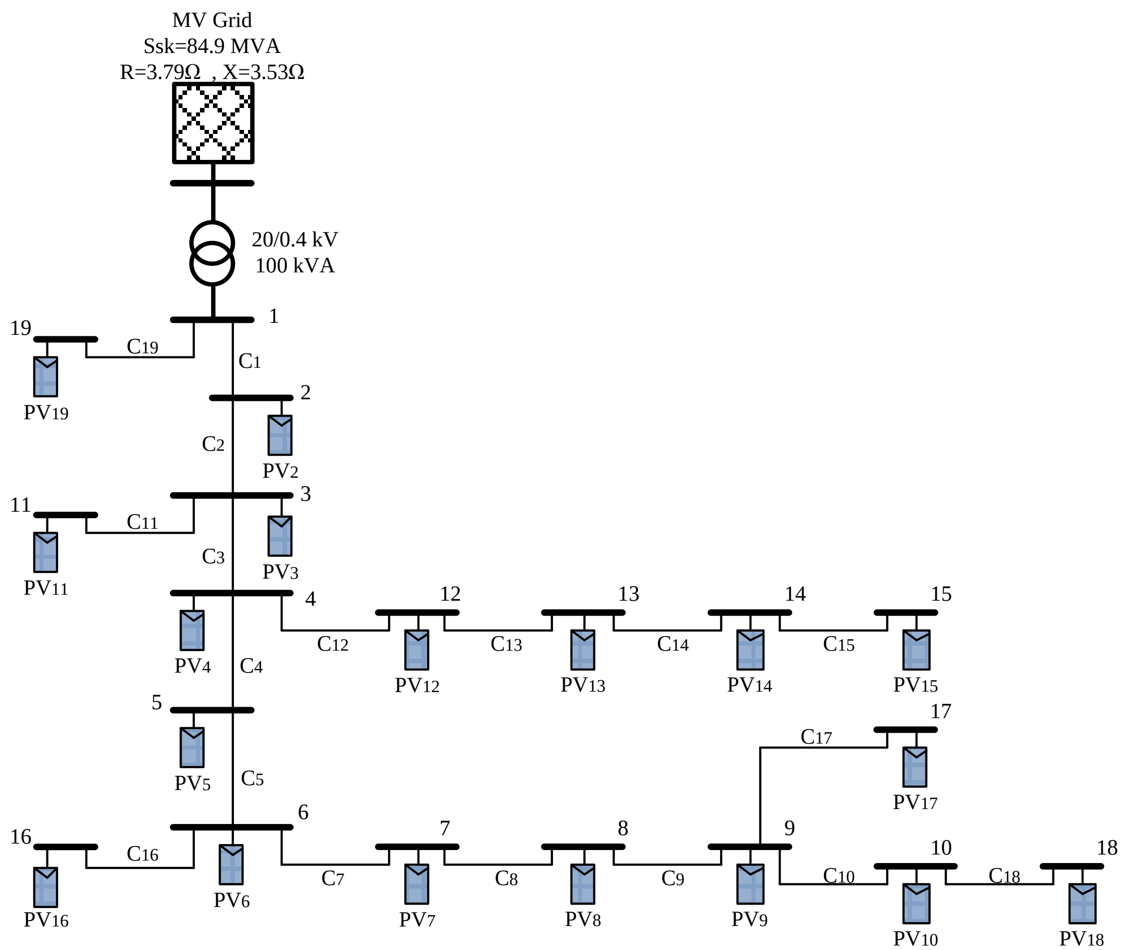

Figure 3-5 European network benchmark [57]

The complete data of the LV network was taken from [58] and it can be found in Table 3-1.

Table 3-1 Rural LV network specifications [57, 58]

External Grid	SSK=84.9 MVA; R=3.79 Ω; X=3.53 Ω
Distribution transformer	S=100 kVA Dy5; 20/0.4 kV; ukr=4%; urr=2%
LV Branch Feeder conductor (C11, C15, C16, C17, C18, C19)	NAYY 4x70 mm2 AL OLH; R=0.413 Ω/km; X=0.3 Ω/km; length=0.3 km
LV Branch Feeder conductor (C1, C2, C3, C4, C5, C7, C8, C9, C10, C12, C13, C14)	NAYY 4x70 mm2 AL OLH; R=0.413 Ω/km; X=0.3 Ω/km; length=0.35 km

The overhead cables between individual systems have impedance which resulted in an R/X ratio of 1.37. Therefore, the active power has greater impact over the grid voltage and causes voltage rise during high PV generation period. In this situation, the probability of voltage violation is higher than in the other typical networks such as urban and suburban given the fact that the character of those networks is more inductive. The voltage variation depending on active and reactive current can be observer in the equation (3.5).

$$\Delta V = R \cdot I_{active} + X \cdot I_{reactive} \tag{3.5}$$

In order to determine the maximum PV capacity which can be installed in residential LV networks and how PV systems are influencing the grid, test studies were performed using the simulation software Power Factory from DigSILENT and MATLAB.

The considered input data in terms of active power production was chosen from a real generation profile [59]. The measurements have a resolution of 15 min and they record the active power generation of a residential PV system during a day with high irradiance in June 2007. For the network presented in Table 3-1, 9 active power generation profiles were developed using the data from [59]. Each generation profile was assigned to 2 PV systems. In Figure 3-6, the PV generation profiles for one day in June 2007 are shown.

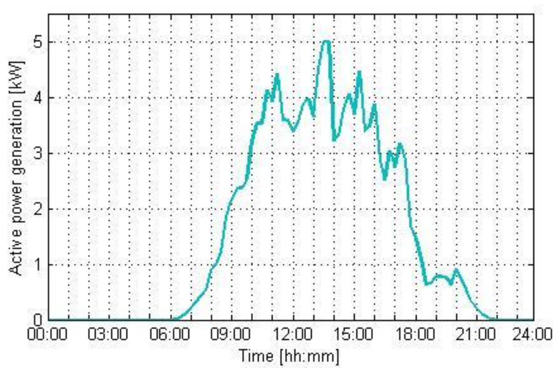

a) Profile 1 for PV2 & PV11 systems

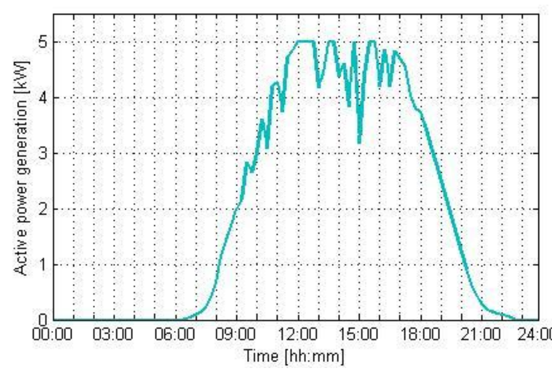

b) Profile 2 for PV3 & PV12 systems

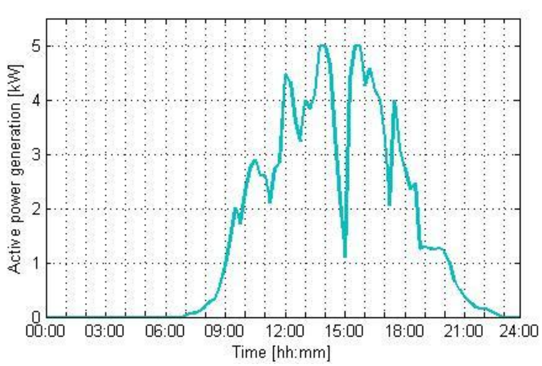

c) Profile 3 for PV4 & PV13 systems

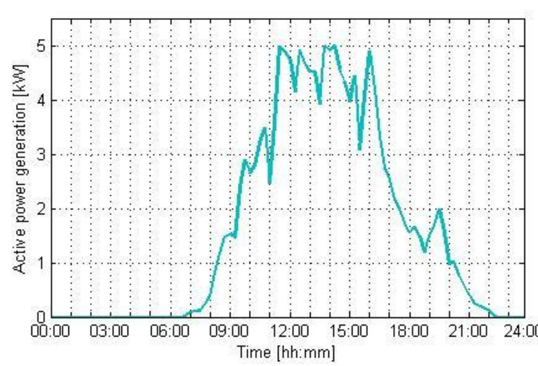

d) Profile 4 for PV5 & PV14 systems

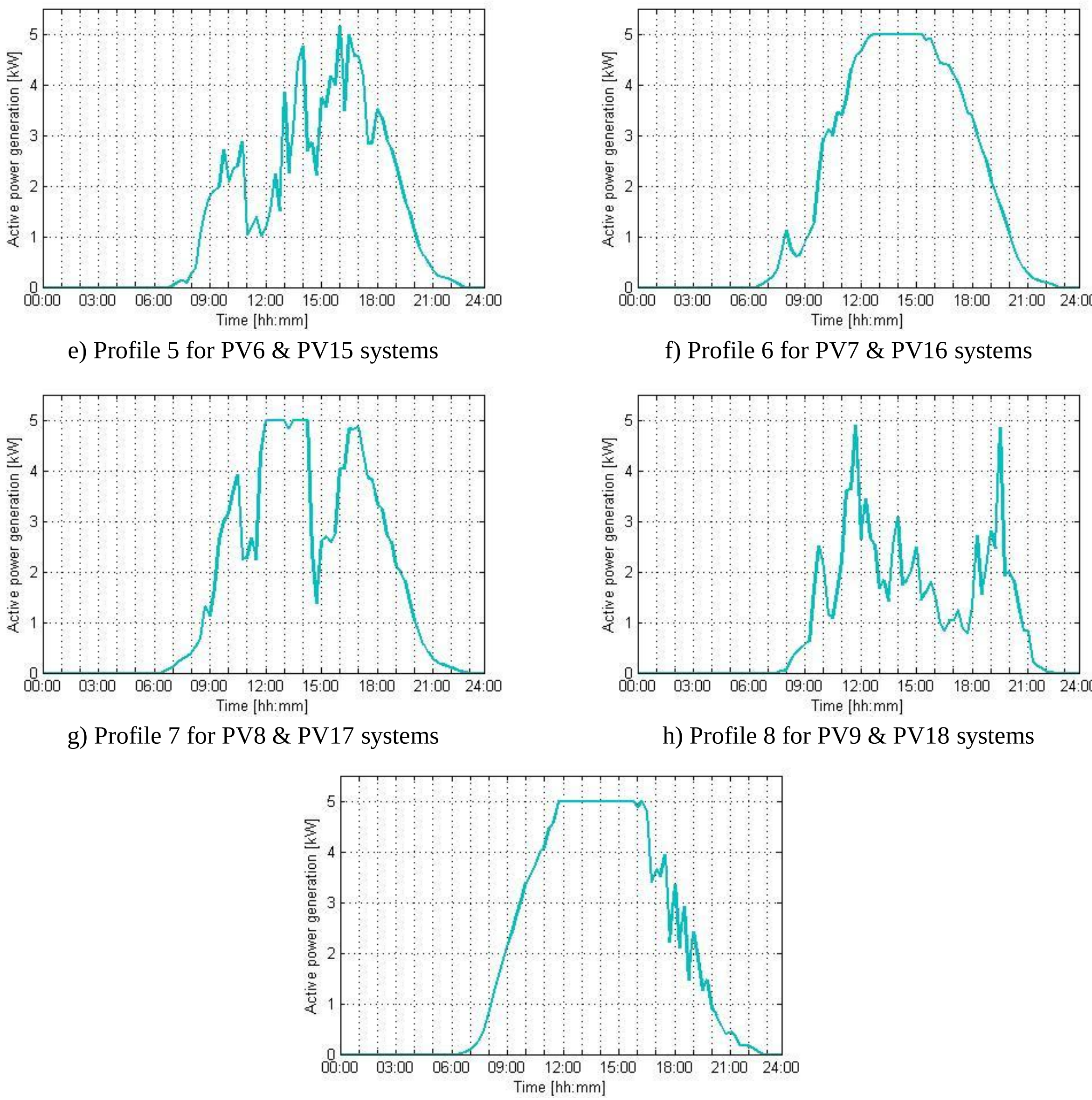

e) Profile 5 for PV6 & PV15 systems

f) Profile 6 for PV7 & PV16 systems

g) Profile 7 for PV8 & PV17 systems

h) Profile 8 for PV9 & PV18 systems

i) Profile 9 for PV10 & PV19 systems

Figure 3-6 Power generation profiles - June 2007 (a - i)

3.5 Load flow analysis

Load flow studies are performed to determine important features of power systems such as: the magnitude and angle of the voltage in each bus and the active and reactive power flow in each line. It also calculates the line losses and determines if the voltages remain within specified limits and whether transformers are overloaded [60].

In order to mitigate the voltage rise problem on the chosen LV network, successive load flow calculations are performed using the simulation software Power Factory from DigSILENT

[61]. This simulator uses Newton-Raphson method for load flow problem solving; therefore, this algorithm will be explained and later implemented using MATLAB software.

Basically, the Newton-Raphson method calculates two unknown variables using the known parameters and the power flow equations which include both types of variables and other known parameters. Depending on the bus type, the unknown variables which can be calculated based on the known variables are shown in Table 3-2.

Table 3-2 Known and unknown variables depending on bus type

	Known variables	Unknown variables
PQ bus	Active and reactive power (P, Q)	Voltage magnitude and angle (|V|, δ)
PV bus	Active power and voltage magnitude (P, |V|)	Reactive power and voltage angle (Q, δ)
Slack bus	Voltage magnitude and angle (|V|, δ)	Active and reactive power (P, Q)

3.5.1 Newton-Raphson method

Further, the Newton-Raphson algorithm will be explained step by step [62]:

Step 1: Reading of data

The bus where the low-voltage side of the transformer is connected (CP1) was chosen to be the slack bus and the rest are PQ buses.

Step 2: Construct the admittance bus (Ybus)

The Y_{bus} is the matrix which contains all the admittances in the network. The form of the matrix is the following:

$$Y_{bus} = \begin{pmatrix} Y_{11} & Y_{12} & \dots & Y_{1N} \\ Y_{21} & Y_{22} & \dots & Y_{2N} \\ \dots & \dots & \dots & \dots \\ Y_{N1} & Y_{N2} & \dots & Y_{NN} \end{pmatrix} = \frac{1}{Z_{bus}} \quad , N = 19 \tag{3.6}$$

Where:

- Y_{ii} is the self-admittance (diagonal) and it is equal to the sum of the admittances of all the branches connected to the i^{th} node
- Y_{ij} is the mutual admittance (off-diagonal) and is equal to the negative of the admittances of all the branches connected between i^{th} and j^{th} node

The impedance matrix Z_{bus} is calculated based on the cable specifications from Table 3-1. The values for all the elements of the Y_{bus} matrix can be found in Appendix A.

Step 3: Start values

The start values refer to the initial conditions for the magnitude and angle of the voltages in all CPs. Usually, when there are no other specifications, the *flat start* values are consider: 1 p.u. and 0 degrees.

The reference values for the active power generation are taken from [59] and the reactive power reference is taken as 0.

Step 4: Number of iterations

The number of iteration is set to 3.

Step 5: Calculation of injected power

The active and reactive powers injected in all buses are calculated using the actual magnitude and phase angles:

$$P_i = \sum_{j=1}^{19} |V_i||V_j||Y_{ij}|\cos(\theta_{ij} + \delta_j - \delta_i) \tag{3.7}$$

$$Q_i = -\sum_{j=1}^{19} |V_i||V_j||Y_{ij}|\sin(\theta_{ij} + \delta_j - \delta_i) \tag{3.8}$$

A detailed description for calculating the above mentioned formulas is presented in Appendix B.

Step 6: Difference between specified and injected power

The difference between the specified and the injected power values comes from the fact that the injected powers are computed based on guessed values of voltage magnitude and angle in the buses, whereas the specified ones are fixed reference values.

$$\Delta P_i = P_i^{ref} - P_i \tag{3.9}$$

$$\Delta Q_i = Q_i^{ref} - Q_i \tag{3.10}$$

Step 7: Maximum difference

The power difference values is calculated and compared to a set tolerance value, in this case 0.0001. If the mismatch is less than the tolerance, proceed to step 11, otherwise continue with step 8.

Step 8: Jacobian matrix

The Newton-Raphson method is responsible with the linearization of the power equations (3.9) and (3.10), therefore the Jacobian matrix is formed of partial derivatives that can be computed. The active and reactive power corrections are found in Step 6. In this way, the unknown variables, voltage magnitude and angle, can be calculated. The general form of the Jacobian matrix is the following [62, 63]:

$$\underbrace{\begin{pmatrix} \frac{\partial P_1}{\partial \delta_1} & \cdots & \frac{\partial P_1}{\partial \delta_N} & \frac{\partial P_1}{\partial V_1} & \cdots & \frac{\partial P_1}{\partial V_N} \\ \vdots & \ddots & \vdots & \vdots & \ddots & \vdots \\ \frac{\partial P_N}{\partial \delta_1} & \cdots & \frac{\partial P_N}{\partial \delta_N} & \frac{\partial P_N}{\partial V_1} & \cdots & \frac{\partial P_N}{\partial V_N} \\ \frac{\partial Q_1}{\partial \delta_1} & \cdots & \frac{\partial Q_1}{\partial \delta_N} & \frac{\partial Q_1}{\partial V_1} & \cdots & \frac{\partial Q_1}{\partial V_N} \\ \vdots & \ddots & \vdots & \vdots & \ddots & \vdots \\ \frac{\partial Q_N}{\partial \delta_1} & \cdots & \frac{\partial Q_N}{\partial \delta_N} & \frac{\partial Q_N}{\partial V_1} & \cdots & \frac{\partial Q_N}{\partial V_N} \end{pmatrix}}_{Jacobian} \underbrace{\begin{pmatrix} \Delta\delta_1 \\ \vdots \\ \Delta\delta_N \\ \Delta V_1 \\ \vdots \\ \Delta V_N \end{pmatrix}}_{Corrections} = \underbrace{\begin{pmatrix} \Delta P_1 \\ \vdots \\ \Delta P_N \\ \Delta Q_1 \\ \vdots \\ \Delta Q_N \end{pmatrix}}_{Mismatches} \tag{3.11}$$

The form of the equation (3.11) can be simplified with the use of submatrixes:

$$\begin{pmatrix} H_{ik} & N'_{ik} \\ J_{ik} & L'_{ik} \end{pmatrix} \cdot \begin{pmatrix} \Delta\delta_i \\ \Delta V_i \end{pmatrix} = \begin{pmatrix} \Delta P_i \\ \Delta Q_i \end{pmatrix} \tag{3.12}$$

The elements of the submatrixes $\left(H, J, N^{'}, L^{'}\right)$ are the partial derivatives from (3.11) which can be calculated taking into consideration also the bus type.

$$\begin{cases} H_{ik} = \dfrac{\partial P_i}{\partial \delta_k} & i \neq \text{ slack bus}, \ k \neq \text{ slack bus} \\ N'_{ik} = \dfrac{\partial P_i}{\partial V_k} & i \neq \text{ slack bus}, \ k \neq \text{ slack bus or PV bus} \\ J_{ik} = \dfrac{\partial Q_i}{\partial \delta_k} & i \neq \text{ slack bus or PV bus}, \ k \neq \text{ slack bus} \\ L'_{ik} = \dfrac{\partial Q_i}{\partial V_k} & i \neq \text{ slack bus or PV bus} \quad k \neq \text{ slack bus or PV bus} \end{cases} \tag{3.13}$$

The LV network analyzed in this project does not contain PV buses, therefore, only the derivatives for the slack bus are not computed. The mismatches for the slack bus are not considered since ΔP_1 and ΔQ_1 are undefined when P_1 and Q_1 are not scheduled and the correction for $\Delta\delta_1$ and ΔV_1 are both 0. In consequence, the dimensions of the submatrixes H, J, N', L' are $(N-1)\times(N-1)$ where N is the total number of buses in the network and in this case is equal to 19.

In order to simplify the expression of the N'_{ik} and L'_{ik} submatrixes, their elements will be multiplied with a voltage magnitude without influencing the result [63]. Therefore the correction will become $\Delta V_i / V_i$ and equation (3.12) can be rewritten in the following form:

$$\begin{pmatrix} H_{ik} & N_{ik} \\ J_{ik} & L_{ik} \end{pmatrix} \cdot \begin{pmatrix} \Delta\delta_i \\ \Delta V_i / V_i \end{pmatrix} = \begin{pmatrix} \Delta P_i \\ \Delta Q_i \end{pmatrix} \tag{3.14}$$

The elements of the Jacobian matrix can now be calculated based on equations (3.7) and (3.8).

- when $i \neq k$:

$$\begin{cases} \mathrm{H}_{ik} = \dfrac{\partial P_i}{\partial \delta_k} = \mathrm{V}_i \mathrm{V}_k \left(G_{ik}\sin(\delta_{ik}) - B_{ik}\cos(\delta_{ik})\right) \\ \mathrm{N}_{ik} = \mathrm{V}_k \mathrm{N}'_{ik} = \mathrm{V}_k \dfrac{\partial P_i}{\partial \mathrm{V}_k} = \mathrm{V}_i \mathrm{V}_k \left(G_{ik}\cos(\delta_{ik}) + B_{ik}\sin(\delta_{ik})\right) \\ J_{ik} = \dfrac{\partial Q_i}{\partial \delta_k} = -\mathrm{V}_i \mathrm{V}_k \left(G_{ik}\cos(\delta_{ik}) + B_{ik}\sin(\delta_{ik})\right) \\ \mathrm{L}_{ik} = \mathrm{V}_k L'_{ik} = \mathrm{V}_k \dfrac{\partial P_i}{\partial \mathrm{V}_k} = \mathrm{V}_i \mathrm{V}_k \left(G_{ik}\sin(\delta_{ik}) - B_{ik}\cos(\delta_{ik})\right) \end{cases} \tag{3.15}$$

- when $i = k$:

$$\begin{cases} \mathrm{H}_{ii} = -Q_i - B_{ii}V_i^2 \\ \mathrm{N}_{ii} = \mathrm{P}_i + G_{ii}V_i^2 \\ J_{ii} = \mathrm{P}_i - G_{ii}V_i^2 \\ \mathrm{L}_{ii} = Q_i - B_{ii}V_i^2 \end{cases} \tag{3.16}$$

A more detailed description of how the Jacobian matrix is formed and how its elements are computed can be found in [63].

Step 9: Calculation of ΔV and Δδ

Using the power mismatches calculated at Step 6 and the elements of the Jacobian matrix computed at Step 8, the corrections can be found using the following formula:

$$\begin{pmatrix} \Delta\delta_i \\ \Delta V_i / V_i \end{pmatrix} = \begin{pmatrix} H_{ik} & N_{ik} \\ J_{ik} & L_{ik} \end{pmatrix}^{-1} \cdot \begin{pmatrix} \Delta P_i \\ \Delta Q_i \end{pmatrix} \tag{3.17}$$

Step 10: New voltage magnitude and angle

Using the calculated corrections in Step 9, the new voltages can be computed using equations (3.18) and (3.19).

$$V_i = V_i\left(1 + \Delta V_i / V_i\right) \qquad i \neq \text{ slack bus} \tag{3.18}$$

$$\delta_i = \delta_i + \Delta\delta_i \qquad i \neq \text{ slack bus} \tag{3.19}$$

Step 11: Power flow and power production

The active and reactive power flows and the net power production in all busses can be calculated with the known voltage magnitude and angle values. Furthermore, the total network losses can also be computed.

3.5.2 Load flow results

The first load flow analysis on the chosen LV network must be performed with the following conditions: maximum active power generation and no reactive power consumption. The purpose of this study is to examine the maximum voltage levels in the network and based on these values, a reactive power compensation strategy can be proposed. Furthermore, based on the measured values, the droop characteristics can be developed for both regulation methods proposed by the German GC VDE-AR-N 4105 [19].

To emphasize the voltage increase due to PV power generation, a study case with zero load demand was considered. The voltage value at the slack bus before the connection of the PV systems is chosen 1 p.u.. In Figure 3-7, the network voltage levels at all CPs are presented. As expected, the network experience voltage rise above the 3% limit with the maximum rise at the end of the feeder.

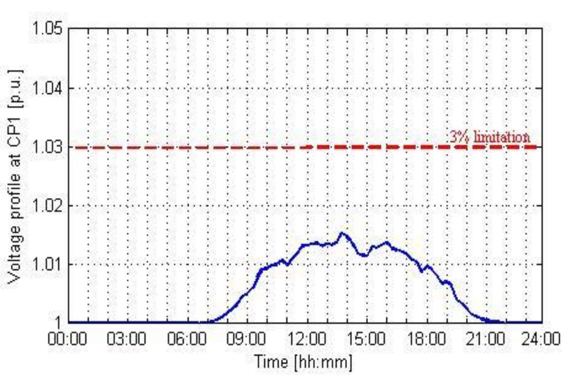

a) Voltage level at CP1

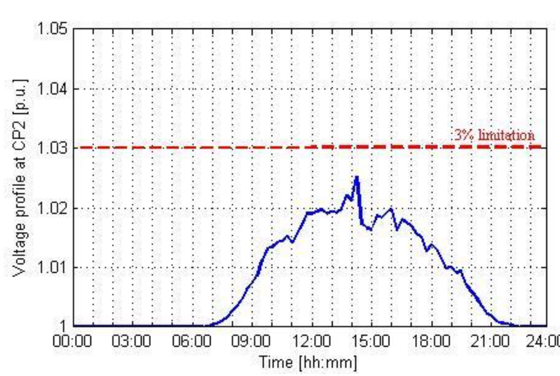

b) Voltage level at CP2

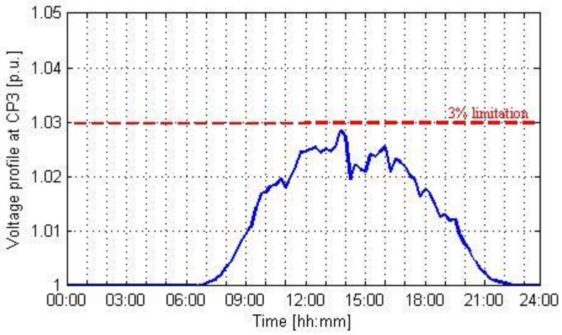

c) Voltage level at CP3

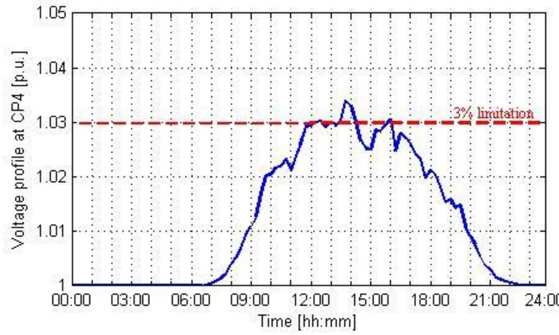

d) Voltage level at CP4

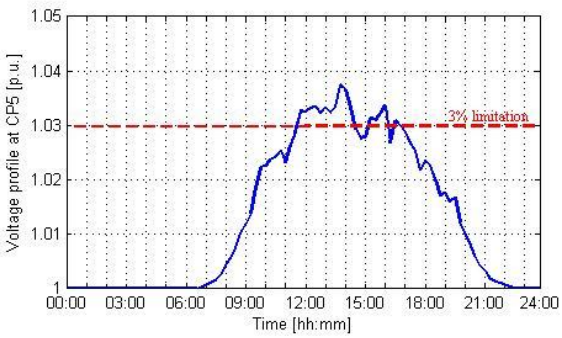

e) Voltage level at CP5

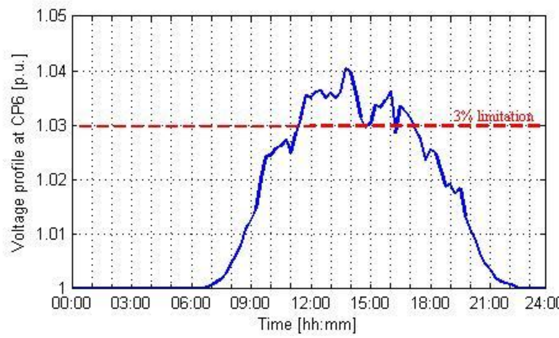

f) Voltage level at CP6

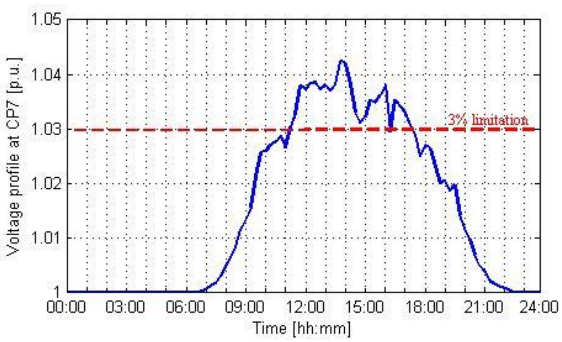

g) Voltage level at CP7

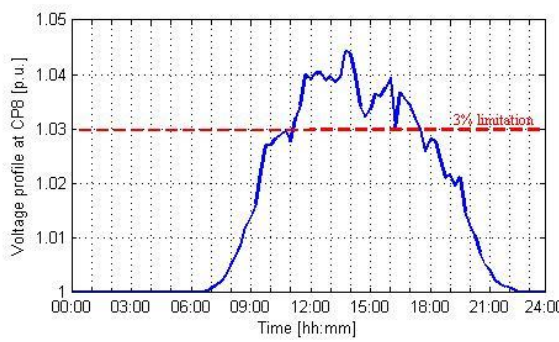

h) Voltage level at CP8

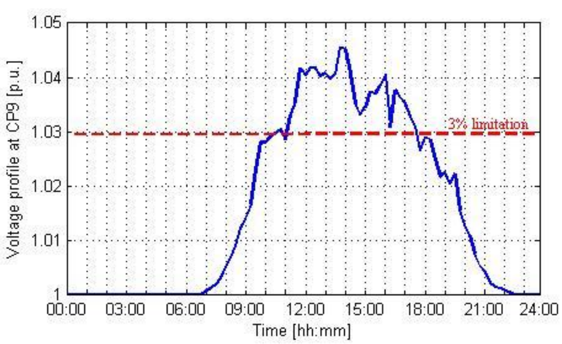

i) Voltage level at CP9

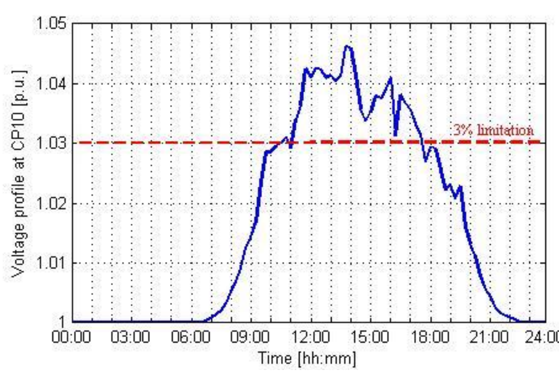

j) Voltage level at CP10

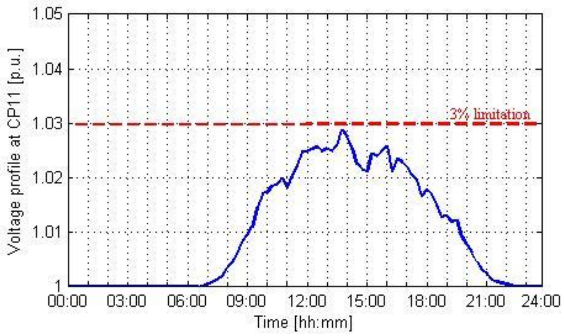

k) Voltage level at CP11

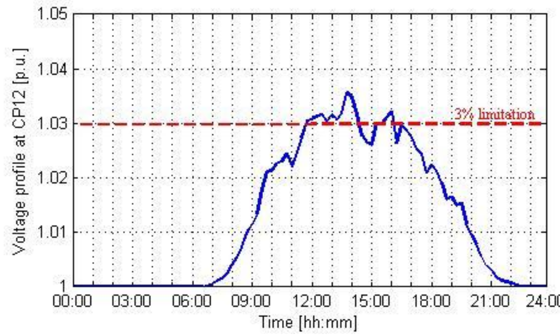

l) Voltage level at CP12

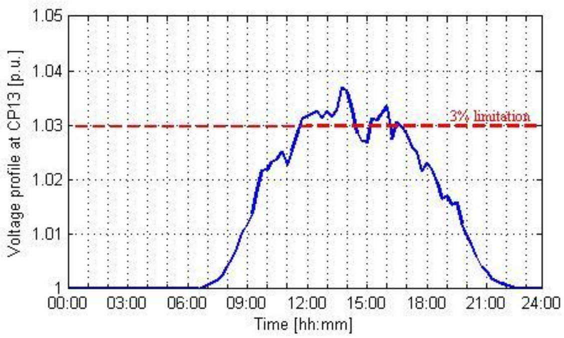

m) Voltage level at CP13

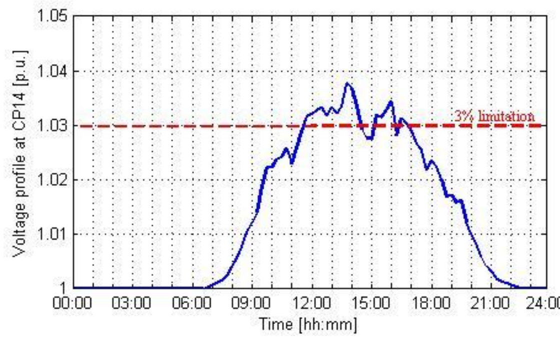

n) Voltage level at CP14

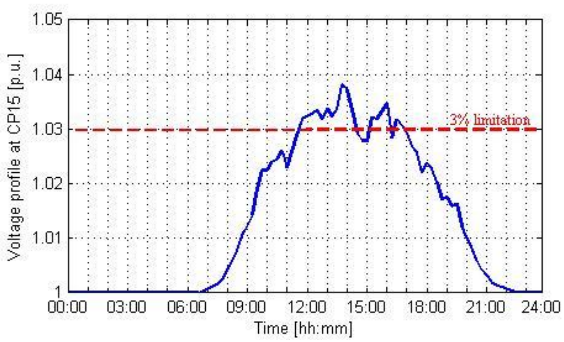

o) Voltage level at CP15

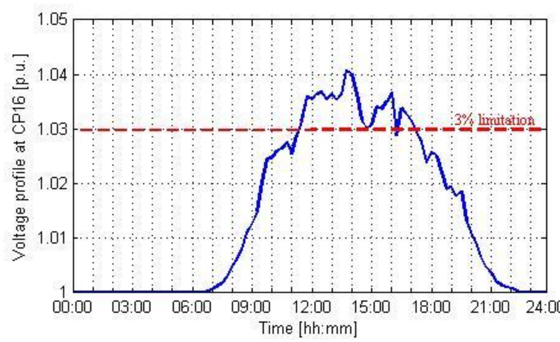

p) Voltage level at CP16

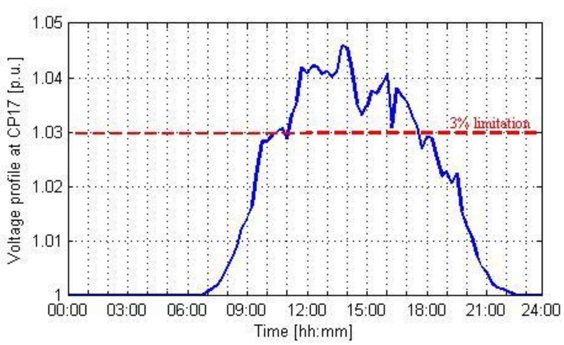

q) Voltage level at CP17

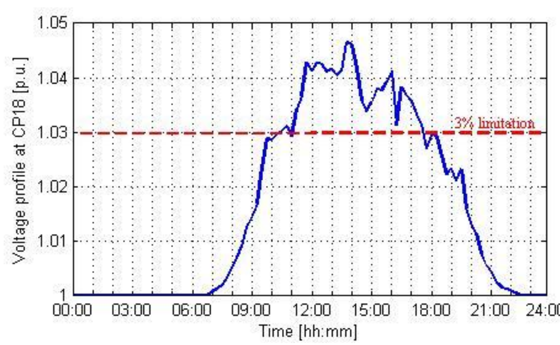

r) Voltage level at CP18

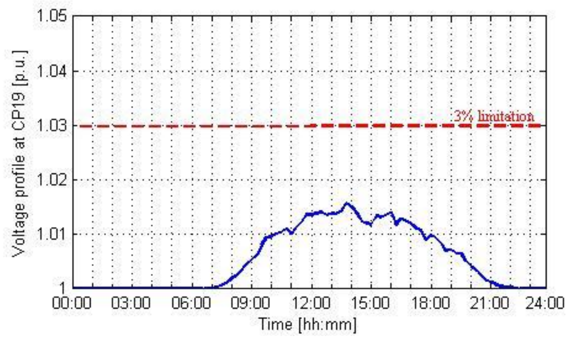

s) Voltage level at CP19

Figure 3-7 Voltage levels at all CPs of the network after performing the load flow analysis (a - s)

In order for the whole system to be inbounded to the 3% voltage limit and to avoid power curtailment, PV generators have to adopt voltage regulation methods.

The transformer loading also calculated after performing the load flow analysis for one day in June 2007 can be seen in Figure 3-8. As it can be observed, the loading level does not exceed 100%.

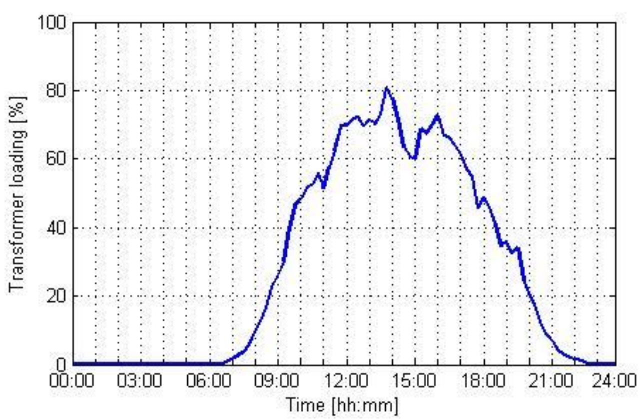

Figure 3-8 Transformer loading when no voltage regulation methods are applied

The source code developed using DigSILENT simulator for the load flow analysis can be found in Appendix C.

3.6 Cosφ(P) method

The first voltage regulation method proposed by the German GC is calculating the reactive power reference depending on the active power generated by the PVs (Figure 3-9). When the power production is low, the risk of overvoltage in the network is small as well. When the power generation increase reaches half of the PV nominal power, the power factor is decreasing towards 0.9 and reactive power is absorbed.

The method does not use grid voltage information and is only assuming that high power generation matches the voltage increase [49, 58].

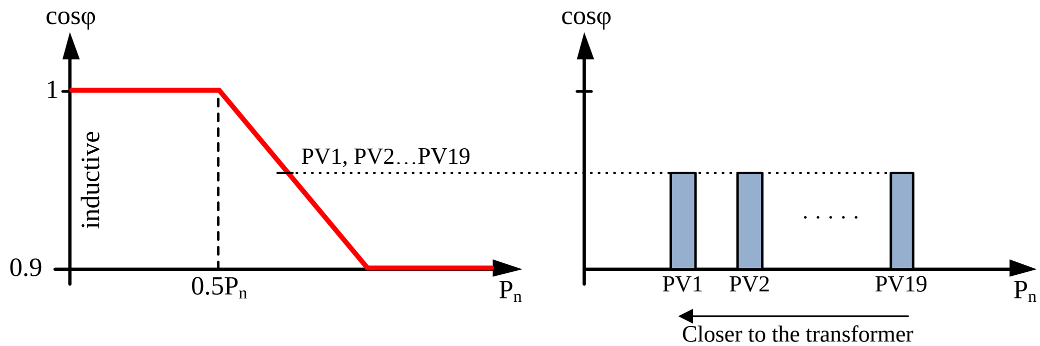

Figure 3-9 Droop characteristic for cosφ (P) method

The main drawback of this method is the possibility of reactive power consumption even though the voltage at the CP is in admissible range. Furthermore, this method does not take into consideration the impedance of the cables and the PV system located nearest to the transformer can absorb the same amount of reactive power as the PV system located at the end of the feeder if they both have the same active power generation [49, 58].

In this case the reactive power reference can be expressed as:

$$Q = tan(a\cos\varphi)\cdot P \tag{3.20}$$

The maximum reactive power the PV inverter can absorb at the rated power of 5kW is:

$$Q_{max} = tan(a\cos(0.9))\cdot P_n = 2.42\ kVar \tag{3.21}$$

The flow chart presented in Figure 3-10 shows the implementation of the cosφ(P) algorithm on the chosen LV network.

The first step consists of assigning the active power reference value (P_i^{ref}). The data will be assigned each 15 minutes during a day; therefore a total of 96 assignments will be performed. Next, the algorithm checks the value of the active power generation value to assign its corresponding cosφ value and calculate the reactive power consumption. If the P_i^{ref} value is less than half the rated power ($P_n = 5kW$), the system works at unitary PF and no reactive power is consumed. If the power reference is higher than the nominal value, the system absorbs the maximum amount of reactive power ($Q_{max} = 2.42kVar$). For any other values of P_i^{ref} a corresponding value for PF is assigned according to Table 3-3 and the reactive power reference Q_i^{ref} is calculated. The algorithm stops when the number of iterations set by user is reached.

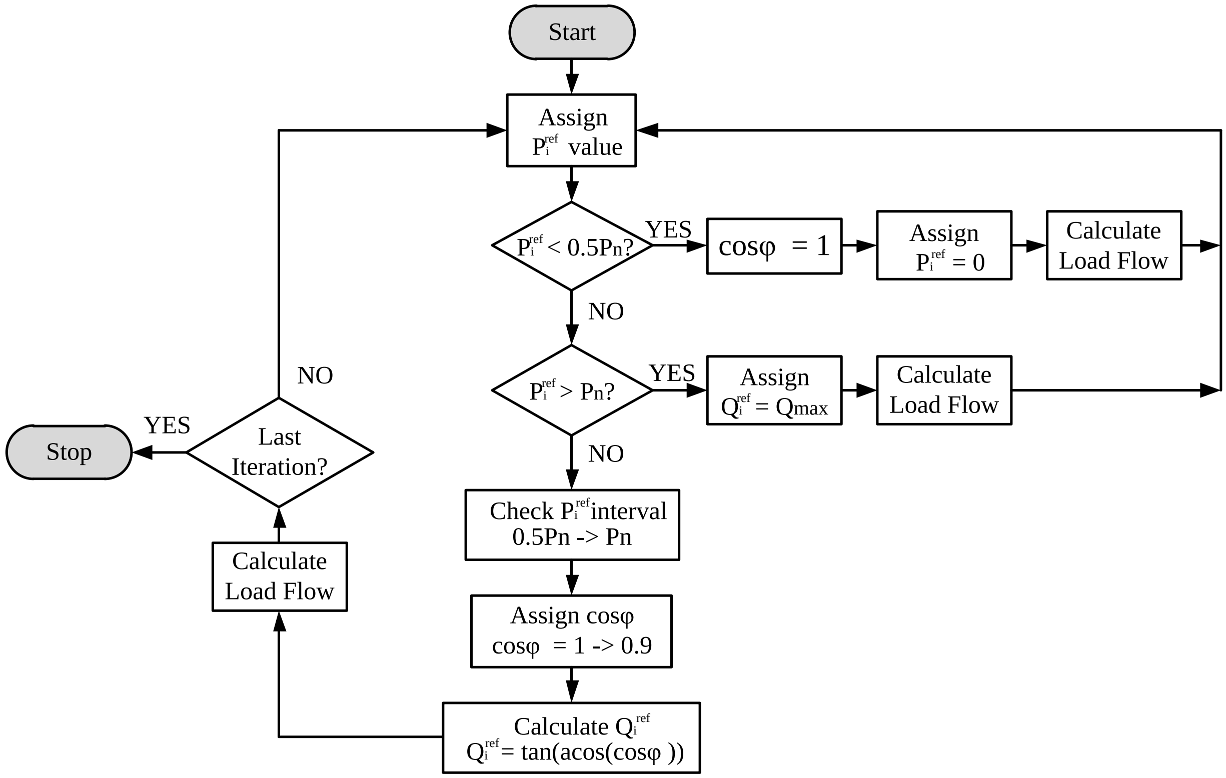

Figure 3-10 Flow chart with the implementation of the cosφ(P) method

Table 3-3 Cosφ values assigned corresponding to P_i^{ref} values when $P_i^{ref} \in [2.5;5]$kW

P_i^{ref} interval (kW)	[2.5, 2.75]	(2.75, 3]	(3, 3.25]	(3.25, 3.5]	(3.5, 3.75]
cosφ	0.99	0.98	0.97	0.96	0.95
P_i^{ref} interval (kW)	(3.75, 4]	(4, 4.25]	(4.25, 4.5]	(4.5, 4.75]	(4.75, 5]
cosφ	0.94	0.93	0.92	0.91	0.9

The source code developed using DigSILENT simulator to implement the cosφ(P) method can be found in Appendix D.

3.7 Q(U) method

The second strategy of voltage regulation proposed by the German GC, presented in Figure 3-11, is calculating the reactive power reference of each PV system depending on the voltage magnitude measured at its corresponding CP. The benefit of this method compared to cosφ(P) is that it uses local voltage information in the regulation process which means the reactive power consumption will be proportional to the voltage level.

The main drawback of this regulation method is the improper use of the inverter available capacity. It is likely the voltage magnitude at the CPs near the transformer to be within limits, therefore the corresponding PV systems will not participate in the regulation process, making the task much difficult for the other PV inverters. Furthermore, the probability that the inverters situated further away from the transformer will work at full capacity or at a capacity higher than the inverters located near the transformer. Because each PV system performs a local regulation process, the inverters with available capacity cannot help the inverters working at full capacity; therefore, in terms of reliability, the inverters located at the end of the feeder will experience reliability problems earlier [50, 58, 64].

As stated in the German GC, the droop curve for the Q(U) method is provided by the network operator. Therefore, the droop characteristic specific for the LV network studied in this project must be designed. Based on the results of the first load flow analysis, for the maximum voltage value, the corresponding reactive power absorption value can be assigned. As it can be seen from Figure 3-11, this value can be taken as 1.05 p.u. because when there is no reactive power absorption in the network, the maximum voltage magnitude does not exceed 1.05 p.u.. The start value for absorbing reactive power is chosen to be 1.02 p.u.. Using these values, the droop characteristic can be achieved and the Q(U) regulation method can be implemented (Figure 3-12) [58].

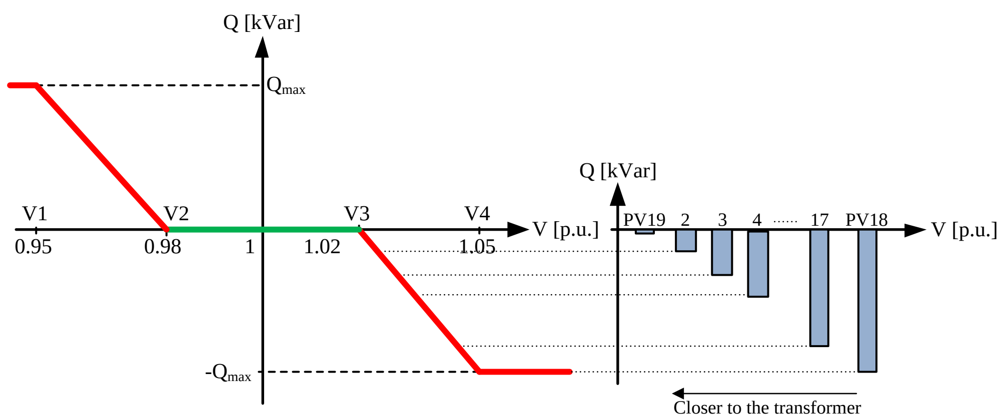

Figure 3-11 Droop characteristic for Q(U) method

The voltage variation is calculated using the following formula:

$$\varsigma = \frac{V_{meas} - V_3}{V_3} \cdot 34\ [\%]\,, \qquad \varsigma \in [0,1] \tag{3.22}$$

The reactive power reference is calculated using the value of the voltage variation found in (3.20):

$$Q_i^{ref} = \varsigma \cdot Q_{\max} \tag{3.23}$$

The flowchart shown in Figure 3-12 presents the implementation of the Q(U) method. For this purpose the DigSilent Power Factory software was used and for each iteration, two load flow analysis are performed. First, the effect of active power generation on the voltage magnitude is investigated. Based on the measured voltage value (V_{meas}), an individual reactive power is assigned to each PV (Q_i^{ref}) and a new load flow analysis is performed in order to check if the problem has been suppressed.

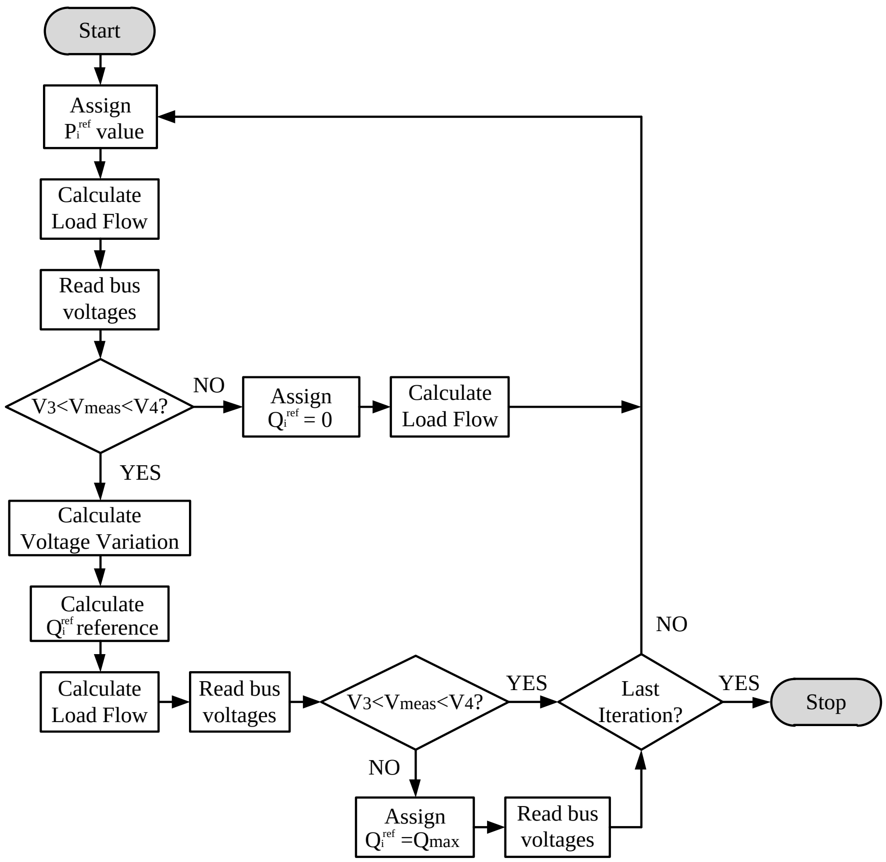

Figure 3-12 Flow chart with the implementation of the Q(U) method

The algorithm for Q(U) method can be summarized by the equation system from (3.24).

$$Q_i^{ref} = \begin{cases} Q_{max}; & V_{meas} > V_1 \\ \dfrac{V_{meas} - V_3}{V_3} \cdot 100 \cdot Q_{max}; & V_1 < V_{meas} < V_2 \\ 0; & V_2 < V_{meas} < V_3 \\ \dfrac{V_{meas} - V_1}{V_1} \cdot 100 \cdot \left(-Q_{max}\right); & V_3 < V_{meas} < V_4 \\ -Q_{max}; & V_{meas} > V_4 \end{cases} \tag{3.24}$$

It can be mentioned that for the LV network studied in this project, the only concern is the voltage rise problem and PV systems are required only to absorb reactive power, therefore only the corresponding part from the equation system was considered for implementation. The source code developed using DigSILENT simulator to implement the Q(U) method can be found in Appendix E.

3.8 Study case results

The performance of the above described methods is investigated based on voltage level, reactive power flow and the transformer loading level. First, the behavior of the PV systems closer to the transformer is investigated. It is expected that these systems will experience less voltage rise at their CPs. When the selected voltage regulation strategies are implemented, each PV system consume a reactive power value corresponding to its active power generation (cosφ (P)) or the local voltage magnitude (Q(U)).

In Figure 3-13a) the voltage profile of the closest system to the transformer (PV19) is shown. As it can be observed the highest voltage level at the CP is around 1.015p.u.. In Figure 3-13b), the generation profile of the PV19 generator is presented together with the levels of reactive power consumed using both regulation methods. The reason there is no reactive power absorption for Q(U) strategy is because the droop-characteristic, defined in Figure 3-11, states that the inverter will start consuming reactive power only when the voltage reaches the value of 1.02 p.u. For this PV system the voltage remains inside the dead band of the droop curve (0.98p.u. – 1.02p.u.). On the other hand, it can be observed that the cosφ(P) algorithm consumes large amounts of reactive power, proportional to the active generation levels, even though no voltage regulation is needed. Although the voltage is between limits, the high amount of reactive absorption leads to a decrease in voltage level to an approximate value of 1.005 p.u..

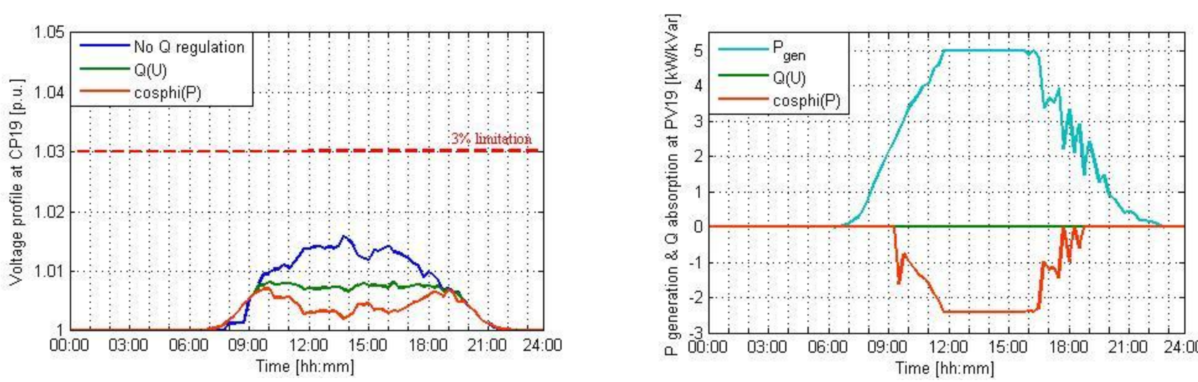

a) b)

Figure 3-13 PV19 system analysis a) Voltage levels with and without regulation methods b) Active power generation and reactive power consumed using regulation methods

The reason the voltage at the CP19 when using the Q(U) algorithm is lower compared to the voltage when no regulation is applied in the network is due to the influence of the reactive power absorbed by the rest of the network and the high impedance of the transformer.

Figure 3-14 presents the analysis results of the second PV system closest to the transformer – PV2. As it can be noticed, the only difference compared to the previously analyzed PV system is the fact that the voltage at the CP slightly increases above 1.02p.u. and for a short period of time, the Q(U) method is absorbing reactive power.

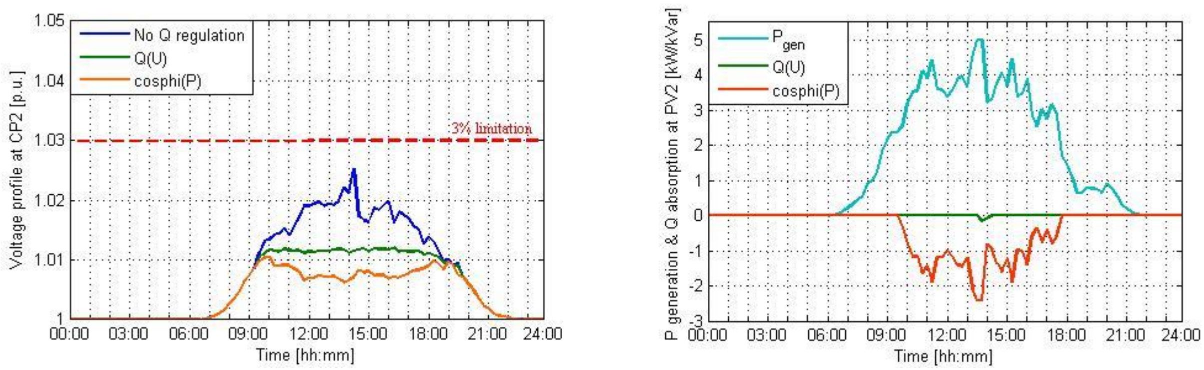

a) b)

Figure 3-14 PV2 system analysis a) Voltage levels with and without regulation methods b) Active power generation and reactive power consumed using regulation methods

For PV19 system, the active power generation profile is different from the previously discussed one, but the high amounts of reactive power absorption when using cosφ(P) algorithm is present in this case also. This fact leads again to having the lowest voltage values at the CP when considering cosφ(P) strategy.

As expected, the CPs near the transformer did not experience voltage rise above the 3% limit. Further on, the PV systems situated at the end of the main feeder and the ones located at the end of the two sub-feeders will be analyzed.

Figure 3-15 describes the simulation results for the PV system located at the end of the main feeder – PV16.

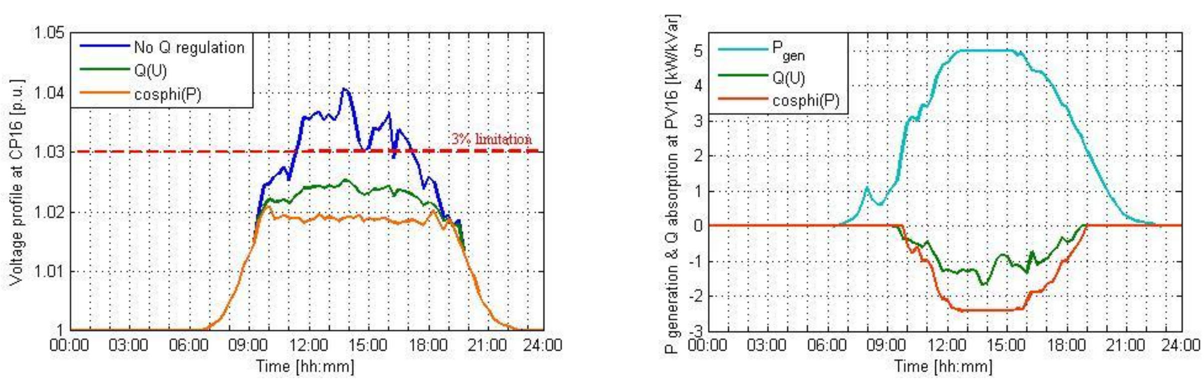

a) b)

Figure 3-15 PV16 system analysis a) Voltage levels with and without regulation methods b) Active power generation and reactive power consumed using regulation methods

The voltage level after performing the first load flow analysis reaches 1.04 p.u., therefore voltage regulation is mandatory to lower the voltage below the imposed limit. Both cosφ(P) and Q(U) strategies perform successfully the regulation process with the same difference in terms of reactive power consumption: the amount absorbed with cosφ(P) is significantly higher than using Q(U).

The analysis of the simulation results continue with the PV system located at the end of the first sub-feeder - PV15. As well as the previous analyzed system, the voltage level at the CP violates the 3% limit and after the regulation process the voltage is reduced and maintained in the specific range (Figure 3-16).

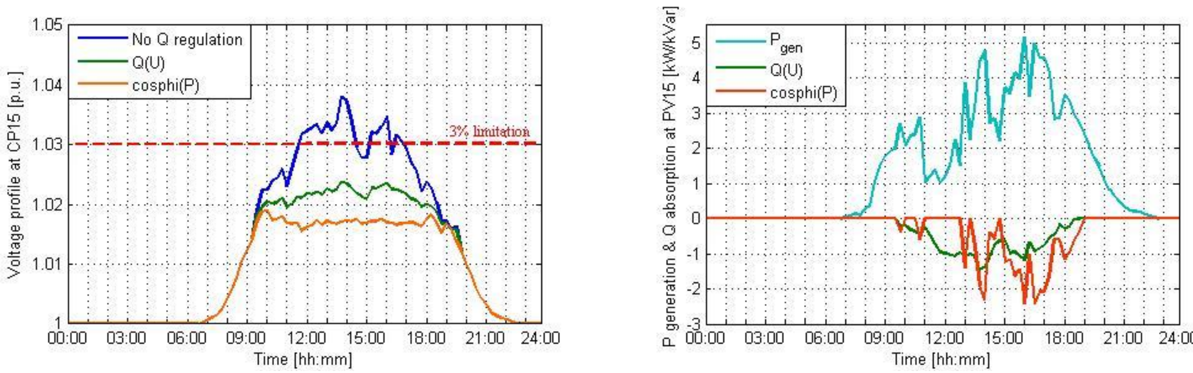

a) b)

Figure 3-16 PV15 system analysis a) Voltage levels with and without regulation methods b) Active power generation and reactive power consumed using regulation methods

Finally, the PV system situated at the end of the second sub-feeder and furthest away from the transformer is discussed – PV18 (Figure 3-17). The highest voltage level in the network, approximately 1.046, is reached at the CP of this system. The interesting part is that in this case the roles are reversed and the Q(U) method consumes more reactive power than cosφ(P) in the first part of the day until around 15:00. The reason this happened is the low levels of active power generation.

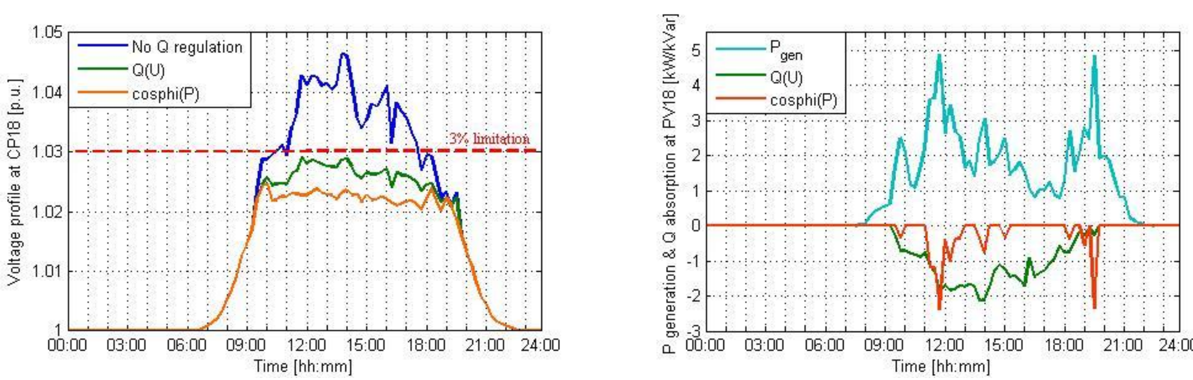

a) b)

Figure 3-17 PV18 system analysis a) Voltage levels with and without regulation methods b) Active power generation and reactive power consumed using regulation methods

In Figure 3-18, the transformer loading for the analyzed strategies is shown. Without the reactive power regulation from the PV systems, the maximum transformer loading is 81%. The Q(U) method minimizes the reactive power absorption and increases the loading of the transformer to a maximum value of 85.5%. On the other hand, the cosφ(P) method limits the further PV capacity achievement due to the high amounts of reactive power consumption which lead to a 91% loading of the transformer.

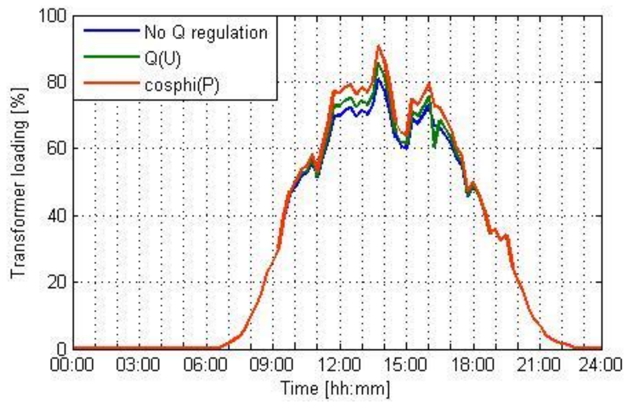

Figure 3-18 Transformer loading for the analyzed strategies

3.9 Discussions

The performance of both cosφ(P) and Q(U) regulation methods was evaluated on the chosen European LV network based on their ability to maintain the voltage between specified limits.

The purpose of having more active power generation profiles for the PV systems is to emphasize the effect of the cosφ(P) method. If all PV generators had the same profile, the amount of reactive power consumed using cosφ(P) would have been the same for all the inverters.

The simulation results show that both methods have achieved their regulation purpose. Although the voltage values using the cosφ(P) are closer to 1 p.u. compared to Q(U) method, the consequence of having a lower voltage is a higher reactive power consumption. As long as the voltage does not exceed the 3% limit, the value is not an issue, therefore the fact that the voltage level is lower using cosφ(P) cannot be seen as an advantage because it does not have any effect on the network.

The difference between the two strategies in terms of reactive power is prominent as both strategies calculate the reactive power consumption in two different ways. Because cosφ(P) method does not consider any feedback from the network nor the voltage sensitivity, all the inverters in the network can consume the same amount of reactive power, regardless of their position and the voltage levels. On the other hand, Q(U) method takes into consideration the above mentioned issues and improves the inverter capacity use. The inverters that do not experience voltage rise over the limit are not as stressed as the other inverters and the reactive power consumption is therefore decreased. From the point of view of reactive power absorption, it can be stated that Q(U) method is better, but improvements can be made so that all inverters can participate in the regulation process with their available capacity.

From the above mentioned, another conclusion can be drawn in terms of reliability. Because of the higher levels of reactive power consumed by all the inverters with cosφ(P) method, the amount of inverters that can experience problems is bigger than in case of using Q(U) strategy; thus leading to a lower life-time of the inverters.

The last performance criterion to evaluate the two control strategies is the level of transformer loading. The simulation results shown that the transformer loading was most increased when using the cosφ(P). It is normal because the higher stress on the transformer is the consequence of the larger amounts of reactive power absorption.

Both methods proposed by the new German GC VDE-AR-N 4105 were implemented on a LV network and analyzed from different points of view. All the results and discussions point in the same direction: the Q(U) algorithm is the best candidate when considering voltage regulation in a LV network with minimum reactive power consumption.

Chapter 4 Improved voltage regulation strategies

The chapter describes an optimization algorithm for voltage regulation in LV network in order to improve the classical methods proposed by the German GC. The implementation of the optimized Q(U) algorithm is explained in detail and simulation results are discussed and compared with the classical Q(U) algorithm which was chosen as best candidate based on the results from the previous chapter.

4.1 Optimized Q(U) method

The main objectives when talking about networks are to find optimal solutions to problems that minimize the costs. The optimization problem treated in this chapter refers to the reactive power dispatch problem with the focus on developing an algorithm with the following purposes:

- Maintain the voltages at the CPs below the specified limit
- Minimize the reactive power consumption of the overall network, hence minimize the losses in the line
- Use the available capacity of all the PV inverters to avoid stressing the ones at the end of the feeder
- Use advanced communication protocols to gather information from all the PV systems on a centralized controller which would calculate the optimal reactive power reference for each PV system

4.1.1 Standard optimization problem

Optimization is a mathematical process in which a search is activated that aims at a best value of an objective function that is optimal [65]. In general, an optimization algorithm has a specific objective function to be minimized while satisfying some predefined equality and inequality constraints.

The objective functions are formed based on a problem definition. In general, there are various features in a network that can be considered problems which can be optimized, for example: minimization of the total generating cost, reduction of active transmission losses, security and stability of the power system [66, 67]. Each of these problems can be define to form the objective function of an optimization algorithm. The standard form of the objective function is $F(x)$ where F is a scalar function and x is the vector of the design variables containing both state and control variables. The state variables describe any unique state of the power system, whereas the control variables can be modified to satisfy predefined conditions.

For any optimization problem, the equality constrains are expressed using the form $g(x) = 0$ where g is a function assumed to be continuous and at least twice differentiable [68]. The most common equality constraints for power systems refer to the nonlinear load flow equations. These constraint functions contain the limits for the state variables.

The inequality constraint function has the form $h(x) \leq 0$. Usually, these functions define some specific bounds such as: voltage levels at the CP in a network, transmission line flow limit, reactive power capabilities of inverters etc.

Therefore, the standard form of the optimization problem can be expressed as:

$$\min F(x) \tag{4.1}$$

Subject to:

$$g(x) = 0 \tag{4.2}$$

$$h(x) \leq 0 \tag{4.3}$$

4.1.2 Problem formulation process for the LV network

In this subchapter, the problem formulation process will be presented step by step based on [69]:

Step 1: Problem Statement

Maintain the voltage levels at all the CPs of the LV network between limits imposed by the German GC considering in the same time the optimization of the reactive power dispatch.

Step 2: Data and Information Collection

- the number of PV systems in the network is 18
- the considered CPs are beginning from the LV-side of the transformer and the total number is 19 (1 slack bus and 18 PQ buses)
- the influence of the transformer impedance is not taken into consideration (Figure 4-1)
- active power generation profile of all PV generators are predefined
- inverter capabilities in terms of active and reactive power are set
- parameters for cables are predefined

Step 3: Identification/Definition of the design variables

The state variables consist of the voltage magnitude $\left(V_i\right)$ and angle $\left(\delta_i\right)$ for each bus in the LV network. The reactive power references $\left(Q_i^{ref}\right)$ of all PV systems are defined as the control variables. Both set of variables have the following vector form:

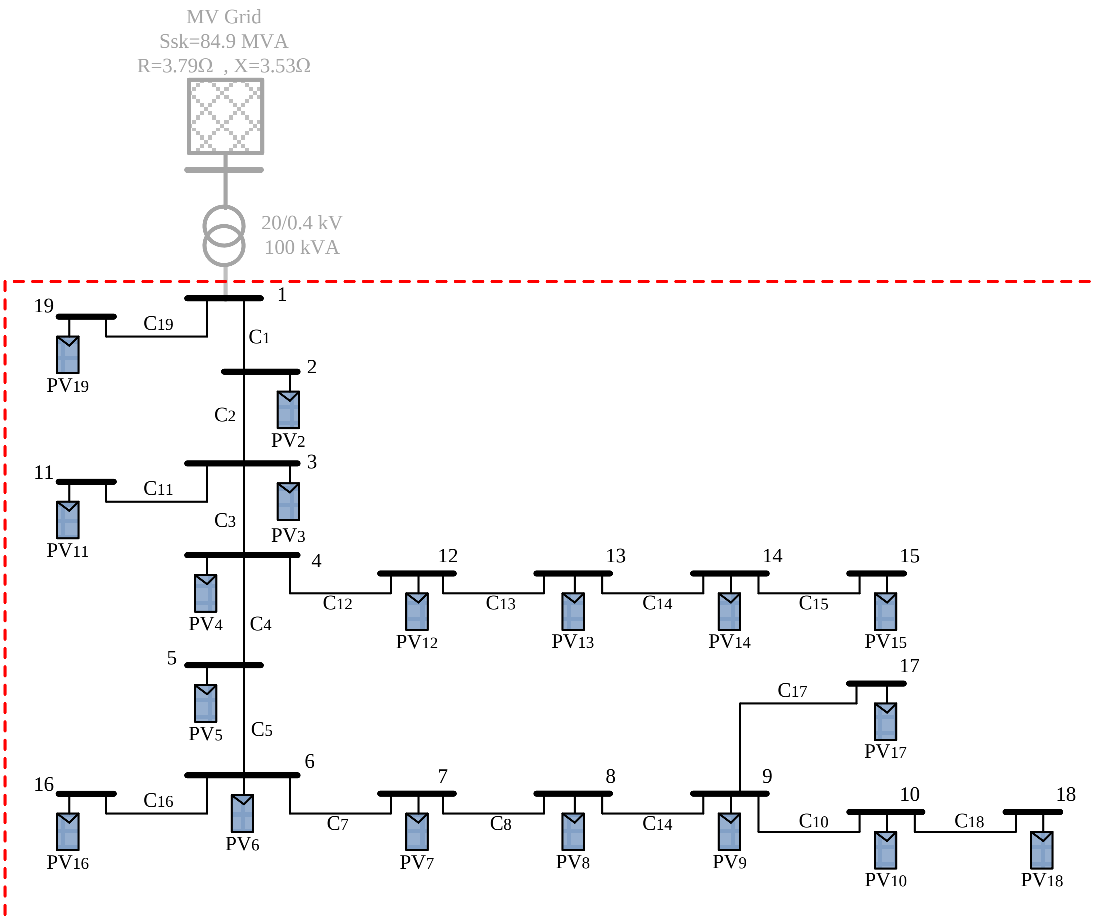

Figure 4-1 LV network under study with the area of interest highlighted

$$X_1 = [V_1, V_2, \ldots\ldots\ldots, V_{19}] \tag{4.4}$$

$$X_2 = [\delta_1, \delta_2, \ldots\ldots\ldots, \delta_{19}] \tag{4.5}$$

$$U = \left[Q_1^{ref}, Q_2^{ref}, \ldots\ldots\ldots, Q_{19}^{ref}\right] \tag{4.6}$$

The design variable vector contains all the variables of the system, therefore its form will be:

$$x_{opt} = \left[V_i, \delta_i, Q_i^{ref}\right] \quad where \ \ i = \overline{1:19} \tag{4.7}$$

Step 4: Identification of Criterion to be optimized

Using the problem statement defined in Step1, the objective function can be formulated as follows:

$$\min \ f(x) = \sum \left(Q_i^{ref}\right)^2 \ , \ i = \overline{2:19} \tag{4.8}$$

Step 5: Identification of Criterion to be optimized

Step 5.1: Identification of Equality Constraints

As stated before, the power flow equations are used as equality constraints:

$$g_1 = P_i^{ref} - V_i \sum_{j=1}^{19} V_j \left(G_{ij} \cos\theta_{ij} + B_{ij} \sin\theta_{ij} \right) = 0 \quad , \; i = \overline{2:19} \tag{4.9}$$

$$g_2 = Q_i^{ref} - V_i \sum_{j=1}^{19} V_j \left(G_{ij} \sin\theta_{ij} - B_{ij} \cos\theta_{ij} \right) = 0 \quad , \; i = \overline{2:19} \tag{4.10}$$

Where V_i, V_j are the voltages at i and j buses, $i = \overline{2:19}$, $j = \overline{1:19}$. P_i^{ref}, Q_i^{ref} are the active and reactive power injected at bus i. G_{ij}, B_{ij} are the conductance and susceptance between bus i and j and θ_{ij} is the voltage angle difference between bus i and j.

The equality constraint for the slack bus refers to the reactive power reference, voltage magnitude and angle:

$$\begin{cases} Q_1^{ref} = 0 \\ V_1 = 1\, p.u. \\ \delta_1 = 0 \end{cases} \Rightarrow \quad g_3 = \begin{cases} Q_1^{ref} = 0 \\ V_1 - 1 = 0 \\ \delta_1 = 0 \end{cases} \tag{4.11}$$

Step 5.2: Identification of Inequality Constraints

First inequality constraint expresses the limits for voltage magnitude for all PQ buses in the network:

$$0.97\, p.u. \le V_i \le 1.03\, p.u. \quad \Rightarrow \quad h_1 = \begin{cases} 0.97 - V_i \le 0 \\ V_i - 1.03 \le 0 \end{cases} \quad , \; i = \overline{2,19} \tag{4.12}$$

Moreover, the reactive power capabilities of the PV inverters are limited:

$$\left(P_i^{ref}\right)^2 + \left(Q_i^{ref}\right)^2 \le S_i^2 \quad \Rightarrow \quad h_2 = \left(P_i^{ref}\right)^2 + \left(Q_i^{ref}\right)^2 - S_i^2 \le 0 \;\; , \; i = \overline{2,19} \tag{4.13}$$

It should be mentioned that a minimization of line losses is also achieved with the load flow equations taken as constraints and the use of *fmincon* function.

Step 6: Initial Conditions

The initial condition for voltage magnitude and angle are the output values of the first load flow performed for the LV network and zero for the reactive power references.

$$x_{init} = \left[V_{i_{load\_flow}}, \delta_{i_{load\_flow}}, Q_{i_{init}}^{ref} \right] \quad where \;\; Q_{i_{init}}^{ref} = 0 \; , \; i = \overline{1:19} \tag{4.14}$$

4.2 Implementation of optimized Q(U) method

The flow chart presented in Figure 4-2 describes the implementation of the optimized Q(U) strategy.

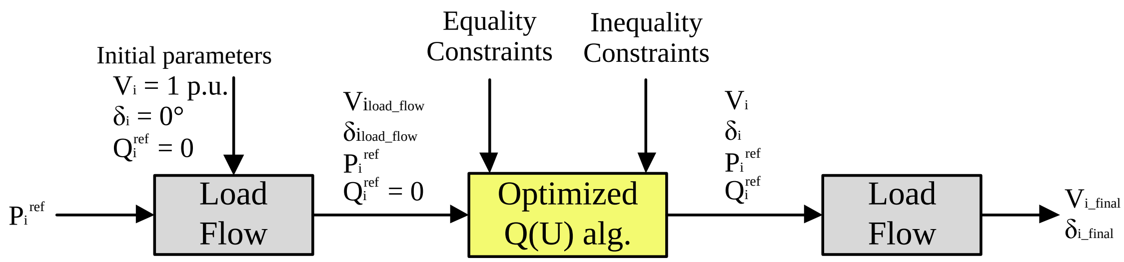

Figure 4-2 Flow chart with the implementation of the optimized Q(U) method

The first step consists of performing a load flow analysis with the *flat start* conditions for voltage magnitude $\left(V_i = 1p.u. \right)$ and angle $\left(\delta_i = 0^\circ \right)$, the set active power generation P_i^{ref} and $Q_i^{ref} = 0$. Afterwards, the optimized Q(U) algorithm takes as reference the output values of the load flow for voltage magnitude and angle. Considering also the equality and inequality constrains, a feasible solution will be obtained for the defined objective function. The output values of the algorithm will be given as reference to the inverters and another load flow analysis will be performed in order to check if the voltage is maintained between limits.

The source code developed using MATLAB to implement the optimized Q(U) method along with a comparison between the DigSILENT and MATLAB load flow results (voltage and angle) can be found in Appendix F.

4.3 Study case results

Further on, the simulation results of the optimized Q(U) strategy will be presented and compared with the results obtained when Q(U) method was analyzed on the LV network.

In Figure 4-3a) the voltage profile and power levels of the closest system to the transformer (PV19) is shown. In Figure 4-3b), the generation profile of the PV19 generator is presented together with the levels of reactive power consumed using both regulation methods. The voltage profile when using the optimized Q(U) method is similar to the one when no regulation methods are applied because the influence of the transformer was not considered when the algorithm was designed. Only very small amounts of reactive power are absorbed in this case because the PV19 system tries to take part in the regulation process, but the distance between this system and the first one which experience voltage rise above the limit at the CP is the highest.

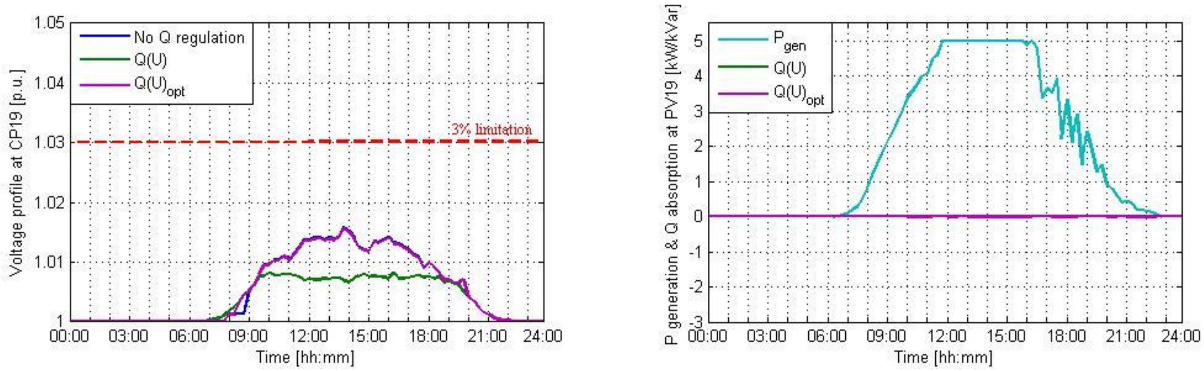

a) b)

Figure 4-3 PV19 system analysis a) Voltage levels with and without regulation methods b) Active power generation and reactive power consumed using regulation methods

Similar results are shown in Figure 4-4 for PV2 system compared with PV19 system because the difference between them is the length of the cables. PV19 system is connected directly to the rest of the system, therefore it takes part in the regulation process with slightly higher amounts of reactive power absorption compared with the previous system, but they are still low compared to the other systems.

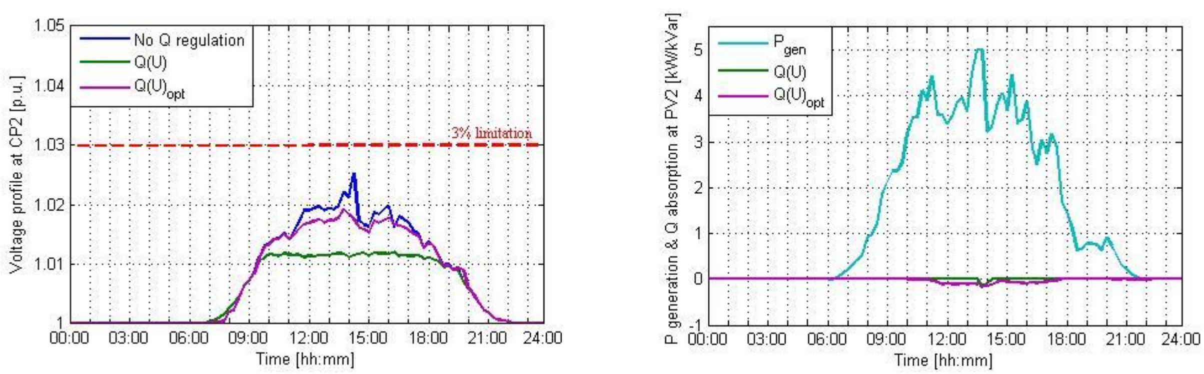

a) b)

Figure 4-4 PV2 system analysis a) Voltage levels with and without regulation methods b) Active power generation and reactive power consumed using regulation methods

In order to see the improvements brought by the optimized Q(U) algorithm the systems located at the end of the main feeder and the two sub-feeders will be presented further on.

Figure 4-5 describes the simulation results for the PV system located at the end of the main feeder – PV16. Although there is a difference between the voltages after performing the regulation strategies, both perform successfully the regulation process, but the reactive power amount absorbed with the optimized Q(U) algorithm is lower than using Q(U).

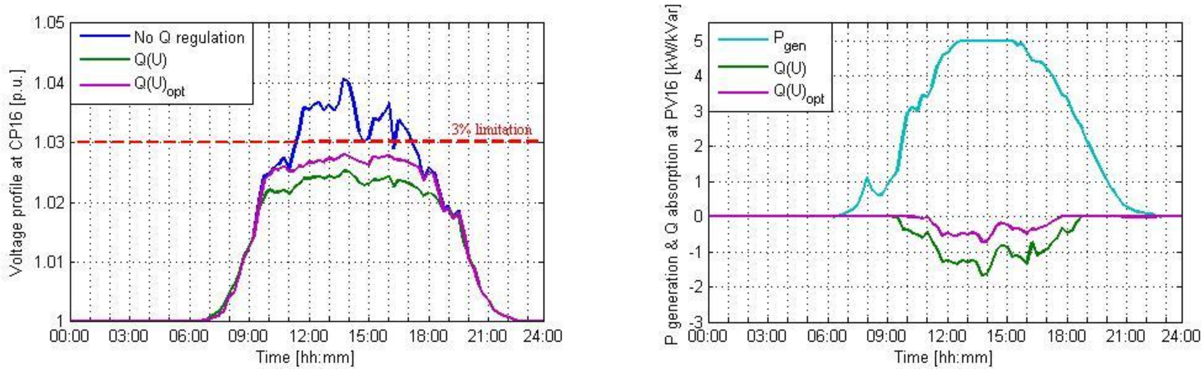

a) b)

Figure 4-5 PV16 system analysis a) Voltage levels with and without regulation methods b) Active power generation and reactive power consumed using regulation methods

The analysis of the simulation results continue with the PV systems located at the end of the two sub-feeders - PV15 and PV18 (Figure 4-6 and Figure 4-7).

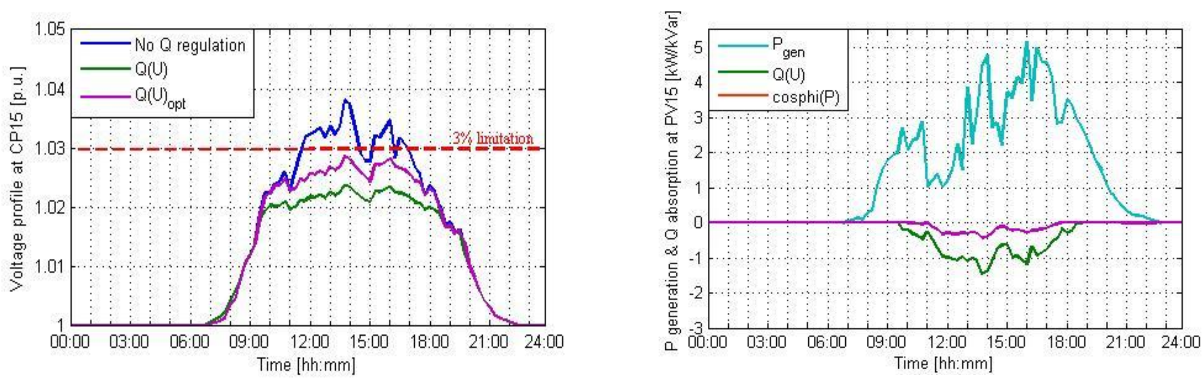

a) b)

Figure 4-6 PV15 system analysis a) Voltage levels with and without regulation methods b) Active power generation and reactive power consumed using regulation methods

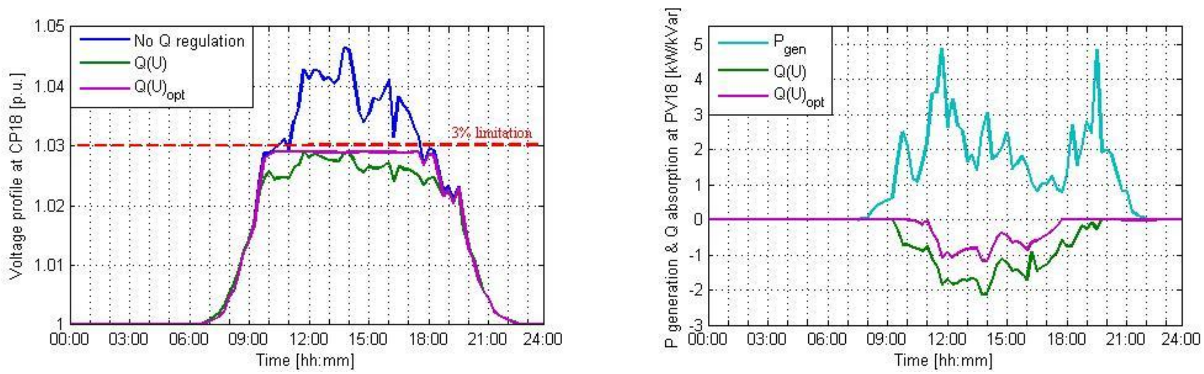

a) b)

Figure 4-7 PV18 system analysis a) Voltage levels with and without regulation methods b) Active power generation and reactive power consumed using regulation methods

It can be noticed that the Q(U) algorithm absorbs unnecessary amounts of reactive power to perform the voltage regulation process. Lower levels of reactive power are possible when using the optimized Q(U) algorithm because these references are calculated based on the information gathered from all the PV systems in the network and it also considers the impedance of the cables between them.

The limitation of the voltage profile from Figure 4-7a) when using the optimized Q(U) method is performed by the inequality constraint (h_1) which is also responsible for keeping the voltage at a constant value of 1.029 p.u. between 10:00 and 18:00.

Figure 4-8 presents the total active power losses before and after performing the Q(U) optimized algorithm.

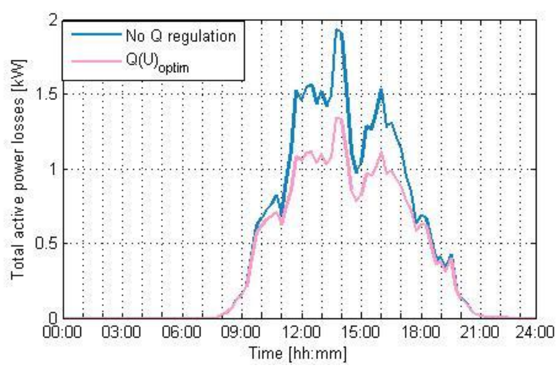

Figure 4-8 Total active power losses in the network

Besides the optimization of the reactive power reference, the proposed algorithm presents the benefit of minimizing the line losses. This is achieved because the optimization algorithm uses the load flow equations as equality constraints and performs the balancing of the power transfer in the network.

Due to the fact that the optimized Q(U) method is absorbing less reactive power than the Q(U) method, it can be stated that the transformer does not exceed the 100% loading in this case also. In addition, the optimized Q(U) method presents the advantage of less stressing the transformer.

4.4 Discussions

The best candidate from the regulation strategies proposed by the German GC, Q(U) was compared with the optimized algorithm. Their performance was evaluated based on their ability to maintain the voltage within limits and to minimize the reactive power absorption.

The main difference between the two strategies is the fact that while for the first one, each PV inverter absorbs a calculated value of reactive power corresponding to its local voltage magnitude, for the second strategy, the amount of reactive power values are computed based on all the PCC voltages of the network. In consequence, the optimized Q(U) algorithm makes the LV network more flexible in terms of connecting more PV systems.

Even though the voltage levels using the optimized Q(U) method are higher, but within limits compared to the voltage using the Q(U) algorithm, the benefit of the optimized method is the minimization of the reactive power absorption while the PV generators maintain their operation in MPPT.

Other benefits of the optimized Q(U) method over the classical Q(U) are the minimization of the line losses and lower transformer loading.

Both methods were implemented on a LV network and analyzed from different points of view. All the results and discussions conclude that the optimized Q(U) algorithm has improved the classical Q(U) method proposed by the new German GC VDE-AR-N 4105.

Chapter 5 Voltage regulation strategies using the communication concept

The chapter presents the analysis of the standards series IEC 61850 together with its experimental validation. In the beginning, an overview of how the standard is structured and a general description of the information model are given. Further on, the experimental setup and the methodology of implementation are presented along with the results.

5.1 Analysis of the IEC 61850 standard

5.1.1 Introduction

The massive integration of renewable energy into the utility grid lead to the necessity of developing modern electricity systems. The new technology based on real-time information exchange, also known as “Smart Grid Concept” aims to optimize the energy power supply and demand by taking advantage of the computing and communication concept. This big task implies changes in the control algorithms and a new configuration of the network which allows two-way data information exchange thus resulting in a well-organized DG integration without affecting the power flow efficiency [70].

One of the biggest challenges to overcome in the development of smart grid systems was the interoperability between intelligent electronic devices (IEDs). Power system equipments which incorporate microprocessor-based controllers such as circuit breakers, transformers, converters, capacitor banks etc. and can exchange information are defined as IEDs. Very often, devices of different manufactures couldn’t interoperate due to compatibility issues and missing communication standard, and therefore the task of implementing a communication system became difficult and complicate. In order to overcome the limitations stated above, the working groups of the Technical Committee 57 of IEC (IEC TC57) issued a new standard IEC 61850 which regulates the communication in substations and defines a common information exchange protocol between interconnected IEDs. In this way, the Smart Grid technology along with its automation and control functions can be integrated into power systems, resulting in benefits for the grid operator [71].

In electric power systems, the management of information and protection functions is done into substations (known as nodes) which include transformers, switching and protection devices. It is the place where the lines and cables are connected for transmission and distribution of electric power. In a substation automation system (SAS) the information can be accessed over the network (eg. TCP/IP) and in consequence the human intervention can be reduced to minimum. The modeling approach is to create a model which comprises all the components defined as IEDs and their functions, by including also the form of communication allowed by the system [72, 73].

5.1.2 Overview and Scope of IEC 61850

The IEC 61850 standard series named "Communication networks and systems in substations" comprises in total 10 major sections, which cover different aspects of the substation communication network. In Figure 5-1, the modeling and implementation methods applied in the parts of the standard are exposed [74].

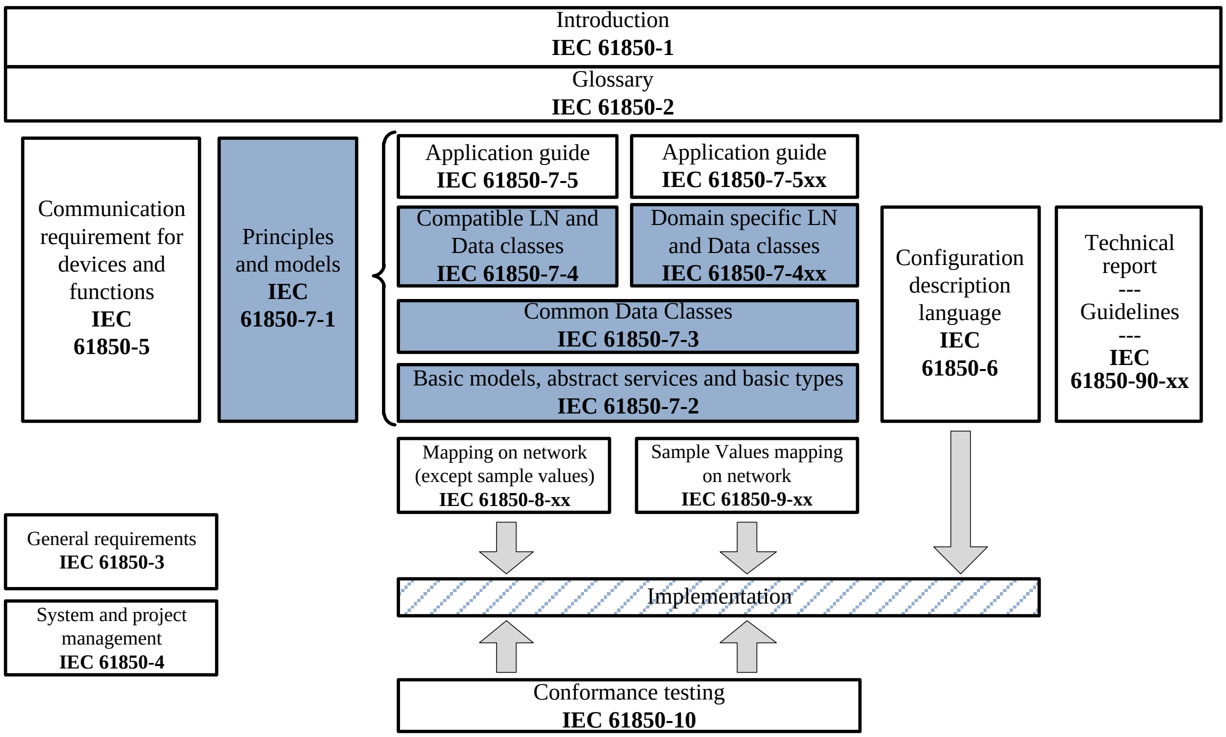

Figure 5-1 Relations between modeling and mapping parts of the IEC 61850 series [74]

The parts 1 and 2 are meant to provide an introduction to the standard series IEC 61850 and contain also the glossary of terms used along with definitions regarding the power utility automation systems context. The general requirements for communication in substations are presented in part 3, with the focus on quality requirements, environmental conditions and auxiliary services. The specific functional communication requirements are described in the 4th and 5th part where all known functions are identified and described in detail. In part 6, the system configuration language (SCL) used by the IEDs to communicate is explained, allowing devices of different manufactures to exchange information in a compatible way [74]. The most important part of the IEC 61850 standard which will be focused in this report is contained by the 7-xx series named "Basic communication structure for substation and feeder equipment".

- **IEC61850-7-1** Principles and models

This part scope is to provide an introduction to the modeling methods, communication principles and information models used in the 7-xx series. Information is given regarding the dependency of this part with the requirements from IEC 61850-5 [74].

- **IEC61850-7-2** Abstract communication service interface (ACSI)

The abstract services definitions are found in this section together with the methodology of client-server communication. The modeling process of IEDs such as information model and exchange are possible by accessing the pre-defined functions [75].

- **IEC61850-7-3** Common data classes

The part 7-3 describes the common data classes (CDCs) such as status information, measured and controllable status information, controllable analogue set point information, status and analogue settings and the common attribute types associated with the substation modeling [76].

- **IEC61850-7-4** Compatible logical node classes and data classes

The information model and functions of the real devices used in substation applications are specified in this part. The logical nodes (LNs) name and data object necessary for developing communication between IEDs are described in particular depending on their class of origin [77].

- **IEC61850-7-420** Distributed energy resources (DER) logical nodes

The part 7-420 describes the LNs specific for DER but which have also applicability to central-station generation units as PVs or fuel cells [78].

In the section 8.1 of the standard, the procedure of mapping the abstract data object and services defined in parts 7-2, 7-3 and 7-4 into the MMS (Manufacturing Messaging Specification) is described [79]. In the part 9-2 the service communication mapping (SCM) which is necessary for the transmission of sample values is specified, while in section 10 the conformance testing methods of devices and engineering tools are defined [74, 80].

5.1.3 Data Model

In IEC 61850 standard, the data model is generated by using the concept of virtualization. This means that only the relevant details of a real device are defined in order to exchange information with other devices. The data model decomposes the application functions of a real device into the smallest possible entities named logical nodes [81]. The information of the physical devices is configured inside the ICD file by using the standardized XML language format according to the rules of IEC 61850.

An example of data model structure in IEC 61850 is depicted in Figure 5-2.

Physical Device (IED)

The top tree structure of the data model is represented by the physical device (PD) which is also defined as server. An electrical network can contain one or several IEDs which have the capability to connect to exchange information by using a unique IP Address [74].

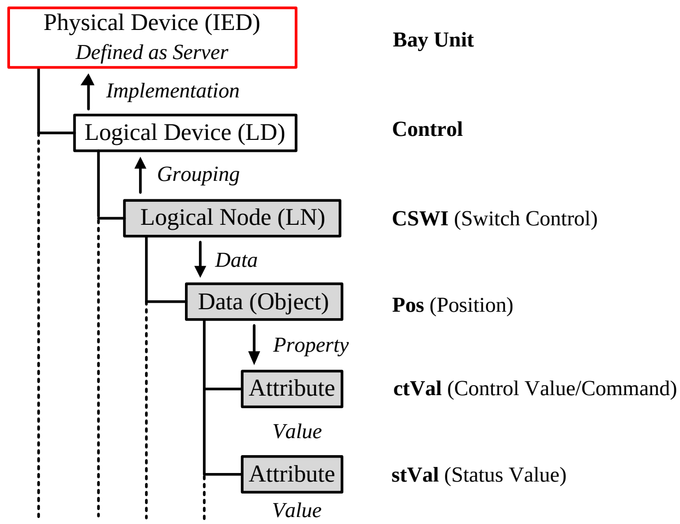

Figure 5-2 The object model of IEC 61850 [71]

Logical Device (LD)

The logical device (LD) inside the server is defined as the main entity of the data model. It contains a group of LNs depending on the functions required by the particular device from the network. It is important to know that an IED contains only one LD and it does not include LNs from other devices. Also it is mandatory that each device contains at least three logical nodes as it is shown in Figure 5-3 where the relationship between the common LNs is exposed [74].

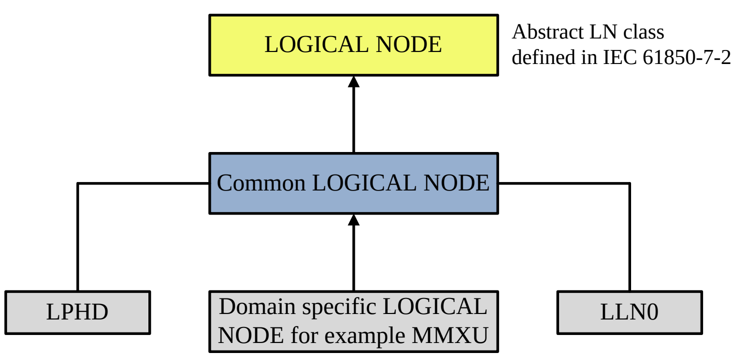

Figure 5-3 LOGICAL NODE relationship [77]

Logical Node (LN)

The logical node (LN) represents a combination of data and services related to a particular function within an IED. As it was previous mentioned, at least three LNs must be contained in a LD, such as LPHD, LLN0 and a domain specific LN (e.g. MMXU). The LLN0 contains the common information for the logical device as "health, mode, beh and NamePlt" while the LPHD represents the common information related to the physical device [74].

The information contained inside the logical nodes can be structured as depicted in Figure 5-4. The data attributes (DAs) and data object (DO) represent the semantic of the LN and can contain up to 100 individual information (points) structured in a hierarchical structure [82].

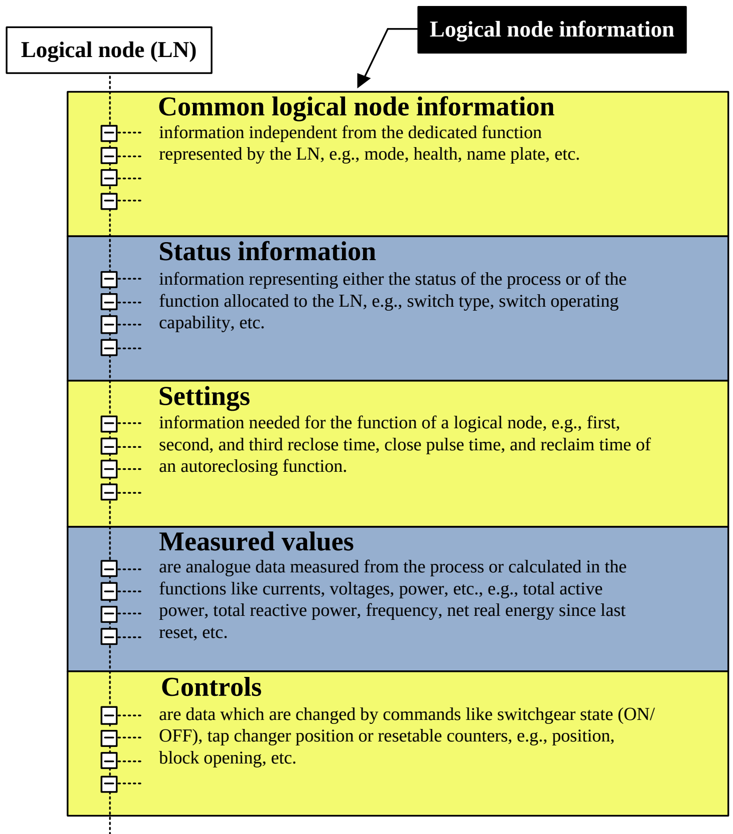

Figure 5-4 LOGICAL NODE information categories [77]

The standard comprises in total over 100 LNs structured into 19 groups, depending on their functionality and are described in detail in part 7-4 [77]. In order to provide further information of how a logical node is modeled, the voltage to ground phase A measurement value from the Metering and Measurement group (LN MMXU) is shown in Table 5-1.

Table 5-1 Example of types: The logical node MMXU. The recursive structure of types DATA and data attributes is illustrated

Object Reference	**Type**	**Remark**
MMXU1	LN	Measurement LN
MMXU1.PhV	DATA	Phase to ground voltages
MMXU1.PhV.phsA	DATA	Value of Phase A
MMXU1.PhV.phsA.cVal	DataAttribute	Complex Value
MMXU1.PhV.phsA.cVal.mag	DataAttribute	Magnitude of complex number
MMXU1.PhV.phsA.cVal.mag.f	DataAttribute	Floating point number

The DATA class represents the information contained by a LN and which is intended to be accessed in the real device. The information can be represented by currents, voltages, power, temperatures, status, quality, timestamps etc. In Figure 5-5 the anatomy of an object name is presented using the example of logical node MMXU. The PD and LD can take any name in the IEC 61850 world, while the other parts as LNs, DOs and DAs are predefined names in the standard.

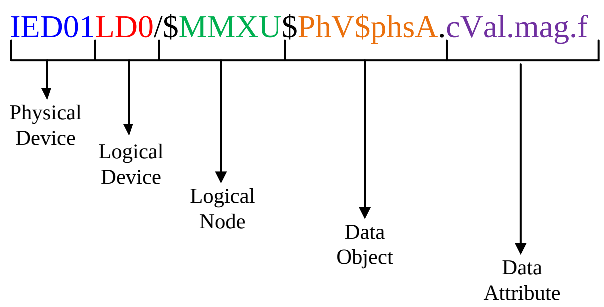

Figure 5-5 The anatomy of an object name according to IEC 61850-8-1 [79]

5.1.4 Services model

After the information has been specified by means of LNs, DAs and service parameters, the data has to be transmitted over the communication network from the IEDs towards the control center or between interconnected devices. The information exchange is defined by the services categorized in part 7-2 of the IEC 61850 which are presented in Figure 5-6 [75].

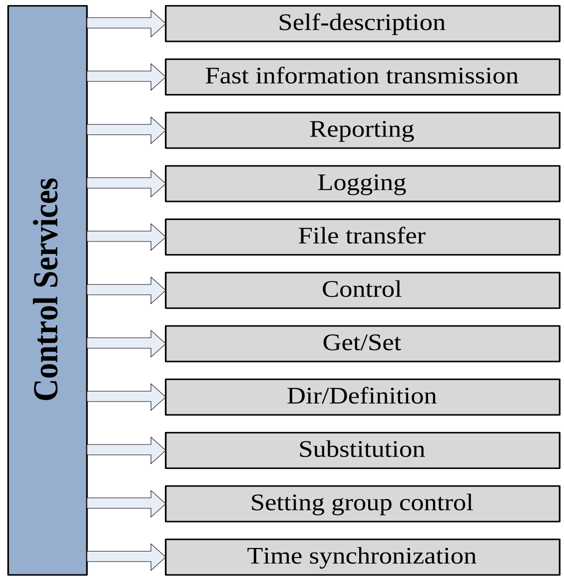

Figure 5-6 Control services provided by IEC 61850-7-2 [74, 83]

1) Self-description – the client is using this service to access the hierarchy of the information model and its subclasses, by using the command GetDirectory.

2) Peer-to-peer information exchange provided by:
   - Generic Object Oriented Substation Events (GOOSE) – transmission of information regarding the status of the devices (e.g. start, stop, trip, etc.)
   - Sample Value (SV) – uses the publisher-subscriber mechanism for fast transmission of multicast synchronized sample values (the data is written into the transmission buffer and its being accessed by the receiving side).
3) Reporting – it contains two report data classes such as buffered-report-control-block (BRCB) and unbuffered-report-control-block (URCB). Ensures the report of the data object values from the logical node to client within a specific configured time.
4) Logging – it is used to store the events occurred and gives the possibility to access them at any time from the internal storage.
5) File transfer – for configuration, disturbance recording or historical data
6) Control – controls the state of internal and external processes by a client. Applies to CDCs and DAs which have enabled this function.
7) Data-Set – Retrieve / Write/ Create/ Delete the data object set values.
8) Dir/Definition – to access the directory information and its data definition
9) Substitution – allow to overwrite manually the value of a DA by using the substitution associated DAs "subEna" and "subVal". In case of reporting, the new value will be transmitted and not the original one.
10) Setting group control –allows a DATA Instance to take multiple values which are used one at a time.
11) Time/Time synchronization – provides accurate synchronization to applications in the server and client substation IEDs.

The services are described in an abstract way, meaning that only the information that is required to perform a desired action will be outlined.

5.1.5 Server /Client architecture

The purpose of a server/client application is to exchange real time information within the electrical network between the interconnected IEDs. The information travels from the server (IED) towards client (Controller) which performs the calculations based on the information received. The data is then transmitted back to the server which execute the desired operations (for e.g. Active/Reactive power new references, Measurements, Start/Stop, Reset etc.). It should be mentioned that after the server transmits the information, its exchange capabilities remain blocked until the further reply from the client.

In Figure 5-7, the configuration of a client-server application is illustrated, by using the Application Programming Interface (API) offered by SystemCorp [84]. The TCP/IP protocol together with the Data Report Service is used to broadcast the information between client and server within the power utility network.

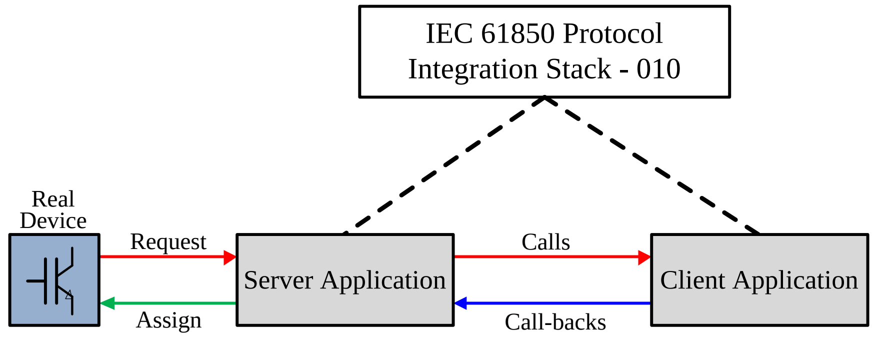

Figure 5-7 Mapping of the Server/Client application to IEC 61850 [84, 85]

. The integration of a client/server application is possible by making use of the Protocol Integration Stack (PIS) which includes separately the IED capability description (ICD), containing the individual data and services that are modeled in a device. The file contains also the LNs field addresses and unique TCP/IP and MAC address required for the information exchange. The data is accessed between client and server using the special Call and Call-back functions also defined in the Protocol Stack [84, 85]. The general steps in the configuration of server/client required to exchange real time information are shown in Figure 5-8.

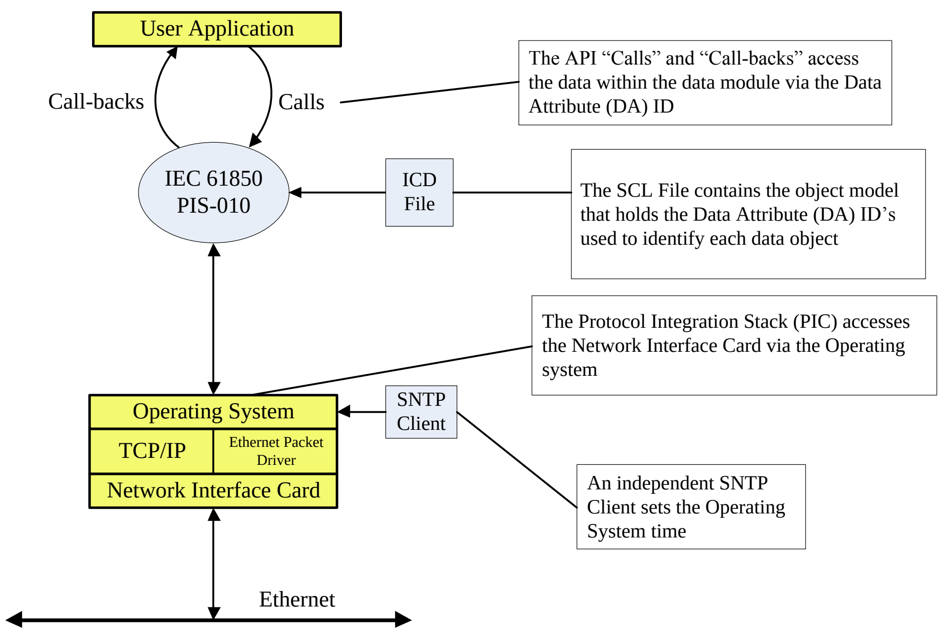

Figure 5-8 Context diagram [84]

In Figure 5-9 the functions used in the client/server application are illustrated, as presented as they have been used in the modeling process of the application.

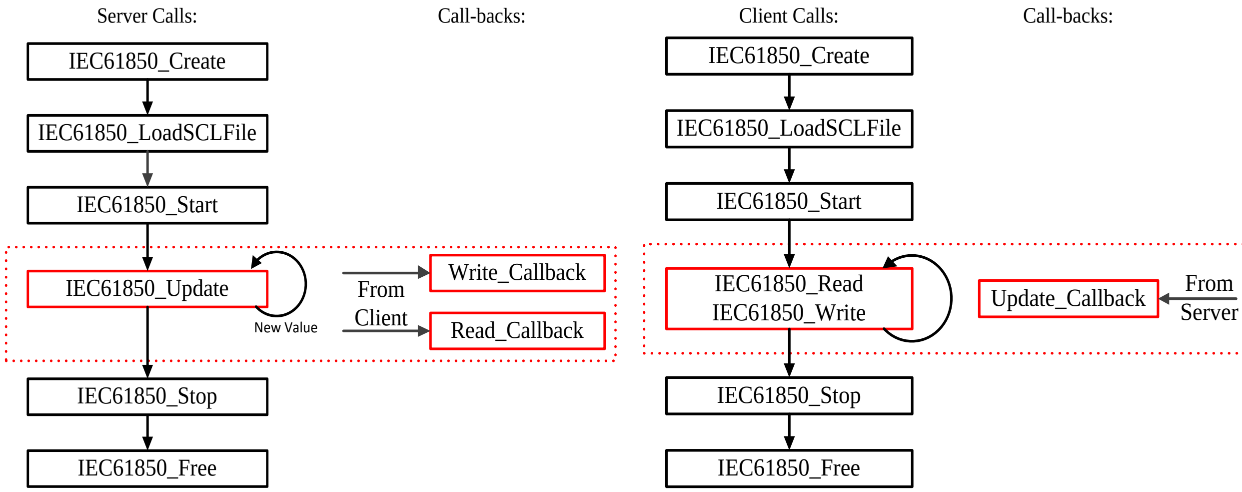

Figure 5-9 Server/client management – API functions [84, 86]

Common functions for client and server application [84]:

- IEC61850_Create – create a new IEC 61850 object as client or server
- IEC61850_LoadSCLFile – load the configured ICD file into the IEC 61850 application
- IEC61850_Start – start the IEC 61850 console application
- IEC61850_Stop – stop the IEC 61850 console application
- IEC61850_Free – free the memory used by IEC 61850 object

The specific functions of the Server are [84]:

- IEC61850_Update – used to send the information to the client
- IEC61850_ReadCallback – used to read the information from the client
- IEC61850_WriteCallback – used to write the information from the client

The specific functions of the Client are [84]:

- IEC61850_UpdateCallback – used to receive the information from the server
- IEC61850_Read – used to send readable information to the Server
- IEC61850_Write – used to send writable information to the Server

By using the above described functions, the client and server source codes can be developed.

5.2 Modeling of the IEC 61850 concept

In this section, the modeling method of the IEC 61850 standard is presented with the main focus on the development of the client/server application. The objective is to create a bi-directional data communication between a server (IED) and a client for the exchange of critical information. The IED is represented by a grid connected three-phase PV inverter and the data exchange consists of measurements (grid current, grid voltage, active and reactive power) and power references (active and reactive power). The chosen tool used to create the ICD configuration file of the server and client is ICD Designer provided by company SystemCORP [85].

The IEC 61850 user application is composed by two consoles which are running separately on the IED computer and respectively client computer and the information inside the LN is accessed via the Ethernet protocol and exchanged using the Report service. The C script code of the IEC 61850 application is written in the software Visual Studio 2010 and can be found in Appendix G.

5.2.1 Server/Client Configuration

In order to build the ICD file required for every IED inside the substation, the functions contained by the LNs which are going to be used have to be identified first. The server application contains the following functions:

- DC Voltage and Current Measurement
- AC Voltage and Current Measurement
- Active and Reactive Power References
- Inverter Start/Stop and Trip (implemented locally only in the server)

Figure 5-10 presents the hierarchical structure of the server ICD file. The configuration contains two main sub headers such as "Communication" where the IP Addresses, Gateway and SubnetMask are included for every particular device connected, and "IED" subheader which comprises the LNs with their specific functionality.

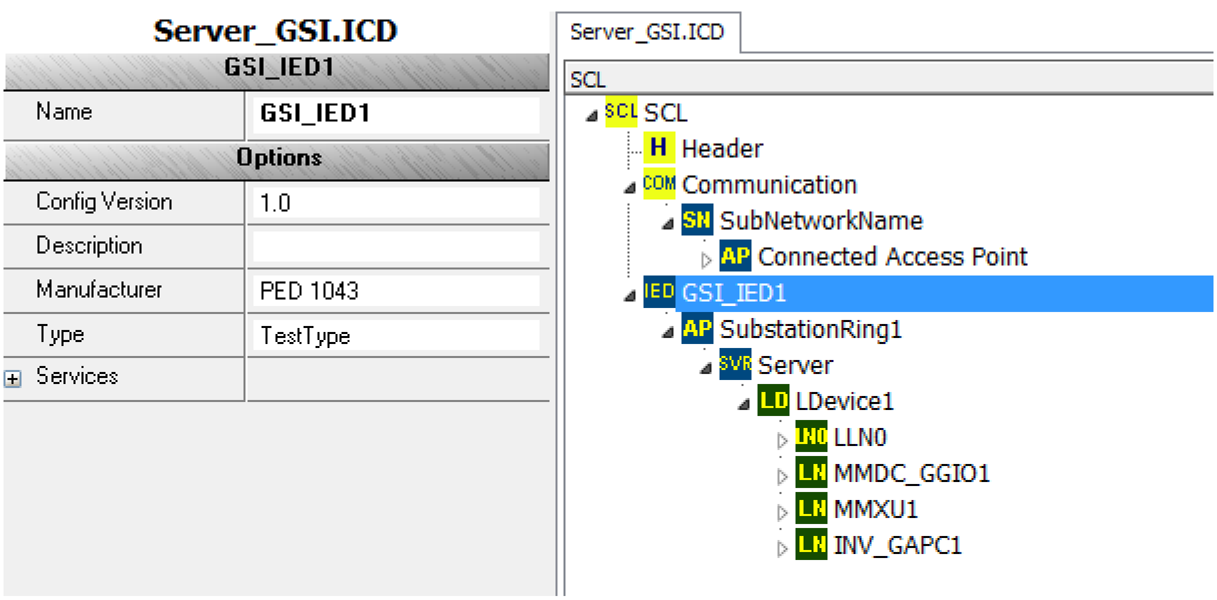

Figure 5-10 Server configuration file hierarchical structure [84]

Further on, each function corresponding LN will be briefly explained. One of the limitations encountered is represented by the fact that not all the LNs are provided by the ICD

Designer software. In consequence, other LNs with similar functionality have been chosen from the standard [77, 84].

The GGIO LN belongs to the group G (Logical nodes for generic references) and shall be used for modeling of functions without a dedicated node. Given the fact that the LN MMDC is not available, it can be successfully replaced with GGIO which will handle the DC voltage and current measurements. The DO values are analog inputs (AnIn) from the CDC "measured and metered values" [77].

The MMXU belongs to the LN group M which is dedicated for measurements and metering in three phase systems. The chosen DOs that are going to be used are the phase voltage represented by "PhV" and the phase current represented by "A".

The ZINV LN offers the functionality of controlling the active and reactive power references by means of DOs within ASG CDC. Again due to software limitations, the LN was replaced with a generic automatic process control (GAPC) LN which has the same functionality. The other functions as Start, Stop and Reset are implemented locally meaning that their status will not be sent to the client.

The LNs specific semantic together with their field addresses are presented in Table 5-2.

Table 5-2 LNs semantic and field addresses used in the Server configuration

Object Reference	**Type**	**Field Address**
LDevice1/GGIOMXAnIn1$mag.f/Val/SystemCorpGeneric	DC Voltage Measurement	1-2-1
LDevice1/GGIOMXAnIn2$mag.f/Val/SystemCorpGeneric	DC Current Measurement	1-3-1
LDevice1/MMXUMXPhV$phsA/mag.f/Val/SystemCorpGeneric	Phase A Voltage Measurement	1-4-1
LDevice1/MMXUMXA$phsA/mag.f/Val/SystemCorpGeneric	Phase A Current Measurement	1-5-1
LDevice1/GAPC $StrVal1$setMag.f/Val/SystemCorpGeneric	Inverter Active Power Reference	1-6-1
LDevice1/GAPC $StrVal4 $setMag.f/Val/SystemCorpGeneric	Inverter Reactive Power Reference	1-7-1

Similar with the Server configuration file, the hierarchically structure of the Client is presented in Figure 5-11. The Communication sub header includes all the addresses of the connected devices (IEDs) and the client application individual IP Address.

The IED sub header includes all the devices which are intended to exchange information with the client application and whose LNs and field addresses must be identical. Two similar IEDs were added to the file in order to experimentally test the IEC 61850, which will be later presented in subchapter 5.3.

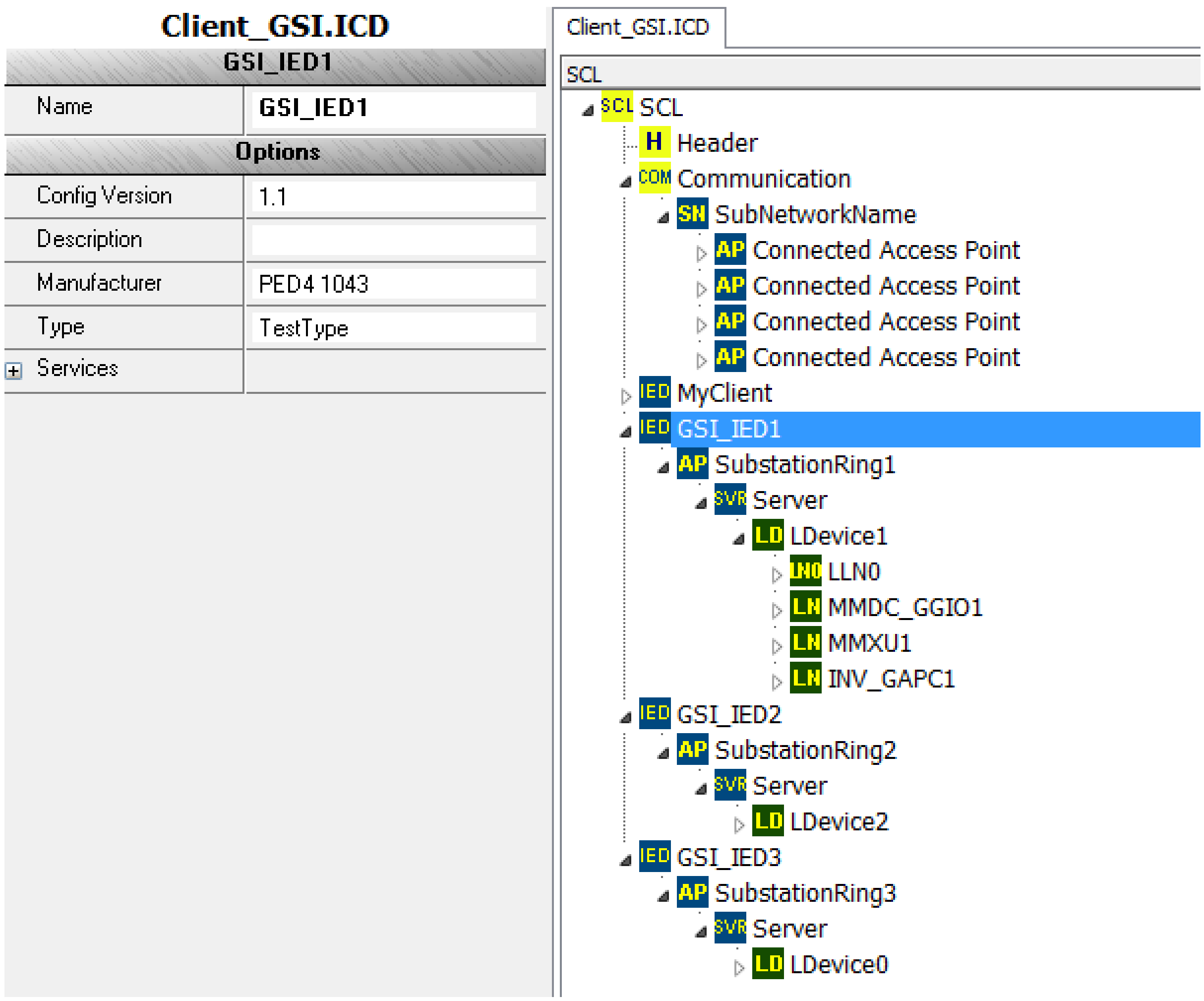

Figure 5-11 Client configuration file hierarchical structure [84]

5.2.2 Validation

In order to validate the IEC 61850 client/server application previously explained, a script code has been developed using the API library provided by SystemCorp. The script flowchart for client/server application is shown in Figure 5-12.

The server and client console applications are running separately on different computers and exchange information using the Ethernet protocol and the Get/Set functions from the report services. The application is loading first the DLL functions contained by the PIS10 library where the services are defined, and which are different for both client and server. Afterwards, the preconfigured ICD files containing the data (LDs, LNs and DOs), IP Addresses and activated report services are imported. The server is reading the grid voltage magnitude and if the value is within the prescribed limits ($0.85 \cdot Vg - 1.15 \cdot Vg$), then it is transmitted to the client. The data is accessed by the receiving end (client) which calculates the reactive power reference using the droop function of the Q(U) method presented in Chapter 3. After calculation, the reference is returned to the server and then the cycle repeats until the number of iteration has been reached. After every function that has been not successfully executed in the script, a failure message will prompt on the console informing the user that an error occurred. The errors list is also provided by the SystemCorp API Library and can be found in [84].

An important aspect is represented by the fact that the Callback functions (Update and Write) used to access the information from the dispatcher are updating permanently and are not limited by the iteration number.

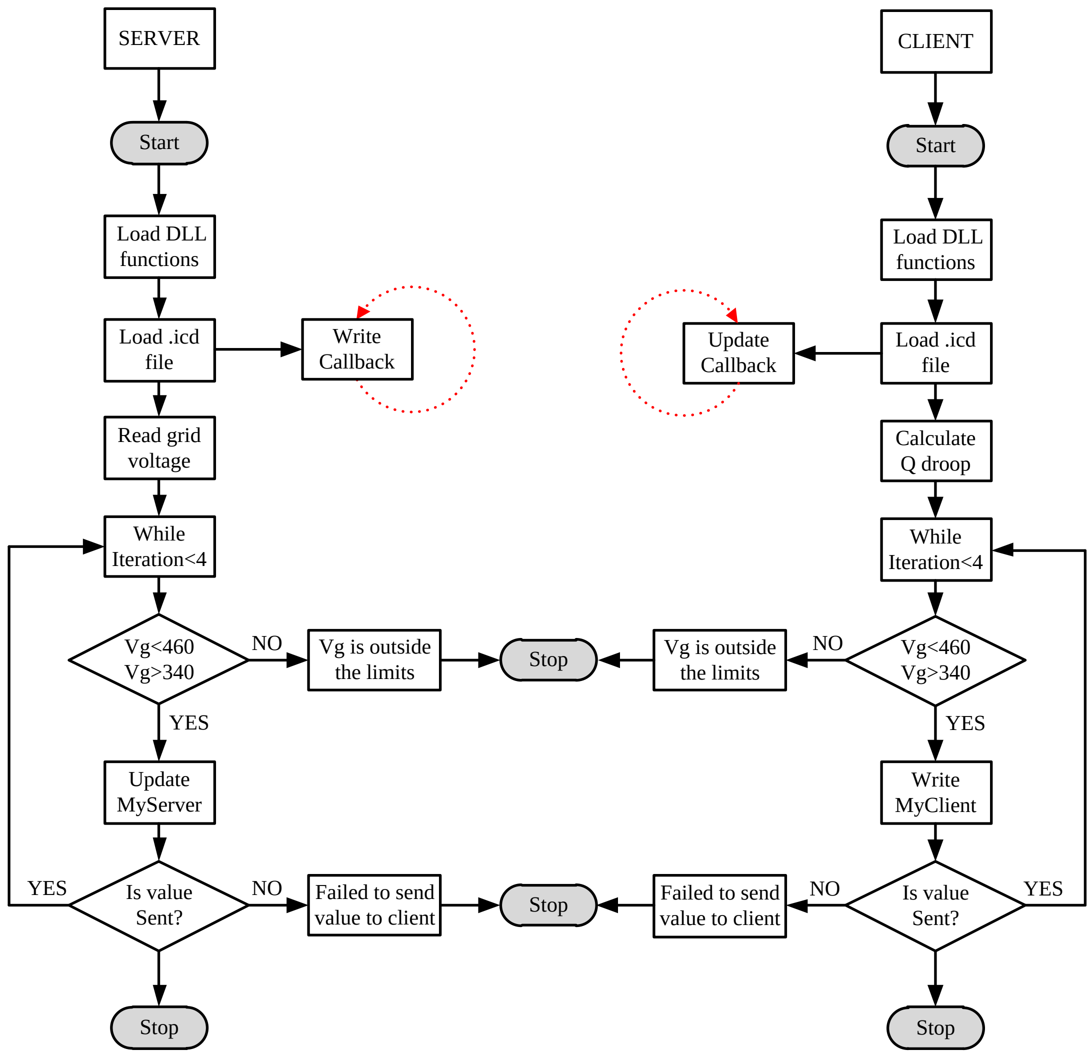

Figure 5-12 Flow chart of the client/server application

The server and client console applications are presented in Figure 5-13, and illustrate the status of the data received and sent by the client respectively server. The main purpose of the validation console is to check that the bi-directional information is transmitted in real-time and can be successfully experimental validated, as it will be later demonstrated in subchapter 5.3.

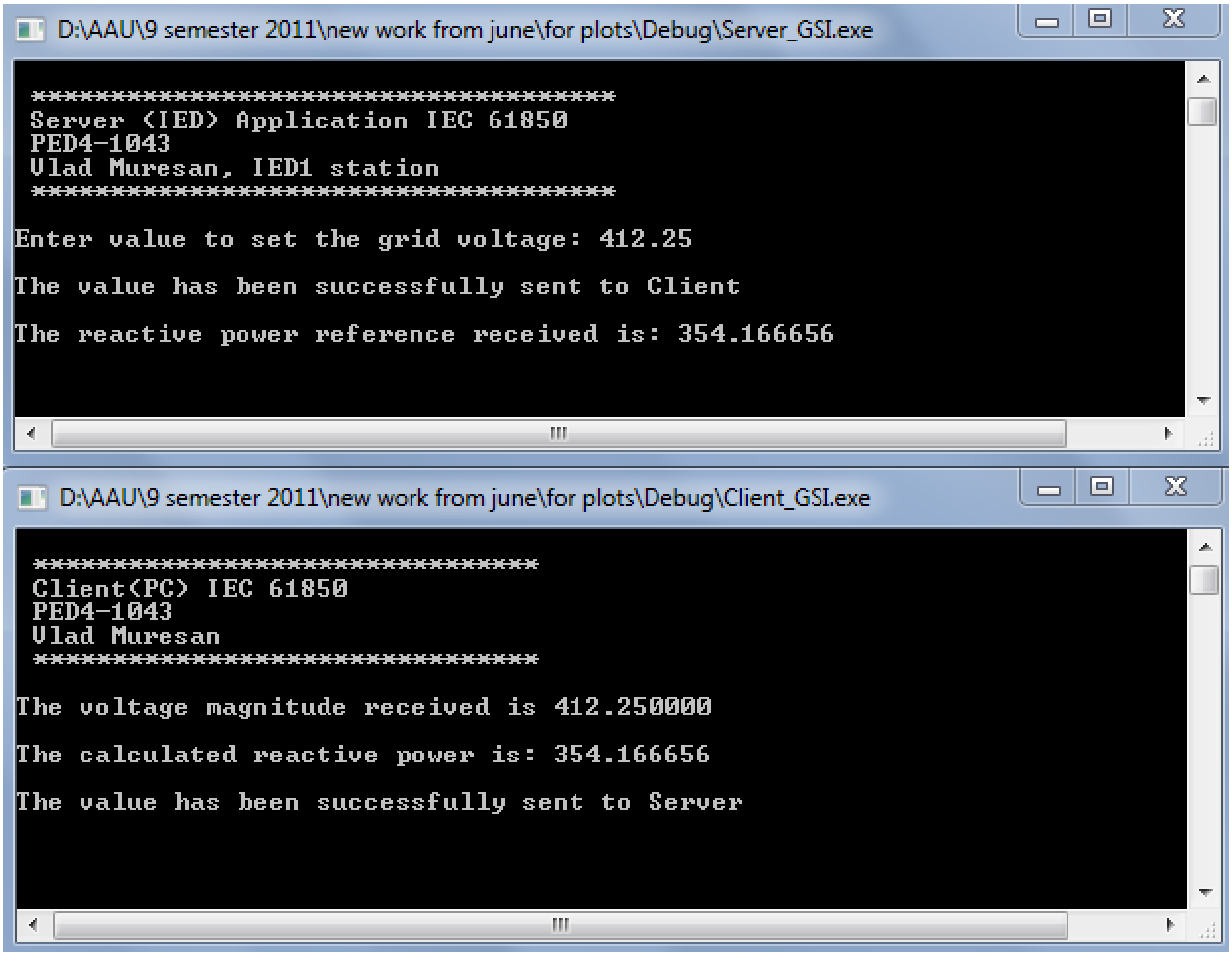

Figure 5-13 Client/Server application console for the validation of IEC 61850

5.3 Experimental implementation of IEC 61850

In Chapter 4, the advantages resulted from the participation of the PV generators in the grid voltage regulation have been discussed, based on the improved voltage regulation method Q(U). The optimization algorithm developed considers that there is a data communication (IEC 61850) between the PVs which are in this case the intelligent electronic devices and a mater controller which calculates the optimum necessary reactive power. It has been shown that the information exchange in the substation results in an optimized distribution of reactive power within the generators with minimum investment costs.

5.3.1 Laboratory setup

In order to experimentally validate the communication protocol IEC 61850 which has been successfully modeled and tested in the previous subchapter, a laboratory setup was developed as shown in Figure 5-14. The LV European Network previously analyzed in chapter 3 and 4 has been downscaled to three PV inverters due to its complexity and due to laboratory limitations.

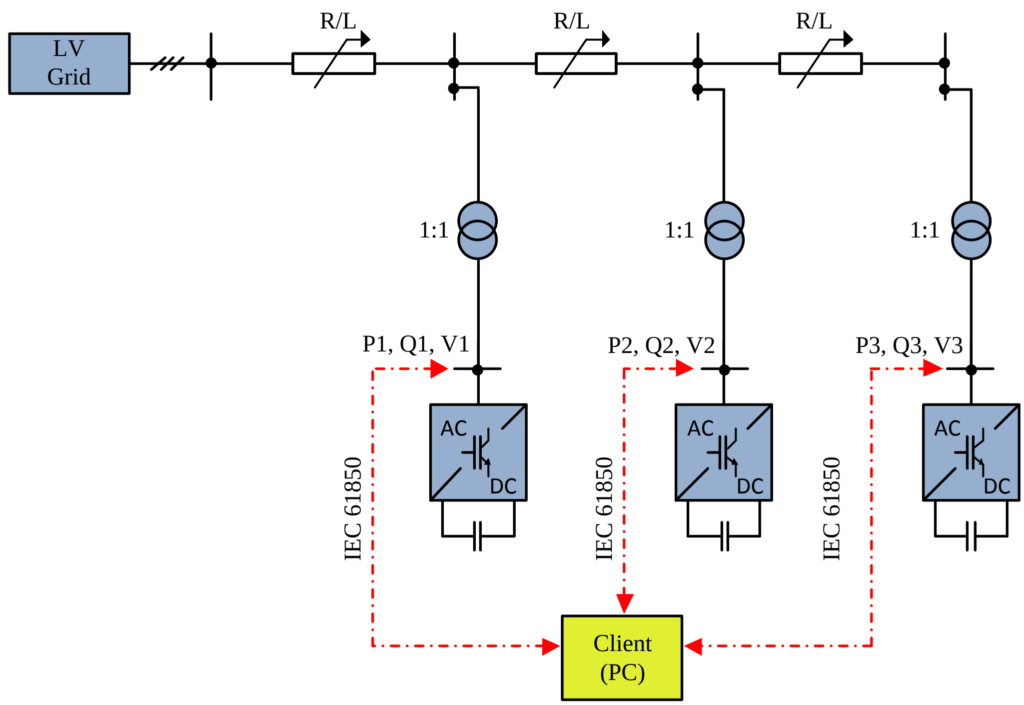

Figure 5-14 Proposed laboratory setup for validation of IEC 61850

The objective of the laboratory setup is to establish a real time bi-directional data communication between the interconnected three-phase inverters and master controller (Client) and further show that the communication concept can be successfully applied in power substations. The individual configuration of each inverter is shown in Figure 5-15. The transmission lines are modeled by means of impedance boxes with variable tap positions for resistance and inductance. This feature gives the possibility to create a more resistive or inductive character of the network. The impedances values can be found in Table 5-3.

Table 5-3 Variable resistors and inductors tap position values

	Tap 1	**Tap2**	**Tap 3**	**Tap 4**	**Tap 5**	**Tap 6**
R /phase	0.3 Ω	0.5 Ω	0.8 Ω	1.1 Ω	1.3 Ω	1.5 Ω
L /phase	1.2 mH	1.5 mH	1.7 mH	1.9 mH	2.1 mH	2.5 mH

The main components of each inverter setup are:

- DC Power Supply 660V, 10A
- Inverter (VLT Danfoss Drive – 3.15 kVA/400V)
- LCL filter

- Isolation Transformer (1:1), S=5 kVA
- 3-phase Grid
- LEM modules for current and voltage measurement
- dSPACE 1103 control system
- CLIB (C library for communication between PC and real-time processor)

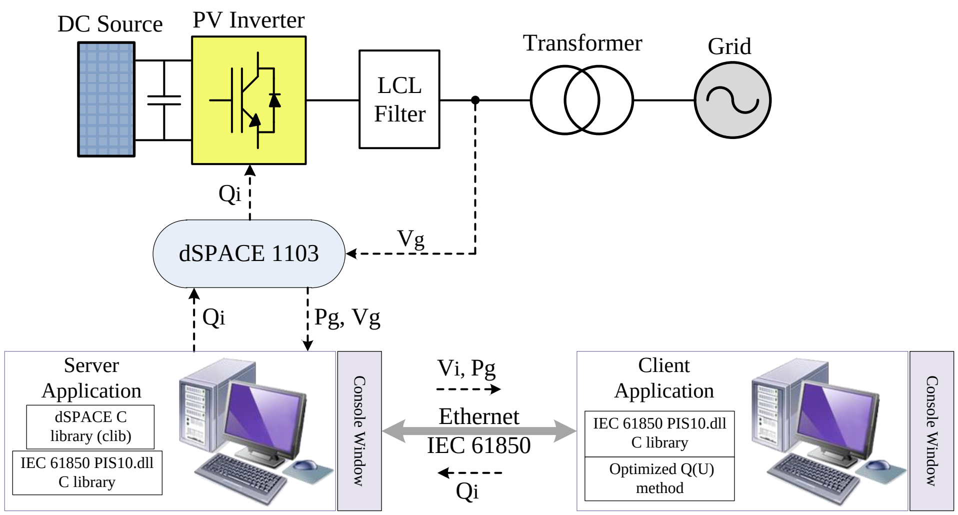

Figure 5-15 PV inverter configuration

The control of the three-phase PV inverter is made in Matlab/Simulink, using the dq synchronous reference frame strategy while the synchronization with the grid voltage is provided by the Phase Loop Lock (PLL) [87]. The PWM signals along with Enable and Reset Trip are transmitted from the dSPACE processor board to the inverter via the IPC2 Card.

Each dSPACE is running on the PC the Control Desk and the Server console application of IEC 61850. After the console application is started, the local functions of the inverter as Reset Trip, Reset PLL and Start are performed within approximately 2 seconds. The variables which have been selected for monitoring and control are being accessed through the CLIB library of the dSPACE.

5.3.2 CLIB Library

One of the project limitations is represented by the lack of physical IED in the laboratory. In order the access the real-time processor which controls the inverter, the communication algorithm is using the C Library which is provided by dSPACE [88]. Any variable used in the control of the three-phase inverter can be accessed by using specific functions to call the DSP Device Driver which interfaces the communication with the hardware.

The main functions used to access the dSPACE processor board are:

- *DS_register_host_app ("app_name")* registers the application with the DSP Device Driver

- *DS_board_spec (board_index, &board_index)* selects and accesses the processor board (in this case DS1103)
- *DS_alloc_mem(board_index, required_size, &memory_address)* allocate a certain amount of memory for the application
- *DS_free_mem(board_index, &memory_address)* free the memory of the previously used application
- DS_unregister_host_app() unregister the application before the exit from the source code

After the connection has been established, the variables are accessed by using the following functions:

- *DS_get_var_addr(board_index, "Desired_signal", &Address_Signal)* accesses the desired variable from the Matlab Simulink model.
- *DS_read_64(board_index, Address_Signal, count, &Value_Signal)* reads the desired variable accessed by the "DS_get_var_address " function.
- *DS_write_64(board_index, Address_Signal, count, &Value_Signal)* writes the desired variable accessed by the "DS_get_var_address " function.

The CLIB functions explained above are implemented locally in every server application, meaning that the client can only read them using IEC 61850. The only variable value decided by the client represents the reactive power reference. The entire script of the client/server application along with the CLIB script can be found in Appendix G.

5.4 Validation

For the validation purpose of communication protocol IEC 61850, the setup presented in Figure 5-14 has been used with the following configuration:

- Tap positions of the impedance boxes were set to R=0.5 Ω/phase and L=1.2 mH, thus resulting in a R/X ratio equal with 1.32
- Four different active power references are applied to each inverter as found in Table 5-4.
- Inverters maximum active power is limited to P=2.85 kW, while the maximum reactive power is Q= ±1.38 kVar (corresponding to 0.9 PF).

Table 5-4 Active power references of the PV Inverters

Power	**PV1**	**PV2**	**PV3**
Iteration 1	1.6	2	1.8
Iteration 2	2	1.7	1.6
Iteration 3	1.3	1.9	2.1
Iteration 4	1	2	2.5

5.4.1 Study Case

For the current study case, a droop function has been implemented in the master controller (Client) which uses the voltage magnitude transmitted by IEC 61850 to calculate the reactive power reference of each inverter. The following formula has been used for the calculation purpose:

$$Q_{ref} = \left(\frac{V_{meas} - V_{base}}{V_{base}} \cdot 34\ [\%] \right) \cdot Q_{\max} \tag{5.1}$$

where $V_{base} = 1.02\,p.u.$,$V_{\max} = 1.05\,p.u.$ and $Q_{\max} = 1.38kVar$. In consequence, for every 0.01 p.u. above the base voltage, 34 % from the reactive capability of the inverter will be absorbed. The voltage deviation after the connection of PV generators has to be of maximum 3% (absolute value).

Each inverter is reading using the CLIB library its voltage magnitude (Vg) and active power reference (Pref) and further sending them to the control unit (client) using the IEC 61850. The droop function calculates the new optimum reactive power references which are being transmitted back to the inverter using the Get/Set Report service and written to the dSPACE. The cycle repeats at a certain refresh time depending on system operator requirements. In case of IEC 61850 data communication failure, the inverters will use locally implemented Stop function to shut down at the end of the current iteration.

In Figure 5-16, the server application of station 3 along with the Control Desk layout is presented. The measured voltage magnitude without and with Q regulation is shown on the console screen along with other measurements as dc-link voltage, grid current, power references and inverter status. Additional information regarding the actions performed by the inverter is illustrated at the bottom end of the screen. The presented configuration is contained in each Server and can be found in Appendix H.

The Client console application which contains the data from all three inverters is presented in Figure 5-17 and corresponds to the iteration 3 data. One of the limitations of ICD Designer demo software is represented by the fact that only 1 server data can be contained in every client application. Therefore three console applications were created, one for each inverter and contain the received measured values from the Server (Vg, Pref and the local time) and the reactive power reference calculated by the droop function. A message which informs about the previous voltage magnitude after the voltage regulation refreshes automatically at every iteration. The console screen allows the network operator/control center to continuously monitor the status of all inverters connected to the network without further investment costs than the IEC 61850 implementation. The complete plots of the client console iterations can be found as well in Appendix H.

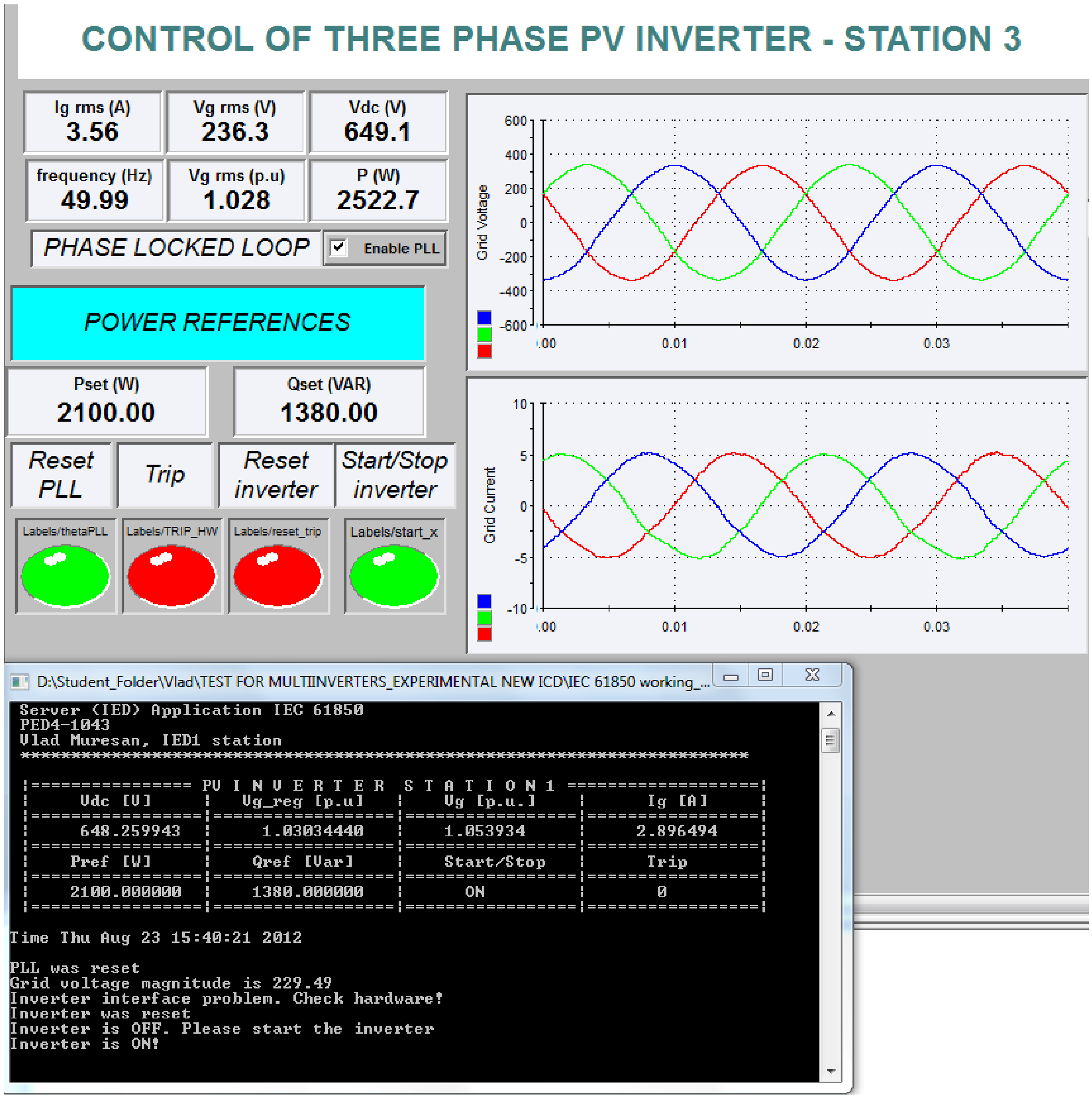

Figure 5-16 Experimental Server Console Application of inverter station along with the dSPACE Control Desk

In order to conclude the IEC 61850 validation part, the experimental results are presented in Figure 5-18. The voltage magnitude before and after the regulation can be observed as well as the amount of reactive power absorbed by each inverter. For the simulated active power references, the voltage magnitude remained in all the cases inside the 3 % voltage deviation (absolute value).

Figure 5-17 Experimental Client Console Application

It can be observed also that although the inverters are sharing information with IEC 61850, the reactive power reference is calculated using local droop function. By using an optimized algorithm which performs better distribution of reactive power, the total losses of the network can be minimized.

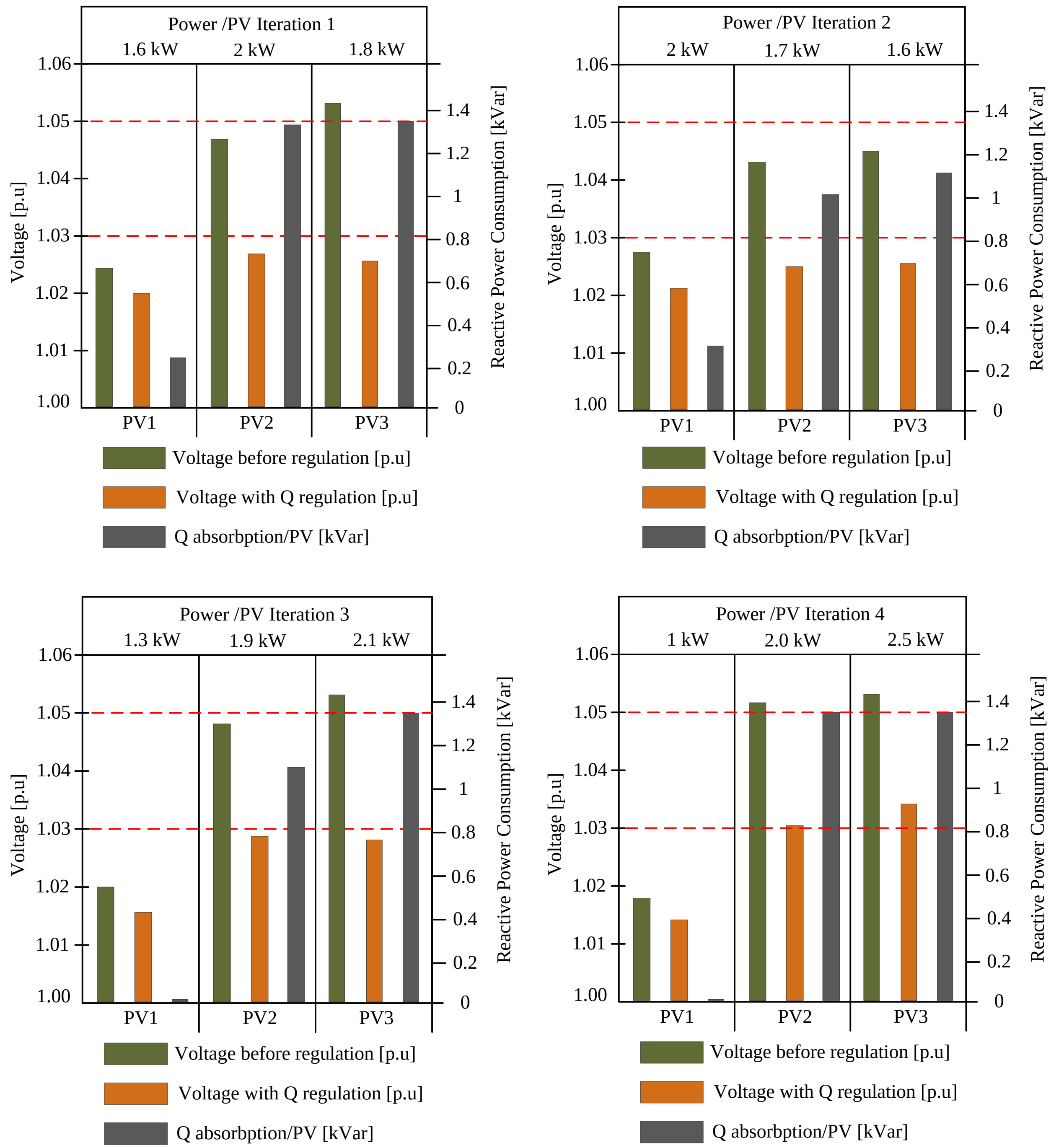

Figure 5-18 Experimental Results for the simulated active power profiles

5.5 Discussions

The main objective of this chapter was to study, design and validate the communication protocol IEC 61850 on a laboratory setup, based on client/server architecture. In the beginning, the SCL files were created depending on the exchange services requirements and variables which have been used.

For the laboratory setup, it has been demonstrated that using the communication concept, critical information can be exchanged between inverters (Servers) and master controller (Client) with the purpose of synchronizing the behavior of the PV generators. The reference has being successfully sent and wrote to the dSPACE through IEC 61850 and CLIB library.

A local droop function has been implemented in the Client application, which calculates the optimum reactive power for each inverter based on the voltage measurements received. Despite the fact that the droop function can be implemented locally without the use of IEC 61850, its main purpose was to decide a real new reference of reactive power without using user input values. Due to the ICD Designer software and time limitations, the optimized algorithm could not be experimentally validated in the laboratory. On the other hand, the communication standard IEC 61850 has been successfully implemented and validated, showing that inverters can share local data for the minimization of network losses and better distribution of reactive power.

Chapter 6 Conclusions and future work

6.1 Conclusions

The current report focused on the analysis and implementation of the voltage regulation methods for PV inverters with ancillary services. The first objective of the project was to investigate and implement the voltage regulation methods by reactive power encouraged by the new German GC VDE-AR-N 4105 on a European LV benchmark grid. The performance of the two strategies was assessed with the purpose of finding the best contender in terms of maintaining the voltage at the CP between limits and to minimize the reactive power consumption. The obtained results concluded that although both methods can maintain the voltage at the CP below the 3% limit, the cosφ(P) strategy is absorbing more reactive power than needed compared to Q(U) method. This is primary because the first method does not use voltage measurement for the calculation purpose. In Chapter 3 is has been concluded that the Q(U) method is the best in terms of voltage stability and reactive power consumption.

The next objective of the project was to model and implement an optimized voltage regulation method able to reduce the reactive power consumption of the PV generators and increase the PV capacity in the LV network. To develop such optimized control strategy, the communication approach is used by the central controller to transmit the optimum values of reactive power for each PV generator which participates in the voltage regulation process. The communication concept is represented by the IEC 61850 and uses client/server architecture. The obtained results concluded that the optimized algorithm presents the following improvements to the network: a better usage of the PV inverter capacity which leads to further PV installments in the network, lower transformer loading and lower network losses.

In order to experimentally validate the communication protocol IEC 61850, a laboratory setup composed of three PV inverters has been developed. First, the information model required by the client/server application has been model, by means of LD, LN and DO. The aim of the laboratory setup is to establish a real time bi-directional data communication between the interconnected three-phase inverters and master controller (Client) and further show that the communication concept can be successfully applied in power substations. The transmission lines were modeled by means of impedance boxes with variable tap positions for resistance and inductance. This feature allowed to create a more resistive or inductive character of the network Each inverter is reading using the CLIB library its voltage magnitude (Vg) and active power reference (Pref) and further sending them to the master controller (client) using the IEC 61850. The droop function calculates the new optimum reactive power references which are being transmitted back to the inverter using the Get/Set Report service and written to the dSPACE. The cycle repeats at a certain refresh time depending on system operator requirements. The communication standard IEC 61850 has been successfully implemented and validated, showing that inverters can share local data for the minimization of network losses and better distribution of reactive power.

6.2 Future work

Because not all the goals of this project were accomplished, several tasks can be considered as future work:

- Graphical User Interface (GUI) can be developed for the IEC 61850 Client/Server application to facilitate the access to the functions.
- The client application should contain only one console with the information from all the inverters.
- The optimization algorithm should be implemented on the client application and the results should be compared with the Q(U) method in terms of power losses.
- For a better investigation of the IEC 61850 advantages compared with the standard voltage regulation methods, the laboratory setup should contain more interconnected PV inverters.

References

[1] A. Timbus, "Grid Monitoring and Advanced Control of Distributed Power Generation Systems," 2007.

[2] M. Rashid, *Power Electronics Handbook- Devices, Circuits and Applications.* 2011.

[3] R. Teodorescu, P. Rodriguez, V. Benda, D. Sera and T. Kerekes, "Industrial/PhD course in photovoltaic power systems - in theory and practice," in Aalborg, Denmark, 2010, .

[4] European Photovoltaic Industry Association, "Market Report 2011," 2012.

[5] X. Yaosuo, D. Kurthakoti, G. Gerd, L. Mihalache, S. Sindhu and M. Madhav, "Towards Next Generation Photovoltaic Inverters," 2010.

[6] European Photovoltaic Industry Association, "Solar generation 6. solar photovoltaic electricity empowering the world," 2011.

[7] Electric Power Research Institute, "Solar Photovoltaics: Status, Costs, and Trends," 2009.

[8] K. Budenbender, M. Braun, T. Stetz and P. Strauss, "Multifunctional PV systems offering additional functionalities and improving grid integration," vol. Volume 7, Number 2 (2011) Pages 109-128, 2011.

[9] ABB, "IEC 61850: Special report," 2010.

[10] A. Mohd, E. Ortjohann, A. Schmelter, N. Hamsic and D. Morton, "Challenges in integrating distributed energy storage systems into future smart grid," in *Industrial Electronics, 2008. ISIE 2008. IEEE International Symposium on,* 2008, pp. 1627-1632.

[11] IMS Research Organization, "The World Market for PV Inverters 2011 Report," 2011.

[12] IEA International Energy Agency, "Trends in photovoltaic applications; survey report of selected IEA countries between 1992 and 2010," .

[13] A. S. Khalifa, "Control and Interfacing of Three Phase Grid Connected Photovoltaic Systems," 2010.

[14] R. Teodorescu, M. Liserre and P. Rodriguez, *Grid Converters for Photovoltaic and Wind Power Systems.* 2011.

[15] S. Evju, "Fundamentals of Grid Connected Photovoltaic Power Electronic Converter Design," 2007.

[16] F. Blaabjerg, Zhe Chen and S. B. Kjaer, "Power electronics as efficient interface in dispersed power generation systems," *Power Electronics, IEEE Transactions on,* vol. 19, pp. 1184-1194, 2004.

[17] T. Kerekes, "Analysis and Modeling of Transformerless Photovoltaic Inverter Systems," 2009.

[18] DKE Deutsche Kommission Elektrotechnik Elektronik Informationstechnik im DIN und VDE, "Entwurf DIN VDE 0126-1-1 (VDE 0126 Teil 1-1)," 2005.

[19] VDE-AR-N 4105, "Generators connected to the low-voltage distribution network - Technical requirements for the connection to and parallel operation with low-voltage distribution networks," 2011.

[20] M. C. Benhabib, J. M. A. Myrzik and J. L. Duarte, "Harmonic effects caused by large scale PV installations in LV network," in *Electrical Power Quality and Utilisation, 2007. EPQU 2007. 9th International Conference on,* 2007, pp. 1-6.

[21] F. Shahnia, A. Ghosh, G. Ledwich and F. Zare, "Voltage unbalance reduction in low voltage distribution networks with rooftop PVs," in *Universities Power Engineering Conference (AUPEC), 2010 20th Australasian,* 2010, pp. 1-5.

[22] F. Shahnia, R. Majumder, A. Ghosh, G. Ledwich and F. Zare, "Sensitivity analysis of voltage imbalance in distribution networks with rooftop PVs," in *Power and Energy Society General Meeting, 2010 IEEE,* 2010, pp. 1-8.

[23] Prof. Dr. Ingo Stadler, "Study about international standards for the connection of small distributed generators to the power grid," 2011.

[24] G. Norbert, G. Kerber, R. Witzmann, M. Sebeck and R. Keck, "Increasing Grid Transmission Capacity and Power Quality by New Solar Inverter Concept and Inbuilt Data Communication," 2009.

[25] E. Paal, Z. Weitzl and C. S. Choi, "Grid management functions built in PV inverters for distributed power generation," in *Power Electronics and ECCE Asia (ICPE & ECCE), 2011 IEEE 8th International Conference on,* 2011, pp. 2637-2644.

[26] N. R. Ullah, T. Thiringer and D. Karlsson, "Voltage and Transient Stability Support by Wind Farms Complying With the E.ON Netz Grid Code," *Power Systems, IEEE Transactions on,* vol. 22, pp. 1647-1656, 2007.

[27] R. A. Walling and K. Clark, "Grid support functions implemented in utility-scale PV systems," in *Transmission and Distribution Conference and Exposition, 2010 IEEE PES,* 2010, pp. 1-5.

[28] Hernan Miranda, "State of the Art on: Grid Interactive Wind Converters," 2008.

[29] EPIA (European Photovoltaic Industry Association), WIP, FIEC (the European Construction Industry Federation), AIE (the European Association of Electrical Contractors), UIA-ARES (International Union of Architects)., "Recommendations for unified technical regulations for grid-connected PV systems," 2009.

[30] T. Degner, G. Arnold, M. Braun, D. Geibel, W. Heckmann and R. Brundlinger, "Utility-scale PV systems: grid connection requirements, test procedures and European harmonisation," 2009.

[31] CIGRE WG14.31, "CUSTOM POWER - STATE OF THE ART," 2000.

[32] E. Fuchs and M. Masoum, *Power Quality in Power Systems and Electrical Machines.* 2008.

[33] IEEE Standards Coordinating Comitee 21 on Fuel Cells Photovoltaics, Dispersed Generation and Energy Storage, "IEEE standard 1547.2 for interconnecting distributed resources with electric power systems," 2008.

[34] A. Baggini, "Handbook of power quality," Wiley, 2008.

[35] M. Tsili, C. Patsiouras and S. Papathanassiou, "Grid code requirements for large wind farms: A review of technical regulations and available wind turbine technologies," .

[36] Commission of the European Communities - Directorate General Joint Research Centre (JRC) - Institute for Energy, "Research, methodologies and technologies for the effective development of pan-european key grid infrastructures to support the achievement of a reliable,competitive and sustainable electricity supply." 2009.

[37] Copper Development Association, "Voltage disturbances standard EN 50160," 2004.

[38] E. Acha, V. G. Agelidis, O. Anaya-Lara and T. Miller, *Power Electronic Control in Electrical Systems.* Oxford, UK: 2002.

[39] E. J. Coster, "Distribution Grid Operation Including Distributed Generation," 2010.

[40] P. Lyons, "Experimental Investigation and Evaluation of Future Active Distribution Networks," 2009.

[41] PV Upscale Report and Inteligent Energy Europe, "Utilities experience and perception of PV distributed generation," 2008.

[42] W. Christiansen and D. T. Johnsen, "Analysis of requirements in selected grid codes," 2006.

[43] A. Kotsopoulos, J. L. Duarte, M. A. M. Hendrix and P. J. M. Heskes, "Islanding behaviour of grid-connected PV inverters operating under different control schemes," in *Power Electronics Specialists Conference, 2002. Pesc 02. 2002 IEEE 33rd Annual*, 2002, pp. 1506-1511 vol.3.

[44] A. D. T. Le, M. A. Kashem, M. Negnevitsky and G. Ledwich, "Control strategy of distributed generation for voltage support in distribution systems," in *Power Electronics, Drives and Energy Systems, 2006. PEDES '06. International Conference on,* 2006, pp. 1-6.

[45] Y. Liu, J. Bebic, B. Kroposki, J. de Bedout and W. Ren, "Distribution system voltage performance analysis for high-penetration PV," in *Energy 2030 Conference, 2008. ENERGY 2008. IEEE,* 2008, pp. 1-8.

[46] C. Rong, "Analysis of STATCOM for Voltage Dip Mitigation," *Göteborg, Sweden,* 2004.

[47] R. Teodorescu, P. Rodriguez, S. Chaudhary and A. Adamczyk, "High Power Converters, Devices and EMI/EMC," *Course at Aalborg University,* 2011.

[48] M. Braun, "Reactive power supply by distributed generators," in *Power and Energy Society General Meeting - Conversion and Delivery of Electrical Energy in the 21st Century, 2008 IEEE,* 2008, pp. 1-8.

[49] E. Demirok, P. Casado González , K. H. B. Frederiksen, D. Sera, P. Rodriguez and R. Teodorescu, "Local Reactive Power Control Methods for Overvoltage Prevention of Distributed Solar Inverters in Low-Voltage Grids," *Photovoltaics, IEEE Journal of,* vol. 1, pp. 174-182, 2011.

[50] G. Kerber, R. Witzmann and H. Sappl, "Voltage limitation by autonomous reactive power control of grid connected photovoltaic inverters," in *Compatibility and Power Electronics, 2009. CPE '09.* 2009, pp. 129-133.

[51] A. Canova, L. Giaccone, F. Spertino and M. Tartaglia, "Electrical impact of photovoltaic plant in distributed network," in *Industry Applications Conference, 2007. 42nd IAS Annual Meeting. Conference Record of the 2007 IEEE,* 2007, pp. 1450-1455.

[52] N. Grass, G. Kerber, R. Witzmann, M. Sebeck and R. Keck, "Increasing Grid Transmission Capacity and Power Quality by new Solar Inverter Concept and Inbuilt Data Communication," *Telecommunication - Energy Special Conference (TELESCON), 2009 4th International Conference on,* pp. 1-5, 2009.

[53] L. Herman, B. Blazic and I. Papic, "Voltage profile support in LV distribution networks with distributed generation," in *Universities Power Engineering Conference (UPEC), 2009 Proceedings of the 44th International,* 2009, pp. 1-5.

[54] T. Stetz, W. Yan and W. Braun, "Voltage Control in distribution systems with high level PV penetration (Improving absorption capacity for PV systems by reactive power supply);" vol. 25th European PV Solar Energy Con-ference and Exhibition, 6th - 10th September 2010, Valencia, Spain, 2010.

[55] E. Demirok, D. Sera, R. Teodorescu, P. Rodriguez and U. Borup, "Clustered PV inverters in LV networks: An overview of impacts and comparison of voltage control strategies," in *Electrical Power & Energy Conference (EPEC), 2009 IEEE*, 2009, pp. 1-6.

[56] G. Kerber, "Statistiche analyse von NS-VErteilungsnetzen und modellierung von referenznetzen," 2208.

[57] Cigre Task Force C6.04.02, "Benchmark Systems for Network Integration of Renewable and Distributed Energy Resources," 2011.

[58] M. Braun, T. Stetz, T. Reimann, B. Valov and G. Arnold, "Optimal reactive power supply in distribution networks; Technological and economic assessment for PV systems ," vol. 24th European Photovoltaic Solar Energy Conference and Exhibition, Hamburg, 2009.

[59] D. EnergiMidt Entreprise A/S, "The SOL-300 project – A 300 roof-top project," 1998-2001.

[60] J. R. Pillai, "Lecture 5: Load flow studies," .

[61] DIgSILENT PowerFactory, "User's manual, volume I, version 14.1," DIgSILENT GmbH, Gomaringen, Germany, 2011.

[62] L. Soder, "EG2030 Power Systems, advanced course - Load flow study and sensitivity analysis of power systems," .

[63] Grainger, J,J, and W. D. Stevenson, Eds., *Power System Analysis.* 1994.

[64] E. Demirok, D. Sera, R. Teodorescu, P. Rodriguez and U. Borup, "Evaluation of the voltage support strategies for the low voltage grid connected PV generators," in *Energy Conversion Congress and Exposition (ECCE), 2010 IEEE*, 2010, pp. 710-717.

[65] J. A. Momoh, "Electric power distribution, automation, protection and control," 2007.

[66] H. Glavitsch and R. Bacher, "OPTIMAL POWER FLOW ALGORITHMS," .

[67] C. E. Bănceanu and I. Vrânceanu, "Coordinated Control of Wind Turbines," 2011.

[68] E. Lund, "Optimization course 2011 - Lecture 1," Department of Mechanical and Manufacturing Engeneering, Aalborg University, Denmark.

[69] J. S. Arora, "Introduction to Optimum Design, Second Edition; ISBN: 0-12-064155-0," 2004.

[70] ByungGwan Yoo, Hyo-Sik Yang, Seungho Yang, Yu-seock Jeong and Won-yong Kim, "CAN to IEC 61850 for microgrid system," in *Advanced Power System Automation and Protection (APAP), 2011 International Conference on*, 2011, pp. 1219-1224.

[71] K. -. Brand, "The standard IEC 61850 as prerequisite for intelligent applications in substations," in *Power Engineering Society General Meeting, 2004. IEEE,* 2004, pp. 714-718 Vol.1.

[72] E. Hammer and S. Eilev, "Analysis and implementation of the IEC 61850 standard," 2008.

[73] C. I. Ciontea and R. N. Beres, "Photovoltaic Power Plant prepared for smart grid," Aalborg University, 2012.

[74] IEC61850, "Communication networks and systems for power utility automation - Part 7-1: Basic communication structure - Principles and models," 2011.

[75] IEC61850, "Communication networks and systems for power utility automation - Part 7-2: Basic information and communication structure - Abstract communication service interface (ACSI)," 2011.

[76] IEC61850, "Communication networks and systems for power utility automation - Part 7-3: Basic communication structure - Common data classes," 2011.

[77] IEC61850, "Communication networks and systems for power utility automation - Part 7-4: Basic communication structure - Compatible logical node classes and data object classes," 2011.

[78] IEC61850, "Communication networks and systems for power utility automation - Part 7-420: Basic communication structure - Distributed energy resources logical nodes," 2011.

[79] IEC61850, "Communication networks and systems for power utility automation - Part 8-1: Specific communication service mapping (SCSM) - Mappings to MMS (ISO 9506-1 and ISO 9506-2) and to ISO/IEC 8802-3," 2011.

[80] R. E. Mackiewicz, "Overview of IEC 61850 and benefits," in *Transmission and Distribution Conference and Exhibition, 2005/2006 IEEE PES,* 2006, pp. 376-383.

[81] P. Nikunj, *IEC 61850 Horizontal Goose Communication and Overview.* 2011.

[82] K. P. Brand, C. Brunner and W. Wimmer, "Design of IEC 61850 based substation automation systems according to customer requirements," vol. Cigre Session B5-103, 2004.

[83] Chul-Hwan Choi, Jong-Ho Park, Jin-Hee Han, Yong-Hark Shin, Yong-Hak Kim and Eung-Bo Shim, "The development of a client conformance tool based on IEC 61850," in *Electrical Machines and Systems (ICEMS), 2011 International Conference on,* 2011, pp. 1-5.

[84] SystemCORP, "IEC 61850 Protocol API User Manual - Protocol Integration Stack," 2009.

[85] SystemCORP, "IEC 61850 Intellingent Electronic Device (IED) Capability Description (ICD) - SystemCorp ICD Designer User Manual," 2010.

[86] E. A. Man, "Control of grid connected PV systems with grid support functions," Aalborg University, Denmark, 2012.

[87] R. Teodorescu, M. Lissere and P. Rodriguez, "Power Electronics in Renewable Energy Sources (PERES) Industrial Phd Course," November 2011, Aalborg University.

[88] dSPACE GmbH, "C Interface Library,", 2011.

Appendix A

Admittance matrix for the European benchmark

Admittance matrix $Y_{bus} = G_{bus} + jB_{bus}$:

- Conductance matrix (G_{bus})

156.9898	-72.4568	0	0	0	0	0	0	0	0	0	0	0	0	0	0	0	0	-84.533
-72.4568	144.9136	-72.4568	0	0	0	0	0	0	0	0	0	0	0	0	0	0	0	0
0	-72.4568	229.4466	-72.4568	0	0	0	0	0	0	-84.533	0	0	0	0	0	0	0	0
0	0	-72.4568	217.3704	-72.4568	0	0	0	0	0	0	-72.4568	0	0	0	0	0	0	0
0	0	0	-72.4568	144.9136	-72.4568	0	0	0	0	0	0	0	0	0	0	0	0	0
0	0	0	0	-72.4568	229.4466	-72.4568	0	0	0	0	0	0	0	0	-84.533	0	0	0
0	0	0	0	0	-72.4568	144.9136	-72.4568	0	0	0	0	0	0	0	0	0	0	0
0	0	0	0	0	0	-72.4568	144.9136	-72.4568	0	0	0	0	0	0	0	0	0	0
0	0	0	0	0	0	0	-72.4568	229.4466	-72.4568	0	0	0	0	0	0	-84.533	0	0
0	0	0	0	0	0	0	0	-72.4568	156.9898	0	0	0	0	0	0	0	-84.533	0
0	0	-84.533	0	0	0	0	0	0	0	84.53295	0	0	0	0	0	0	0	0
0	0	0	-72.4568	0	0	0	0	0	0	0	144.9136	-72.4568	0	0	0	0	0	0
0	0	0	0	0	0	0	0	0	0	0	-72.4568	144.9136	-72.4568	0	0	0	0	0
0	0	0	0	0	0	0	0	0	0	0	0	-72.4568	156.9898	-84.533	0	0	0	0
0	0	0	0	0	0	0	0	0	0	0	0	0	-84.533	84.53295	0	0	0	0
0	0	0	0	0	-84.533	0	0	0	0	0	0	0	0	0	84.53295	0	0	0
0	0	0	0	0	0	0	0	-84.533	0	0	0	0	0	0	0	84.53295	0	0
0	0	0	0	0	0	0	0	0	-84.533	0	0	0	0	0	0	0	84.53295	0
-84.533	0	0	0	0	0	0	0	0	0	0	0	0	0	0	0	0	0	84.53295

- Susceptance matrix (B_{bus})

-114.036	52.63207	0	0	0	0	0	0	0	0	0	0	0	0	0	0	0	0	61.40408
52.63207	-105.264	52.63207	0	0	0	0	0	0	0	0	0	0	0	0	0	0	0	0
0	52.63207	-166.668	52.63207	0	0	0	0	0	0	61.40408	0	0	0	0	0	0	0	0
0	0	52.63207	-157.896	52.63207	0	0	0	0	0	0	52.63207	0	0	0	0	0	0	0
0	0	0	52.63207	-105.264	52.63207	0	0	0	0	0	0	0	0	0	0	0	0	0
0	0	0	0	52.63207	-166.668	52.63207	0	0	0	0	0	0	0	0	61.40408	0	0	0
0	0	0	0	0	52.63207	-105.264	52.63207	0	0	0	0	0	0	0	0	0	0	0
0	0	0	0	0	0	52.63207	-105.264	52.63207	0	0	0	0	0	0	0	0	0	0
0	0	0	0	0	0	0	52.63207	-166.668	52.63207	0	0	0	0	0	0	61.40408	0	0
0	0	0	0	0	0	0	0	52.63207	-114.036	0	0	0	0	0	0	0	61.40408	0
0	0	61.40408	0	0	0	0	0	0	0	-61.4041	0	0	0	0	0	0	0	0
0	0	0	52.63207	0	0	0	0	0	0	0	-105.264	52.63207	0	0	0	0	0	0
0	0	0	0	0	0	0	0	0	0	0	52.63207	-105.264	52.63207	0	0	0	0	0
0	0	0	0	0	0	0	0	0	0	0	0	52.63207	-114.036	61.40408	0	0	0	0
0	0	0	0	0	0	0	0	0	0	0	0	0	61.40408	-61.4041	0	0	0	0
0	0	0	0	0	61.40408	0	0	0	0	0	0	0	0	0	-61.4041	0	0	0
0	0	0	0	0	0	0	0	61.40408	0	0	0	0	0	0	0	-61.4041	0	0
0	0	0	0	0	0	0	0	0	61.40408	0	0	0	0	0	0	0	-61.4041	0
61.40408	0	0	0	0	0	0	0	0	0	0	0	0	0	0	0	0	0	-61.4041

Appendix B

Calculation of injected power in a bus

Figure B-6-1 shows a general representation of each bus in the network presented in Figure 3-5. Further on, the load flow equations will be determined and the first step consists of applying Kirchoff's current law for the LV network in order to obtain the load flow equations.

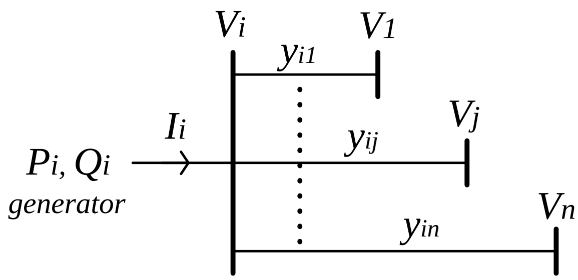

Figure B-6-1A typical bus of a power system

The general formula of the current I_i injected to bus *i* from the PV generators is:

$$I_i = y_{i1}(V_i - V_1) + y_{i2}(V_i - V_2) + ... + y_{in}(V_i - V_n) \quad \text{(B.1)}$$

$$I_i = (y_{i1} + y_{i2} + ... + y_{in})V_i - y_{i1}V_1 - y_{i2}V_2 - .... - y_{in}V_n \quad \text{(B.2)}$$

$$I_i = V_i \sum_{j=1}^{19} y_{ij} - \sum_{j=1}^{19} y_{ij}V_j, \quad i = \overline{2,19}, \quad i \neq j \quad \text{(B.3)}$$

Denoting $\sum_{j=1}^{19} y_{ij} = Y_{ii}$ and $-y_{ij} = Y_{ij}$, $i \neq j$, it results:

$$I_i = V_i Y_{ii} + \sum_{j=1}^{19} Y_{ij} V_j \quad \text{(B.4)}$$

The active and reactive power formula at bus *i* is:

$$S_i = P_i + jQ_i = V_i I_i^* \quad \text{(B.5)}$$

Therefore, from (B.4) and (B.5) it results:

$$I_i = \frac{P_i - jQ_i}{V_i^*} = V_i Y_{ii} + \sum_{j=1}^{19} Y_{ij} V_j \quad \text{(B.6)}$$

Denote:

$$V_i = |V_i| e^{j\delta_i} \quad \text{(B.7)}$$

$$Y_{ij} = \left|Y_{ij}\right| e^{j\theta_{ij}} \tag{B.8}$$

Substituting (B.7) and (B.8) in (B.6), it results that the polar form of the active and reactive power is:

$$P_i = \mathrm{Re}\left\{S_i\right\} = \sum_{j=1}^{19} \left|V_i\right|\left|V_j\right|\left|Y_{ij}\right| \cos(\theta_{ij} + \delta_j - \delta_i) \tag{B.9}$$

$$Q_i = \mathrm{Im}\left\{S_i\right\} = -\sum_{j=1}^{19} \left|V_i\right|\left|V_j\right|\left|Y_{ij}\right| \sin(\theta_{ij} + \delta_j - \delta_i) \tag{B.10}$$

Appendix C

Source code for load flow analysis:

```
object LDF, oPV, oTerm, oTrafo, oFeeder;
set sPV, sTerm, sTrafo, sFeeder;
int ierr,i;
double p2,p3,p4,p5,p6,p7,p8,p9,p10;
string s,s1,s2;

!!!!!!!!This part opens a connection with Excel and read values from it!!!
! open a DDE connection to Sheet1 : #ITERATION 1
s = sprintf('%s%s', ExcelPath, 'Excel.exe');
ierr = ddeOpen(s, 'Excel', 'System');
if (.not.ierr) {
  ! ok, excel can be opened. Now close and connect to a specific sheet
  ddeClose();
  ierr = ddeOpen('', 'Excel', 'Sheet1');
}
!!Connecting to the next row
 i = ddeRequest('R79C2',s,p2); ! get the contents of a cell
! if (i=1) printf('%f', p2); ! i=1 means a number

 i = ddeRequest('R79C6',s,p3); ! get the contents of a cell
! if (i=1) printf('%f', p3); ! i=1 means a number

 i = ddeRequest('R79C9',s,p4); ! get the contents of a cell
! if (i=1) printf('%f', p4); ! i=1 means a number

 i = ddeRequest('R79C12',s,p5); ! get the contents of a cell
! if (i=1) printf('%f', p5); ! i=1 means a number

 i = ddeRequest('R79C15',s,p6); ! get the contents of a cell
! if (i=1) printf('%f', p6); ! i=1 means a number

 i = ddeRequest('R79C18',s,p7); ! get the contents of a cell
! if (i=1) printf('%f', p7); ! i=1 means a number

 i = ddeRequest('R79C21',s,p8); ! get the contents of a cell
! if (i=1) printf('%f', p8); ! i=1 means a number

 i = ddeRequest('R79C24',s,p9); ! get the contents of a cell
! if (i=1) printf('%f', p9); ! i=1 means a number

 i = ddeRequest('R79C27',s,p10); ! get the contents of a cell
! if (i=1) printf('%f', p10); ! i=1 means a number
```

```
!This part assigns a P value to the PV -> do this for all PVs
! Further only PV19 is taken as example

LDF=GetCaseCommand('ComLdf'); !to calculate the load flow

sPV = AllRelevant('PV19*.ElmLod');  !select here for which PV to assign value
oPV=sPV.First();  !takes the first one
oPV:plini=p10; !active power reference for all PV
oPV:qlini=0; !reactive power reference for all PV

!Perform a load flow!!!!!
LDF.Execute();

!VOLTAGE MAGNITUDE AT CP -> do this for all PVs
!Only CP19 is defined as example

sTerm = AllRelevant('R19*.ElmTerm');
oTerm = sTerm.First();
printf('%f',oTerm:m:u);

!Transformer loading

sTrafo=AllRelevant('*.ElmTr2');
oTrafo=sTrafo.First();
printf('%f',oTrafo:c:loading);
```

Appendix D

Source code for cosφ(P) method:

```
object LDF, oPV, oTerm, oTrafo, oFeeder;
set sPV, sTerm, sTrafo, sFeeder;
int ierr,i;
double PF19,p2,p3,p4,p5,p6,p7,p8,p9,p10,Q19;
string s,s1,s2;

!!!!!!!!This part opens a connection with Excel and read values from it!!!
! open a DDE connection to Sheet1 : #ITERATION 1
s = sprintf('%s%s', ExcelPath, 'Excel.exe');
ierr = ddeOpen(s, 'Excel', 'System');
if (.not.ierr) {
! ok, excel can be opened. Now close and connect to a specific sheet
  ddeClose();
  ierr = ddeOpen('', 'Excel', 'Sheet1');
}
!!Connecting to the next row
 i = ddeRequest('R55C2',s,p2); ! get the contents of a cell
if (i=1) printf('%f', p2); ! i=1 means a number

 i = ddeRequest('R55C6',s,p3); ! get the contents of a cell
if (i=1) printf('%f', p3); ! i=1 means a number

 i = ddeRequest('R55C9',s,p4); ! get the contents of a cell
if (i=1) printf('%f', p4); ! i=1 means a number

 i = ddeRequest('R55C12',s,p5); ! get the contents of a cell
if (i=1) printf('%f', p5); ! i=1 means a number

 i = ddeRequest('R55C15',s,p6); ! get the contents of a cell
if (i=1) printf('%f', p6); ! i=1 means a number

 i = ddeRequest('R55C18',s,p7); ! get the contents of a cell
if (i=1) printf('%f', p7); ! i=1 means a number

 i = ddeRequest('R55C21',s,p8); ! get the contents of a cell
if (i=1) printf('%f', p8); ! i=1 means a number

 i = ddeRequest('R55C24',s,p9); ! get the contents of a cell
if (i=1) printf('%f', p9); ! i=1 means a number

 i = ddeRequest('R55C27',s,p10); ! get the contents of a cell
if (i=1) printf('%f', p10); ! i=1 means a number
```

```
! Calculate the power factor and reactive power -> do this for all PVs
! Further only PV19 is taken as example

if (-2.5>p10>-2.75) {
PF19=0.99;
}
if (-2.75>p10>-3) {
PF19=0.98;
}
if (-3>p10>-3.25) {
PF19=0.97;
}
if (-3.25>p10>-3.5) {
PF19=0.96;
}
if (-3.5>p10>-3.75) {
PF19=0.95;
}
if (-3.75>p10>-4) {
PF19=0.94;
}
if (-4>p10>-4.25) {
PF19=0.93;
}
if (-4.25>p10>-4.5) {
PF19=0.92;
}
if (-4.5>p10>-4.75) {
PF19=0.91;
}
if (-4.75>p10>-5) {
PF19=0.90;
}
if (p10<-5) {
 p10=-5;
}
if (p10>-2.5) {
  Q19 = 0;
  }
  else {
   Q19=tan(acos(PF19))*(-p10);
  }
printf('%f',Q19);

!This part assigns a P value to the PV -> do this for all PVs
! Further only PV19 is taken as example
LDF=GetCaseCommand('ComLdf'); !calculate the load flow

sPV = AllRelevant('PV19*.ElmLod');  !select here for which PV to assign value
oPV=sPV.First();  !takes the first one
oPV:plini=p10; !active power reference for all PV
oPV:qlini=Q19; !reactive power reference for all PV

!Perform a load flow!!!!!
LDF.Execute();
```

```
!VOLTAGE MAGNITUDE AT CP -> do this for all PVs
!Only CP19 is defined as example
sTerm = AllRelevant('R19*.ElmTerm');
oTerm = sTerm.First();
printf('%f',oTerm:m:u);

!Transformer loading
sTrafo=AllRelevant('*.ElmTr2');
oTrafo=sTrafo.First();
printf('%f',oTrafo:c:loading);
```

Appendix E

Source code for Q(U) method:

```
object LDF, oPV, oTerm, oTrafo, oFeeder;
set sPV, sTerm, sTrafo, sFeeder;
int ierr,i;
double
p2,p3,p4,p5,p6,p7,p8,p9,p10,PF,Q2,Q3,Q4,Q5,Q6,Q7,Q8,Q9,Q10,Q11,Q12,Q13,Q14,Q1
5,Q16,Q17,Q18,Q19,Er,Vmes,Vbase;
string s,s1,s2;

!!!!!!!!This part opens a connection with Excel and read values from it!!!
! open a DDE connection to Sheet1 : #ITERATION 1
s = sprintf('%s%s', ExcelPath, 'Excel.exe');
ierr = ddeOpen(s, 'Excel', 'System');
if (.not.ierr) {
! ok, excel can be opened. Now close and connect to a specific sheet
  ddeClose();
  ierr = ddeOpen('', 'Excel', 'Sheet1');
}
!!Connecting to the next row
 i = ddeRequest('R59C2',s,p2); ! get the contents of a cel
if (i=1) printf('%f', p2); ! i=1 means a number

 i = ddeRequest('R59C6',s,p3); ! get the contents of a cel
if (i=1) printf('%f', p3); ! i=1 means a number

 i = ddeRequest('R59C9',s,p4); ! get the contents of a cel
if (i=1) printf('%f', p4); ! i=1 means a number

 i = ddeRequest('R59C12',s,p5); ! get the contents of a cel
if (i=1) printf('%f', p5); ! i=1 means a number

 i = ddeRequest('R59C15',s,p6); ! get the contents of a cel
if (i=1) printf('%f', p6); ! i=1 means a number

 i = ddeRequest('R59C18',s,p7); ! get the contents of a cel
if (i=1) printf('%f', p7); ! i=1 means a number

 i = ddeRequest('R59C21',s,p8); ! get the contents of a cel
if (i=1) printf('%f', p8); ! i=1 means a number

 i = ddeRequest('R59C24',s,p9); ! get the contents of a cel
if (i=1) printf('%f', p9); ! i=1 means a number

 i = ddeRequest('R59C27',s,p10); ! get the contents of a cel
if (i=1) printf('%f', p10); ! i=1 means a number
```

```
!This part assigns a P value to the PV -> do this for all PVs
! Further only PV19 is taken as example

LDF=GetCaseCommand('ComLdf'); !calculate the load flow

sPV = AllRelevant('PV19*.ElmLod');  !select here for which PV to assign value
oPV=sPV.First();  !takes the first one
oPV:plini=p10; !active power reference for all PV
oPV:qlini=0; !reactive power reference for all PV

!Perform load flow
LDF.Execute();

! Read voltage at CP and calculate reactive power -> do this for all PVs
! Further only PV19 is taken as example

sTerm = AllRelevant('R19*.ElmTerm');
oTerm = sTerm.First();
Vmes=oTerm:m:u;
Vbase=1.02;
if (1.02<oTerm:m:u<1.05) {
  Er=((Vmes-Vbase)/Vbase)*34;
  Q19=Er*2.42;
  }
else {
    Q19=0;
    }
if (oTerm:m:u>1.05) {
    Q19=2.42;
    }
printf('%f',oTerm:m:u);

LDF=GetCaseCommand('ComLdf'); !calculate the load flow

! Assign reactive power reference to PVs -> do this for all PVs
! Further only PV19 is taken as example
sPV = AllRelevant('PV19*.ElmLod');  !select here for which PV to assign value
oPV=sPV.First(); !takes the first one
oPV:plini=p10; !active power reference for all PV
oPV:qlini=Q19; !reactive power reference for all PV
!Perform load flow
LDF.Execute();

! Read measured reactive power & voltage at CPs -> do this for all PVs
! Further only PV19 is taken as example
sTerm = AllRelevant('R19*.ElmTerm');
oTerm = sTerm.First();
printf('%f',oTerm:m:u);
printf('%f',Q19);

! Read transformer loading value
sTrafo=AllRelevant('*.ElmTr2');
oTrafo=sTrafo.First();
printf('%f',oTrafo:c:loading);
printf('%f',oTrafo:m:Qsum:buslv);
```

Appendix F

Source code for optimized Q(U) method:

- Parameters initialization

```
%% Parameters initialization for the electric system
tole=1e-4;
deg=180/pi;
rad=1/deg ;
Sbase=100000;
Vbase=400;
Zbase=1.6;
Ybase=0.625;
%%%%%%%%%%%%%%%%%%%%%%%%%%%%%%%%%%%%%%%
%% All variables are expressed in p.u.
%%%%%%%%%%%%%%%%%%%%%%%%%%%%%%%%%%%%%%%
% Type=1 means slack-bus, Type=2 means PQ-bus, Type=3 means PU-bus
%Bus Types
bt1 = 1;
bt2 = 2;
bt3 = 2;
bt4 = 2;
bt5 = 2;
bt6 = 2;
bt7 = 2;
bt8 = 2;
bt9 = 2;
bt10 = 2;
bt11 = 2;
bt12 = 2;
bt13 = 2;
bt14 = 2;
bt15 = 2;
bt16 = 2;
bt17 = 2;
bt18 = 2;
bt19 = 2;
%voltage magnitude & angle  at buses
V1=1;           % voltage magnitute in p.u. at buses
angl=0/deg;     % angle in radians
%Assign Pgen and Qgen in each node
PG1=0/100;              QG1=0/100;
PG2=-P2/100;            QG2=0/100;
PG3=-P3/100;            QG3=0/100;
PG4=-P4/100;            QG4=0/100;
PG5=-P5/100;            QG5=0/100;
PG6=-P6/100;            QG6=0/100;
PG7=-P7/100;            QG7=0/100;
PG8=-P8/100;            QG8=0/100;
PG9=-P9/100;            QG9=0/100;
PG10=-P10/100;          QG10=0/100;
PG11=-P2/100;           QG11=0/100;
PG12=-P3/100;           QG12=0/100;
PG13=-P4/100;           QG13=0/100;
```

```
PG14=-P5/100;          QG14=0/100;
PG15=-P6/100;          QG15=0/100;
PG16=-P7/100;          QG16=0/100;
PG17=-P8/100;          QG17=0/100;
PG18=-P9/100;          QG18=0/100;
PG19=-P10/100;         QG19=0/100;
%%%%%%%%%%%
% Bus Data
%%%%%%%%%%%
BUSDATA=[
%         1      2        3       4         5        6
%        Node   Type      V      Angle     Pgen     Qgen
          1      bt1      V2     angl      PG1      QG1
          2      bt2      V1     angl      PG2      QG2
          3      bt3      V1     angl      PG3      QG3
          4      bt4      V1     angl      PG4      QG4
          5      bt5      V1     angl      PG5      QG5
          6      bt6      V1     angl      PG6      QG6
          7      bt7      V1     angl      PG7      QG7
          8      bt8      V1     angl      PG8      QG8
          9      bt9      V1     angl      PG9      QG9
          10     bt10     V1     angl      PG10     QG10
          11     bt11     V1     angl      PG11     QG11
          12     bt12     V1     angl      PG12     QG12
          13     bt13     V1     angl      PG13     QG13
          14     bt14     V1     angl      PG14     QG14
          15     bt15     V1     angl      PG15     QG15
          16     bt16     V1     angl      PG16     QG16
          17     bt17     V1     angl      PG17     QG17
          18     bt18     V1     angl      PG18     QG18
          19     bt19     V1     angl      PG19     QG19];
%%%%%%%%%%%%
% Line Data
%%%%%%%%%%%%
R35 = 0.014455;     %% resistence for 35m cable
X35 = 0.0105;       %% reactance for 35m cable
R30 = 0.01239;      %% resistence for 30m cable
X30 = 0.009;        %% reactance for 30m cable
R12=R35/Zbase;        X12=X35/Zbase;          % 35m cable
R119=R30/Zbase;       X119=X30/Zbase;         % 30m cable
R23=R35/Zbase;        X23=X35/Zbase;          % 35m cable
R34=R35/Zbase;        X34=X35/Zbase;          % 35m cable
R311=R30/Zbase;       X311=X30/Zbase;         % 30m cable
R45=R35/Zbase;        X45=X35/Zbase;          % 35m cable
R412=R35/Zbase;       X412=X35/Zbase;         % 35m cable
R56=R35/Zbase;        X56=X35/Zbase;          % 35m cable
R67=R35/Zbase;        X67=X35/Zbase;          % 35m cable
R616=R30/Zbase;       X616=X30/Zbase;         % 30m cable
R78=R35/Zbase;        X78=X35/Zbase;          % 35m cable
R89=R35/Zbase;        X89=X35/Zbase;          % for 35m cable
R910=R35/Zbase;       X910=X35/Zbase;         % 35m cable
R917=R30/Zbase;       X917=X30/Zbase;         % 30m cable
R1018=R30/Zbase;      X1018=X30/Zbase;        % 30m cable
R1213=R35/Zbase;      X1213=X35/Zbase;        % 35m cable
R1314=R35/Zbase;      X1314=X35/Zbase;        % 35m cable
R1415=R30/Zbase;      X1415=X30/Zbase;        % 30m cable
```

```
LINEDATA = [
% Line  from  to       R        X
   1     1     2      R12      X12
   2     1     19     R119     X119
   3     2     3      R23      X23
   4     3     4      R34      X34
   5     3     11     R311     X311
   6     4     5      R45      X45
   7     4     12     R412     X412
   8     5     6      R56      X56
   9     6     7      R67      X67
   10    6     16     R616     X616
   11    7     8      R78      X78
   12    8     9      R89      X89
   13    9     10     R910     X910
   14    9     17     R917     X917
   15    10    18     R1018    X1018
   16    12    13     R1213    X1213
   17    13    14     R1314    X1314
   18    14    15     R1415    X1415];
%%%%%%%%%%%%%%%%%%%%%%%%%%%%%%%%%%%%%%%%%%%%
%%%%% Rated power for each PV system %%%%%

nl = size(BUSDATA,1);
S = zeros(1,nl);
for N = 1:nl
if BUSDATA(N,2) ~= 1
          S(1,N) = 5.55/100;
else
          S(1,N) = 0/100;
end
end
```

- Admittance matrix

```
%%%%%%Constructing YBUS Admitance Matrix%%%%%%%%%%%%%%%%%%
%%%%%%%%%%%%%%%%%%%%%%%%%%%%%%%%%%%%%%%%%%%%%%%%%%%%%%%%%%%
% Bus and Line Numbers
[busnumber, busproperty] = size(BUSDATA);
[linenumber,lineproperty] = size(LINEDATA);
YBUS = zeros(busnumber);

%Adding line impedances and capacitances
for N = 1:linenumber
%For digonal elements
    YBUS(LINEDATA(N,2),LINEDATA(N,2)) = YBUS(LINEDATA(N,2),LINEDATA(N,2))+...
           1 / (LINEDATA(N,4)+1j*LINEDATA(N,5));


    YBUS(LINEDATA(N,3),LINEDATA(N,3)) = YBUS(LINEDATA(N,3),LINEDATA(N,3))+...
             1 / (LINEDATA(N,4)+1j*LINEDATA(N,5));

%For off-digonal elements
    YBUS(LINEDATA(N,2),LINEDATA(N,3)) = YBUS(LINEDATA(N,2),LINEDATA(N,3))-...
             1 / (LINEDATA(N,4)+1j*LINEDATA(N,5));
```

```
    YBUS(LINEDATA(N,3),LINEDATA(N,2)) = YBUS(LINEDATA(N,3),LINEDATA(N,2))-...
             1 / (LINEDATA(N,4)+1j*LINEDATA(N,5));
end
```

- Jacobian matrix

```
%Create Jacobian Matrix
%%%%%%%%%%%%%%%%%%%%%%%%%%
% Bus and Line Numbers
[busnumber, busproperty] = size(BUSDATA);
[linenumber,lineproperty] = size(LINEDATA);
[admitnumber,admitproperty] = size(YBUS);

%Set scheduled active and reactive power
PGDi = BUSDATA(:,5);
QGDi = BUSDATA(:,6);

%Start of the iterations
%number of iterations
deltaP = ones(busnumber,1);
deltaQ = ones(busnumber,1);
iteration = 0;

while max(abs(deltaP)) > tole && iteration<=3
   Pi = zeros(busnumber,1);
   Qi = zeros(busnumber,1);

%Calculate injected powers
for N = 1:busnumber
if BUSDATA(N,2) ~= 1 % if bus type not slack bus

for M = 1:admitnumber
if  N ~= M && YBUS(N,M) ~= 0
                Pi(N) = Pi(N) +
BUSDATA(N,3)*BUSDATA(M,3)*abs(YBUS(N,M))*cos(angle(YBUS(N,M))+BUSDATA(M,4)-
BUSDATA(N,4));
                Qi(N) = Qi(N) +
BUSDATA(N,3)*BUSDATA(M,3)*abs(YBUS(N,M))*sin(angle(YBUS(N,M))+BUSDATA(M,4)-
BUSDATA(N,4));
end
end
        Pi(N,1) = BUSDATA(N,3)*BUSDATA(N,3)*real(YBUS(N,N)) + Pi(N);
        Qi(N,1) = -BUSDATA(N,3)*BUSDATA(N,3)*imag(YBUS(N,N)) - Qi(N);
end
end

%Maximum differences
   deltaP = PGDi - Pi;
    deltaQ = QGDi - Qi;

%The number of iterations start with zero and will be increased with
%one for each cycle.
    iteration = iteration +1;
```

```
%First create Jacobian N and Jacobian M matrices
    JacobM = zeros(busnumber);
    JacobN = zeros(busnumber);

for N = 1:busnumber
%check slack bus
if BUSDATA(N,2) ~= 1
for M = 1:busnumber
%check slack bus and N is not equal to M
if N ~= M
                    dPdAng = -
BUSDATA(N,3)*BUSDATA(M,3)*abs(YBUS(N,M))*sin(angle(YBUS(N,M))+BUSDATA(M,4)-
BUSDATA(N,4));
                    dQdAng = -
BUSDATA(N,3)*BUSDATA(M,3)*abs(YBUS(N,M))*cos(angle(YBUS(N,M))+BUSDATA(M,4)-
BUSDATA(N,4));
if BUSDATA(M,2) ~= 1
%for off-diagonal Jacobian M, Jacobian N matrix
                        JacobM(N,M) = dPdAng;
                        JacobN(N,M) = dQdAng;
end
%for diagonal Jacobian M, Jacobian N matrix
                    JacobM(N,N) = -Qi(N)-imag(YBUS(N,N))*BUSDATA(N,3)^2;
                    JacobN(N,N) = Pi(N)-real(YBUS(N,N))*BUSDATA(N,3)^2;
end
end
end
end
%Second derivative Jacobian Npr and Jacobian Mpr matrices
    JacobMpr = zeros(busnumber);
    JacobNpr = zeros(busnumber);

for N = 1:busnumber
%check slack bus
if BUSDATA(N,2) ~= 1
for M = 1:busnumber
%check slack bus and N is not equal to M
if N ~= M
                    dPdV =
BUSDATA(N,3)*abs(YBUS(N,M))*cos(angle(YBUS(N,M))+BUSDATA(M,4)-BUSDATA(N,4));
                    dQdV = -
BUSDATA(M,3)*abs(YBUS(N,M))*sin(angle(YBUS(N,M))+BUSDATA(M,4)-BUSDATA(N,4));
if BUSDATA(M,2) ~= 1
%for off-diagonal Jacobian M, Jacobian N matrix
                        JacobMpr(N,M) = dQdV;
                        JacobNpr(N,M) = dPdV;
end
%for diagonal Jacobian M, Jacobian N matrix
                    JacobMpr(N,N) = Qi(N)-imag(YBUS(N,N))*BUSDATA(N,3)^2;
                    JacobNpr(N,N) = Pi(N)+real(YBUS(N,N))*BUSDATA(N,3)^2;

end
end
end
end
end
```

```
    tempbusnumber = busnumber;

while tempbusnumber > 0,

% the row and column for Jacobian is cut out if slack bus

if BUSDATA(tempbusnumber,2) == 1
            JacobM(tempbusnumber,:) = [];
            JacobM(:,tempbusnumber) = [];

            JacobN(tempbusnumber,:) = [];
            JacobN(:,tempbusnumber) = [];

            JacobMpr(tempbusnumber,:) = [];
            JacobMpr(:,tempbusnumber) = [];

            JacobNpr(tempbusnumber,:) = [];
            JacobNpr(:,tempbusnumber) = [];
            deltaP(tempbusnumber,:) = [];
            deltaQ(tempbusnumber,:) = [];

end
    tempbusnumber = tempbusnumber-1;
end

% construct Jacobian from the 4 matrices

    J1 = vertcat(JacobM,JacobN);
    J2 = vertcat(JacobNpr,JacobMpr);
    Jacobian = horzcat(J1,J2);
    deltaPQ = vertcat(deltaP,deltaQ);

    deltaAngV = (Jacobian)\deltaPQ;

    deltaAng = deltaAngV(1:busnumber-1);
    deltaV = deltaAngV(busnumber:end);

    tempAng = zeros(busnumber,1);
    tempV = zeros(busnumber,1);
    delta1 = 1;  %counter for deltaAng
    delta2 = 1;  %counter for deltaV

for N = 1:busnumber
if BUSDATA(N,2) ~= 1
            tempAng(N,1) = deltaAng(delta1,1) + BUSDATA(N,4);
            delta1 = delta1 + 1;

if BUSDATA(N,2) ~= 1
                tempV(N,1) = BUSDATA(N,3)*(deltaV(delta2,1) + 1);
                delta2 = delta2 + 1;
end
else
            tempAng(N,1) = BUSDATA(N,4);
            tempV(N,1) = BUSDATA(N,3);
```

```
end
end

%Update bus voltage magnitudes and angles
    BUSDATA(:,3) = tempV;
    BUSDATA(:,4) = tempAng;

%xlswrite('Results.xlsm',tempV,6,'A1:A19');

%Print iteration results only
    fprintf('-----Results after iteration %d -----\n', iteration);
    fprintf('Bus Number    V(p.u.)         Phase angle (degrees) \n');

for N = 1:busnumber
        fprintf('%d',N);
        fprintf('             %6.4f',BUSDATA(N,3));
        fprintf('       %6.4f\n',BUSDATA(N,4)*deg);
end
```

- Objective function

```
function y = QFunction_correct(x,PG, G, B, BUSDATA)
% LINE LOSSES FUNCTION

[busnumber, busproperty] = size(BUSDATA);
G1 = zeros(1,busnumber);
G2 = zeros(1,busnumber);

y = sum(power(x(2*busnumber+2:end),2));
```

- Contraints

```
function [c, ceq] = Constraints(x,PG,S,BUSDATA, V2)
%NONLINEARCONSTRAINT Summary of this function goes here

[busnumber, busproperty] = size(BUSDATA);
H = zeros(1,busnumber);
H1 = zeros(1,busnumber);
H2 = zeros(1,busnumber);
H3 = zeros(1,busnumber);
H4 = zeros(1,busnumber);

%%%%%%% equality constraints %%%%%%%%%%%%%%
G1 = zeros(1,busnumber);
G2 = zeros(1,busnumber);

%%%%% Balanced power equations %%%%%
for N = 1:busnumber
if BUSDATA(N,2) ~= 1
for M = 1:busnumber
if  N ~= M && G(N,M) ~= 0
            G1(1,N) = G1(1,N)-(x(N)^2*G(N,M)-
x(N)*x(M)*(G(N,M)*cos((x(busnumber+N)-
x(busnumber+M)))+B(N,M)*sin((x(busnumber+N)-x(busnumber+M)))));
```

```
            G2(1,N) = G2(1,N)-(-x(N)^2*B(N,M)-
x(N)*x(M)*(G(N,M)*sin((x(busnumber+N)-x(busnumber+M))-
B(N,M)*cos((x(busnumber+N)-x(busnumber+M)))));
end
end
end
      G1(1,N) = PG(1,N)-G1(1,N);
      G2(1,N) = x(2*busnumber+N)-G2(1,N);
end

 G1(1,1) = 0;
 G2(1,1) = 0;

G3=x(20);       % slack bus angle
G4=x(39);       % slack bus reactive power reference
G5=x(1)-V2;     % slack bus voltage magnitude

%%%%%%%%%%%%%%%%%%%%%%%%%%%%%%%%%%%%%%%%%%%%%%%%%%%%%%%
%%%%%%%%% inequality constraints %%%%%%%%%%%%%

for N = 1:busnumber
if BUSDATA(N,2) ~= 1
        H(1,N) = power(PG(1,N),2)+power(x(1,2*busnumber+N),2)-
power(S(1,N),2);
        H1(1,N) = x(1,N)-1.026;      %upper limit for voltage
        H2(1,N) = 1-x(1,N);          %lower limit for voltage
        H3(1,N) = x(2*busnumber+N); % inverters only inject reactive power
        H4(1,N) = -x(busnumber+N);  % positive angles
end
end

%%%%%%%%%%%%%%%%%%%%%%%%%%%%%%%%%%%%%%%%%%%%%%%%%

ceq = [G1, G2, G3, G4, G5];                   % equality constraints
c = [H, H1, H2, H3, H4];              % inequality constraints

end
```

DigSILENT and MATLAB Load flow Results

In the Table F-1, the load flow results at each bus (voltage and angle) calculated using DigSILENT and MATLAB are compared.

Table F-1 DigSILENT and MATLAB load flow results comparison for 1 iteration

	DigSILENT RESULTS		MATLAB RESULTS	
Bus number	Voltage (p.u.)	Angle (deg.)	Voltage (p.u.)	Angle (deg.)
1	1.0136	0	1.0136	0
2	1.01955	0.2509	1.0201	0.2559
3	1.0252	0.4871	1.026	0.5029
4	1.0302	0.6927	1.0312	0.72
5	1.0334	0.8204	1.0345	0.8561
6	1.0361	0.9298	1.0373	0.9733
7	1.0381	1.0118	1.0394	1.0615
8	1.0397	1.0761	1.0411	1.131
9	1.0409	1.1229	1.0423	1.1817
10	1.0415	1.1463	1.0429	1.207
11	1.0255	0.4972	1.0263	0.5135
12	1.0317	0.7526	1.0328	0.7838
13	1.0328	0.7962	1.0339	0.8302
14	1.0335	0.8233	1.0346	0.8591
15	1.0337	0.8314	1.0348	0.8678
16	1.0364	0.9448	1.0377	0.9894
17	1.0412	1.1378	1.0427	1.1978
18	1.0416	1.1514	1.0431	1.2126
19	1.0139	0.0156	1.0142	0.0159

The maximum difference between the MATLAB and DigSILENT load flow results occurs at bus 18. The voltage error is 0.0016 p.u. which represents 0.57 [V] phase to ground and therefore can be considered negligible.

Appendix G

Source code for the client IEC 61850 application:

```
*********************************************************************************/
/*     ClientMain.c
                                  Includes
********************************************************************************/
#include <stdio.h>
#include <sys/stat.h>      //file stat check
#include "IEC61850API.h"
#include <conio.h>
#include <time.h>
#include "libxl.h"
/* Windows Headers */
#include <windows.h>

/*********************************************************************************
                                  Defines
*********************************************************************************/
#define FUNCTION_NAME_LEN 50
float Qref;
float Vg_input1=0;
float Pset1=0;
time_t t;

}ePrivateObjectType;

/*********************************************************************************
                    Callback function for Update from Server
/*********************************************************************************
void UpdateFunction(struct IEC61850_DataAttributeID* ptObjectID_DAID, const
IEC61850_ObjectData * ptNewValue)
{

GetConsoleScreenBufferInfo(hOut, &SBInfo);
if (ptNewValue->ucType == IEC61850_DATATYPE_FLOAT32)
{

if ((ptObjectID->uiField1==1)&&(ptObjectID->uiField2==2)&&(ptObjectID->uiField3==1))
       {

              memcpy(&Vg_input1,ptNewValue->pvData,(ptNewValue->uiBitLength/8));
              SetConsoleCursorPosition(hOut,VgRefIs1);
              printf("%f",Vg_input1);
              SetConsoleCursorPosition(hOut,SBInfo.dwCursorPosition);
       }

if ((ptObjectID->uiField1==1)&&(ptObjectID->uiField2==3)&&(ptObjectID->uiField3==1))
       {
              memcpy(&Pset1,ptNewValue->pvData,(ptNewValue->uiBitLength/8));
              SetConsoleCursorPosition(hOut,PRefIs1);
              printf("%f",Pset1);
              SetConsoleCursorPosition(hOut,SBInfo.dwCursorPosition);
       }
```

```
/*******************************************************************************************
                                        Client Main
 /*******************************************************************************************
int main(void)
{
       IEC61850      myClient = NULL;
       struct IEC61850_Parameters  tClientParam;
       int            iError = 0;
       unsigned char DLL_Loading_Failed=0;

       printf("\r\n *****************************************************************");
       printf("\r\n Client(PC) IEC 61850");
       printf("\r\n PED4-1043");
       printf("\r\n Vlad Muresan");
       printf("\r\n *****************************************************************");


//Load the Client ICD file
iError = DLL_IEC61850_LoadSCLFile(myClient,"Client_GSI.ICD");
if(iError != IEC61850_ERROR_NONE)
       {
       printf("\r\n Error loading Client_GSI.ICD %d. Please refer to API user manual for
       error message.", iError);
       SetConsoleCursorPosition(hOut,Position);
       printf("     "); //clear previous command
       SetConsoleCursorPosition(hOut,Position);
       break;
       }
//Start the 61850 Client
       iError = DLL_IEC61850_Start(myClient);
if(iError != IEC61850_ERROR_NONE)
       {
       printf("\r\n Client Start Error %d. Please refer to API user manual for error
       message.", iError);
       SetConsoleCursorPosition(hOut,Position);
       printf("     "); //clear previous command
       SetConsoleCursorPosition(hOut,Position);
       break;
       }

       *******************************************************************************
                                   Main processing loop
        *******************************************************************************

       Sleep(8000);
while(1)
       {
       //char c;
       IEC61850_ObjectData Value;
       struct IEC61850_DataAttributeID_Generic   Object = {0} ;


       if (Vg_input1!=0)
              {

                     Qref=(((Vg_input1-230.0)/230.0)*50)*1000; //Droop function
                     memset(&Object,0,sizeof(Object));
                     Object.uiField1 = 4;
```

```
                    Object.uiField2=1;
                    Object.uiField3=1;
                    Object.uiField4=0;
                    Object.uiField5=0;
                    Object.Generic_type = IEC61850_DAID_GENERIC;
                    Value.ucType =  IEC61850_DATATYPE_FLOAT32;
                    Value.uiBitLength = sizeof(Qref)*8;
                    Value.pvData = &Qref;


       iError = DLL_IEC61850_Write(myClient, (struct IEC61850_DataAttributeID*)&Object,
       &Value);
                    if(iError != IEC61850_ERROR_NONE)
                           {
printf("Failed to write the Qptimal to server ErrorCode:%d. Please refer to API user
manual for error message\n.",iError);
                                  SetConsoleCursorPosition(hOut,Position);
                                  printf("      "); //clear previous command
                                  SetConsoleCursorPosition(hOut,Position);
                           }
                           else {

                                  SetConsoleCursorPosition(hOut,QRefIs1);
                                  printf("%f",Qref);
                                  SetConsoleCursorPosition(hOut,Position);

                           }
                    }
                    Sleep(63000);
             }

/*****************************************************************************************
                                   Shutting down client
/*****************************************************************************************
             iError = DLL_IEC61850_Stop(myClient);
                    if(iError != IEC61850_ERROR_NONE)
                           {
                                  SetConsoleCursorPosition(hOut,ErrorPos);
printf("Failed to stop client: %i. Please refer to API user manual for error message.",
iError);
                           }
       } while(0);

       if( myClient != NULL )
       {
             DLL_IEC61850_Free(myClient);
       }
       if (hinst_61850DLL)
             FreeLibrary(hinst_61850DLL);
       SetConsoleCursorPosition(hOut,ErrorPos);
       printf("\r\n Application \'SystemCorp 61850 Client\' has terminated. Press Return
Key to Exit.");
       getchar();
       return(0);
}   // End main()
```

Source code for the server IEC 61850 application:

```
/**********************************************************************************
Servermain.c
                                         Includes
**********************************************************************************
#include <stdio.h>
#include <sys/stat.h>      //file stat check
#include <direct.h>  //file stat check
#include <conio.h>
#include <time.h>
#include <clib32.h>
#include "dSpaceClibInterface.h"

#include "IEC61850API.h"

typedef struct tag_61850ObjectInt // pointer to IEC61850 object
{
   int              iObjectValue;          /* Object Value */
}t61850IntObject;

enum
{
       VALUE  =1, // field 3 description
}e61850ObjectType;


}ePrivateObjectType;

/* Windows Headers */
#include <windows.h>

/**********************************************************************************
                                          Defines
**********************************************************************************

#define FUNCTION_NAME_LEN 50
t61850IntObject INVERTER;
int error;
int Qset=0;
float Vgnew;
double Vgnew_double;
UInt32 required_size = 500, mem_address;
float Vg_input;

/**********************************************************************************
                   Callback functions (read and write from the client)
/**********************************************************************************

int myIEC61850_WriteCallback(struct IEC61850_DataAttributeID* ptObjectID_DAID, const
IEC61850_ObjectData * ptNewValue)
       {
       float *float32=NULL;
       int ErrorCode = IEC61850_CB_ERROR_NONE;
       switch (ptNewValue->ucType) //The value is updated with the new value
       {
```

```
            case IEC61850_DATATYPE_FLOAT32:
            float32=(float *)ptNewValue->pvData;
            Vgnew=*float32;
if ((ptObjectID->uiField1==4)&&(ptObjectID->uiField2==1)&&(ptObjectID->uiField3==1))
            {
                   SetConsoleCursorPosition(hOut,QRefIs);
                   printf("%f",Vgnew);
                   SetConsoleCursorPosition(hOut,SetVgPos);
            }
          //*************WRITE VALUE TO DSPACE******************************
       error = initializedSpace(); //this part starts the board_register part
       if (error != 0)
       exit(1);

       error= initializedSpaceVariables(); //this part starts the functions part
       if (error != 0)
       exit(1);
       Vgnew_double=(double)(Vgnew);
       if (Vgnew_double!=0) {
       writeParameterValue((double)Vgnew_double, ReactivePowerAddress);
       error=DS_free_mem(board_index, &mem_address);
              }

       //*************************************************************************
              ErrorCode=IEC61850_CB_ERROR_NONE;
              break;
              }

       return ErrorCode;
       }

/*****************************************************************************
                                    61850 SERVER MAIN
/*****************************************************************************
int main(void)
{
       IEC61850 myServer = NULL;

       double  GridVoltageMagnitude, trip, inverter_state, VgRMS, IgRMS, PgRMS,
DCVoltage, DCCurrent, ActivePower, ReactivePower, Ref_ActivePower;
       float Vg=0, Pset=0;

*************************************************************************");
       printf("\r\n Server (IED) Application IEC 61850");
       printf("\r\n PED4-1043");
       printf("\r\n Vlad Muresan, IED1 station");
       printf("\r\n
*************************************************************************");

              //Load the Client ICD file
iError = DLL_IEC61850_LoadSCLFile(myServer,"Server_GSI.ICD");
if(iError != IEC61850_ERROR_NONE)
       {
printf("\r\n Error loading Server_GSI.ICD. %d. Please refer to API user manual for error
message.", iError);
              SetConsoleCursorPosition(hOut,Position);
              printf("     "); //clear previous command
              SetConsoleCursorPosition(hOut,Position);
```

```
              break;
       }
              //Start the 61850 Server
iError = DLL_IEC61850_Start(myServer);
if(iError != IEC61850_ERROR_NONE)
       {
printf("\r\n Server Start Error %d. Please refer to API user manual for error message.",
iError);
              SetConsoleCursorPosition(hOut,Position);
              printf("     "); //clear previous command
              SetConsoleCursorPosition(hOut,Position);
              break;
       }


/****************************************CLIB PART ************************************
// CLIB functions check & start inverter
// MEASUREMENTS of signals
**************************************************************************************

    error = initializedSpace();
       if (error != 0)
              exit(1);

       error= initializedSpaceVariables();
       if (error != 0)
              exit(1);

       writeParameterValue((double)0, ActivePowerAddress);
       writeParameterValue((double)0, ReactivePowerAddress);


       error = writePLL(0);
       error = writePLL(1);
       printf("\n");
       printf("\n");
       time(&t);
       printf("Time %s\n", ctime(&t));
       printf("PLL was reset\n");
       error = readGrigVoltageMagnitude(&GridVoltageMagnitude);
       printf("Grid voltage magnitude is %.2f\n", GridVoltageMagnitude);
       Sleep(500);

       error = readTripValue(&trip);
       if (trip==0)
              printf("Inverter interface problem. Check hardware!\n");
       else
              printf("No trip detected\n");

       error = writeInverterReset(1);
       Sleep(500);
       error = writeInverterReset(0);
       printf("Inverter was reset\n");
       Sleep(500);

       error = readInverterStartValue(&inverter_state);
       if (inverter_state==0)
       printf("Inverter is OFF. Please start the inverter\n");
```

```
	//START INVERTER

	error = writeInverterStartValue(1);
	printf("Inverter is ON!\n");
	Sleep(500);

	//WRITE ACTIVE POWER REFERENCE

	writeParameterValue((double)300, ActivePowerAddress);
	printf("\n");


		//PRINT VALUES FOR ENABLE AND TRIP
		SetConsoleCursorPosition(hOut,Enab);//enable
		if (inverter_state==1)
			{
			printf("ON");
		}
		if (inverter_state==0)
		{
			printf("OFF");
		}
		SetConsoleCursorPosition(hOut,SetTrip);
		if (trip==0)
			{
			printf("0");
		}
		else
		{
			printf("1");
		}


		Sleep(6000);

/*******************************main processing loop ***************************/

	while(x<4) {


			IEC61850_ObjectData Value;
			struct IEC61850_DataAttributeID_Generic  Object = {0} ;
			SetConsoleCursorPosition(hOut,SetVgRef);
			SetConsoleCursorPosition(hOut,InputPos);
			Position.Y=InputPos.Y;

				//MEASUREMENTS FROM DSPACE
			error = readParameterValue(&VgRMS, GridVoltageAddress);
			error = readParameterValue(&IgRMS, GridCurrentAddress);
			SetConsoleCursorPosition(hOut,IgPos);//Pref
			printf("%lf", IgRMS);
			error = readParameterValue(&PgRMS, GridPowerAddress);
			error = readParameterValue(&DCVoltage, DCVoltageAddress);
			SetConsoleCursorPosition(hOut,VdcRefIs);//Pref
			printf("%lf", DCVoltage);
			error = readParameterValue(&DCCurrent, DCCurrentAddress);
```

```
                    SetConsoleCursorPosition(hOut,IdcRefIs);//Pref
                    printf("%lf", DCCurrent);
                    error = readParameterValue(&ActivePower, ActivePowerAddress);
                    error = readParameterValue(&ReactivePower, ReactivePowerAddress);
                    Sleep(500);



                        Vg=(float)(VgRMS);
                           if  (Vg!=0) {

                           SetConsoleCursorPosition(hOut,Position);

                           memset(&Object,0,sizeof(Object));
                           Object.uiField1 = 1;
                           Object.uiField2=2;
                           Object.uiField3=1;
                           Object.uiField4=0;
                           Object.uiField5=0;
                           Object.Generic_type = IEC61850_DAID_GENERIC;
                           Value.ucType =  IEC61850_DATATYPE_FLOAT32;
                           Value.uiBitLength = sizeof(Vg)*8;
                           Value.pvData = &Vg;
                           //write to the control
iError = DLL_IEC61850_Update(myServer, (struct IEC61850_DataAttributeID*)&Object,
&Value);
                           if(iError != IEC61850_ERROR_NONE)
                           {
                                  SetConsoleCursorPosition(hOut,ErrorPos);
                                  printf("Failed to write the grid voltage ErrorCode:%d.
Please refer to API user manual for error message.",iError);
                                  SetConsoleCursorPosition(hOut,Position);

                           }
                           else {
                                  SetConsoleCursorPosition(hOut,VgPos);
                                  printf("%f",Vg);
                                  SetConsoleCursorPosition(hOut,Position);
                                   }
                                                }

                    if  (Vg!=0){

                           SetConsoleCursorPosition(hOut,Position);
                           Pset=(float)(ActivePower);
                           memset(&Object,0,sizeof(Object));
                           Object.uiField1 = 1;
                           Object.uiField2=3;
                           Object.uiField3=1;
                           Object.uiField4=0;
                           Object.uiField5=0;
                           Object.Generic_type = IEC61850_DAID_GENERIC;
                           Value.ucType =  IEC61850_DATATYPE_FLOAT32;
                           Value.uiBitLength = sizeof(Pset)*8;
                           Value.pvData = &Pset;
                           //write to the control
                           iError = DLL_IEC61850_Update(myServer, (struct
IEC61850_DataAttributeID*)&Object, &Value);
```

```
                                if(iError != IEC61850_ERROR_NONE)
                                {
                                        SetConsoleCursorPosition(hOut,ErrorPos);
                                        printf("Failed to write the grid voltage ErrorCode:%d. 
Please refer to API user manual for error message.",iError);
                                        SetConsoleCursorPosition(hOut,Position);

                                }
                                else {
                                        SetConsoleCursorPosition(hOut,PRefIs);
                                        printf("%f",Pset);
                                        SetConsoleCursorPosition(hOut,Position);
                                         }
                                                     }



                                else{//exit
                                        SetConsoleCursorPosition(hOut,ErrorPos);
                                        printf("Voltage magnitude is not in the prescribed 
limits 0.85Vg.....1.15Vg ",iError);

                                                _getch();
                                        break;
                                        }
                        x++;
                        Sleep(20000);
                        }

        /*********************************************************************************
                                        Shutting down client
        *********************************************************************************
                iError = DLL_IEC61850_Stop(myServer);
                error = writeInverterStartValue(0); //stop the inverter
                if(iError != IEC61850_ERROR_NONE)
                {
                        SetConsoleCursorPosition(hOut,ErrorPos);
                        printf("Failed to stop client: %i. Please refer to API user manual 
for error message.", iError);
                }
        } while(0);

        if( myServer != NULL )
        {
                // End of program
                DLL_IEC61850_Free(myServer);
        }
        if (hinst_61850DLL)
                FreeLibrary(hinst_61850DLL);
        SetConsoleCursorPosition(hOut,ErrorPos);
        printf("\r\n Application \'SystemCorp 61850 Server\' has terminated. Press Return 
Key to Exit.");

        return(0);
}
```

Appendix H

Validation plots of IEC 61850 Client/Server Application

This section presents the complete experimentally validation plots for the client/server application from Chapter 5, section 5.3. Each simulated iteration is shown.

I. Iteration 1

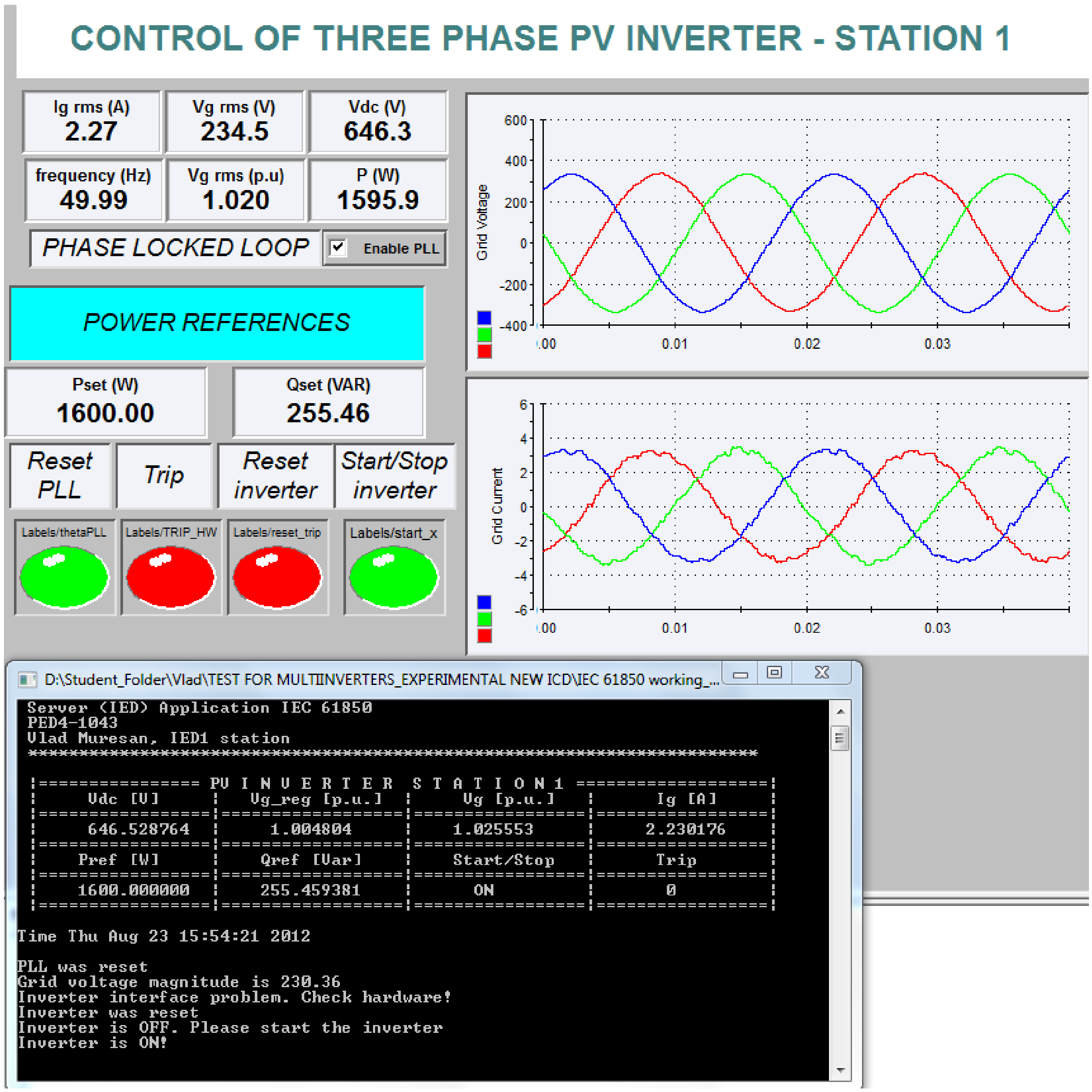

Figure H-1 Iteration 1, Station 1 server console application and Control Desk

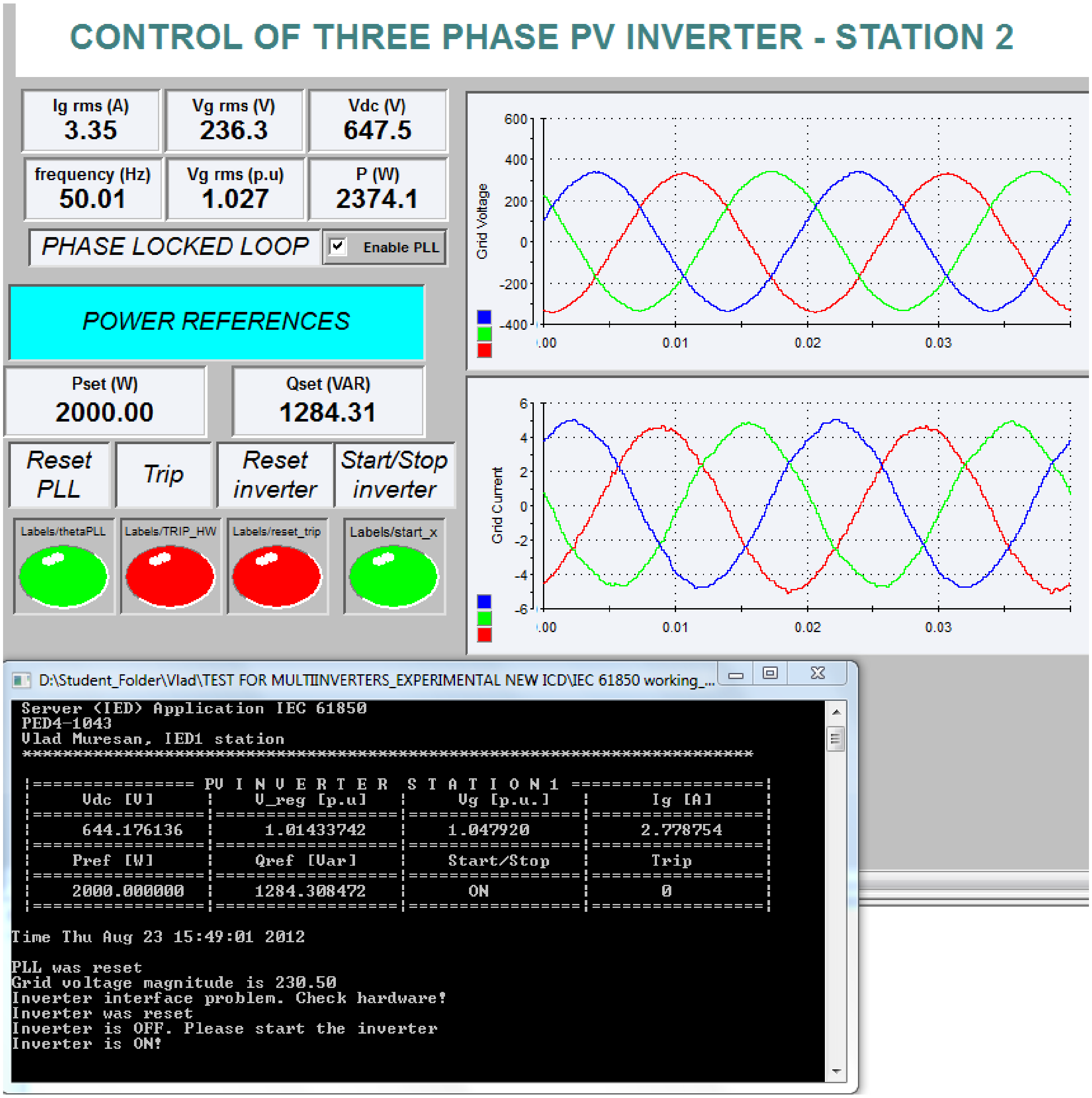

Figure H-2 Iteration 1, Station 2 server console application and Control Desk

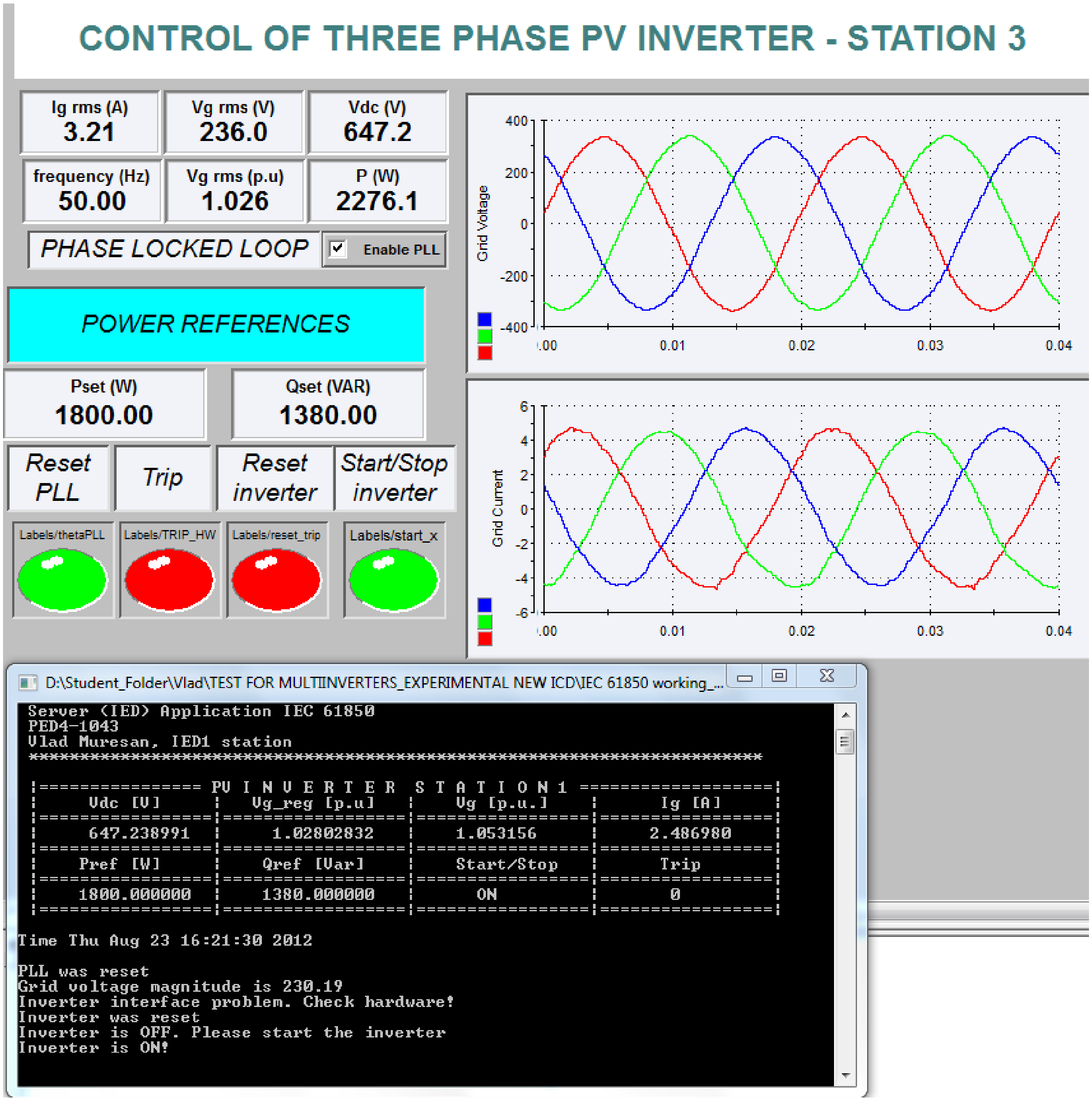

Figure H-3 Iteration 1, Station 3 server console application and Control Desk

Figure H-4 Iteration 1, Client console applications

II. Iteration 2

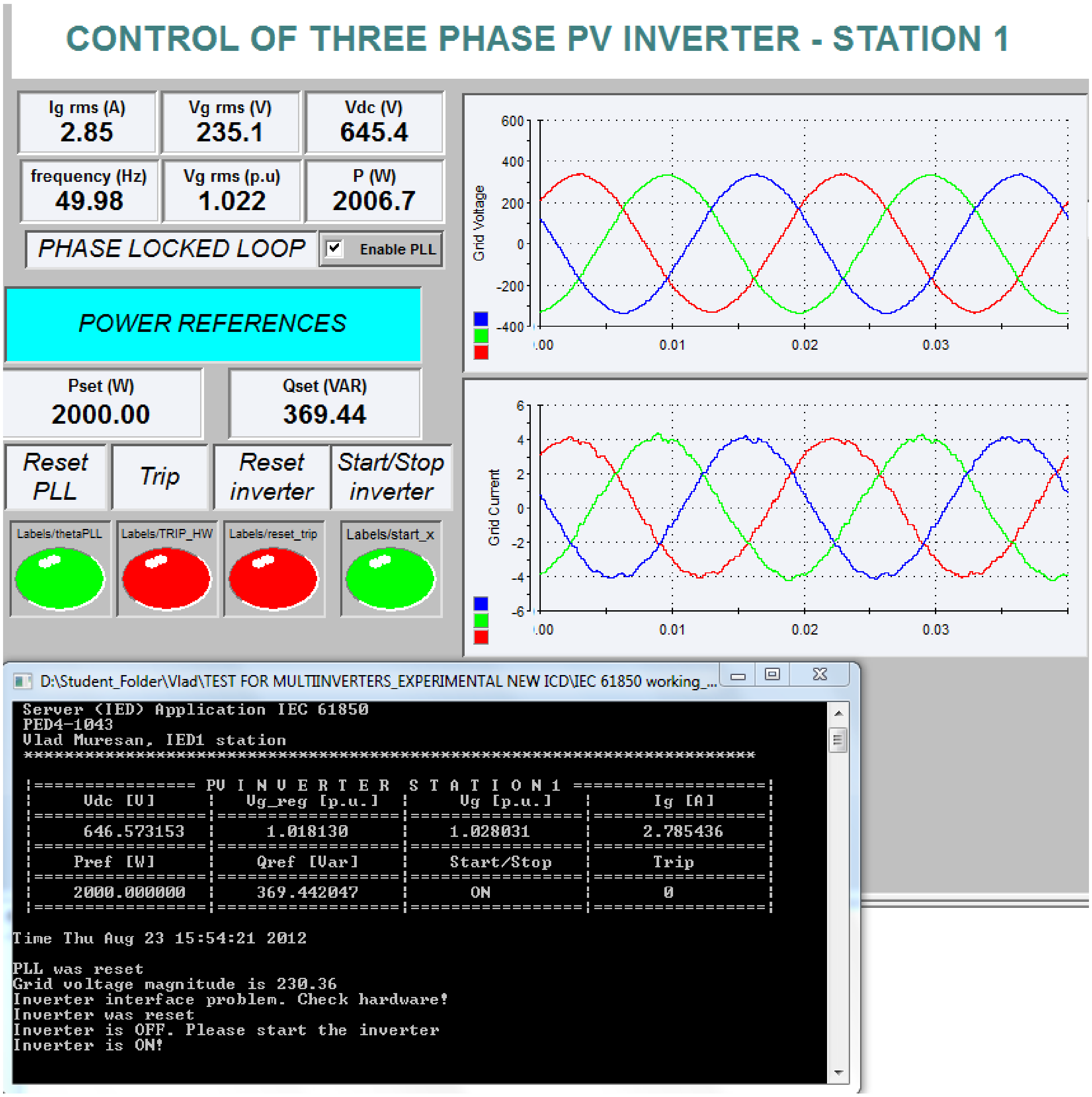

Figure H-5 Iteration 2, Station 1 server console application and Control Desk

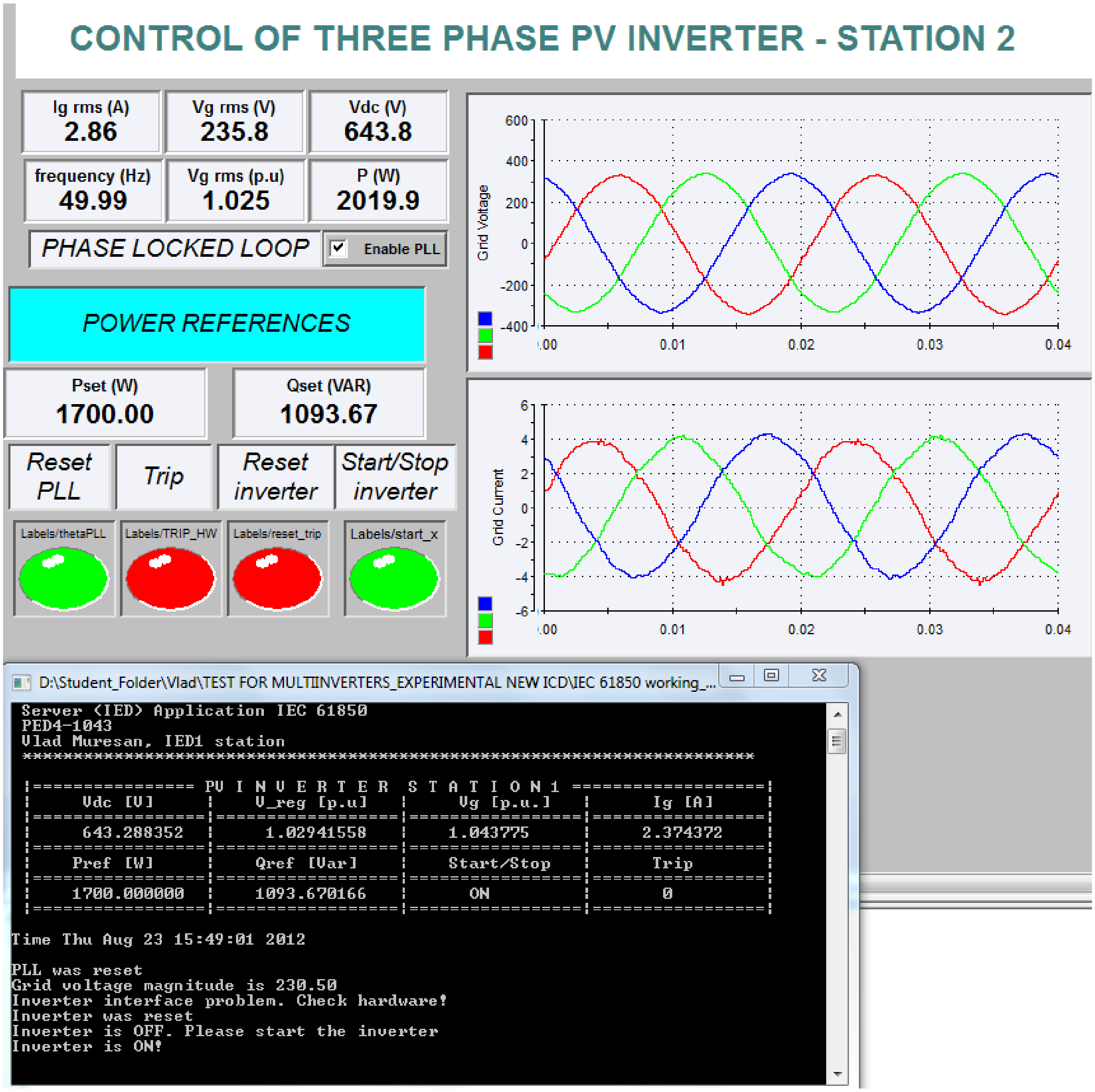

Figure H-6 Iteration 2, Station 2 server console application and Control Desk

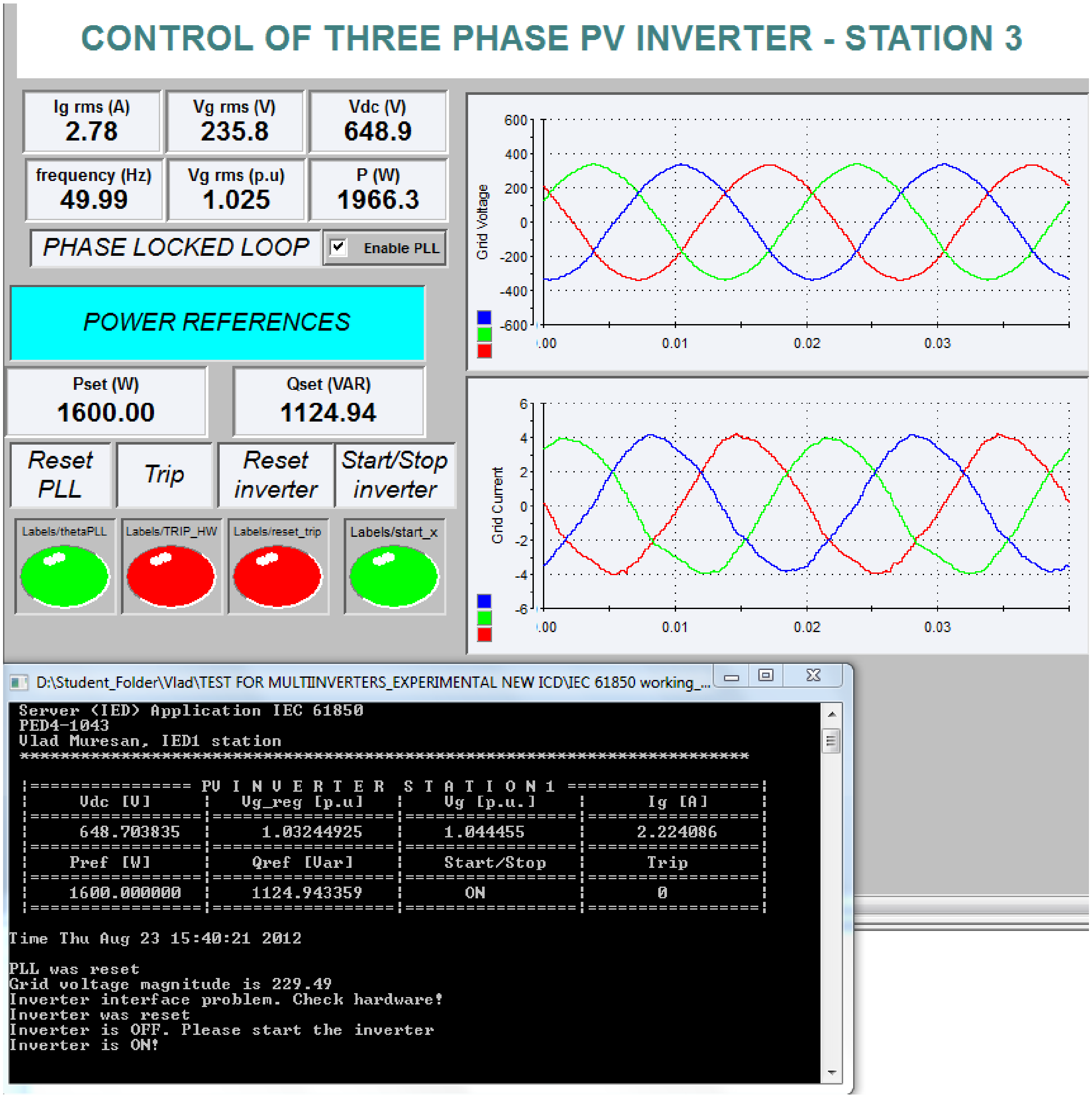

Figure H-7 Iteration 2, Station 3 server console application and Control Desk

Figure H-8 Iteration 2, Client console applications

III. Iteration 3

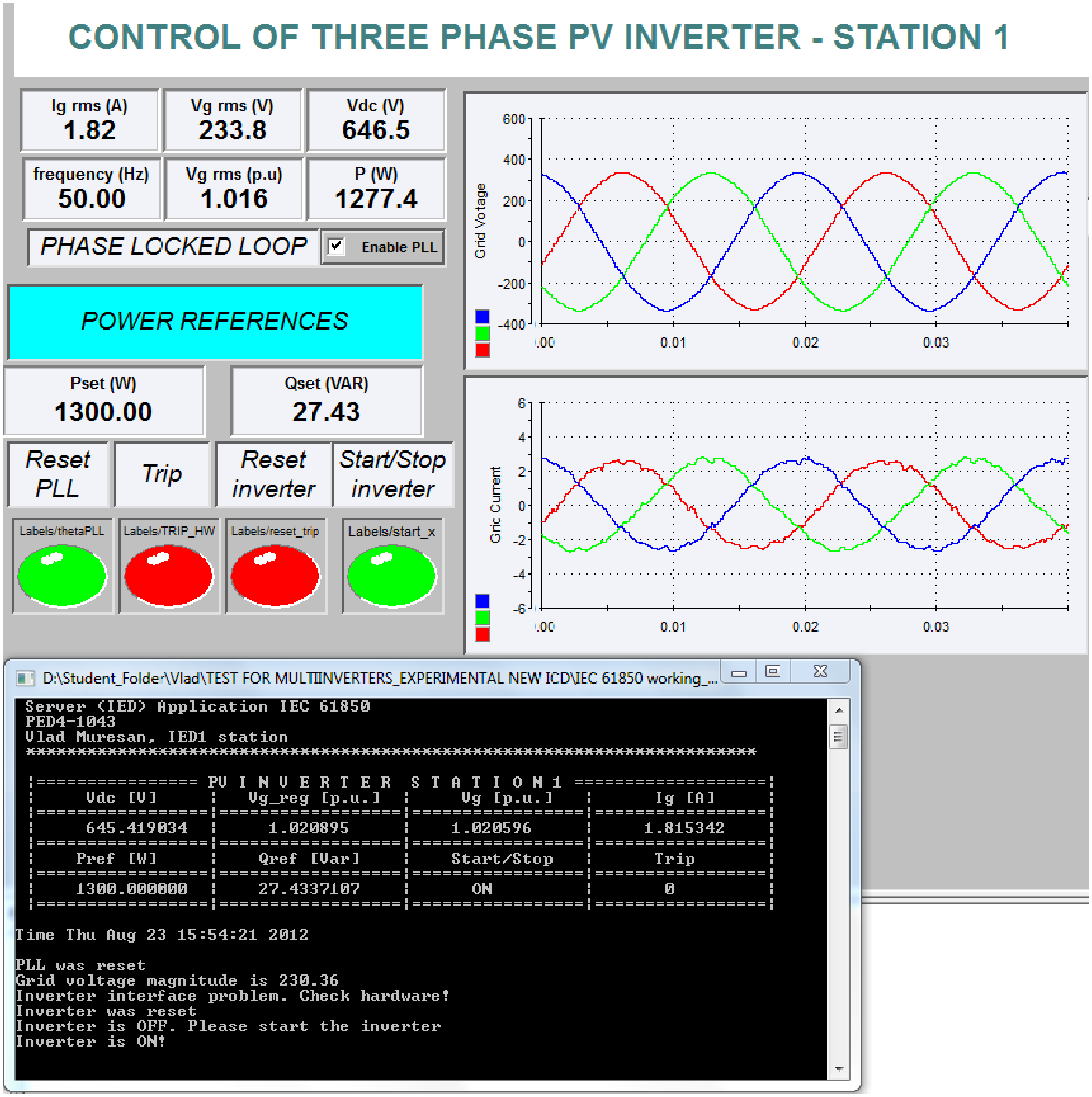

Figure H-9 Iteration 3, Station 1 server console application and Control Desk

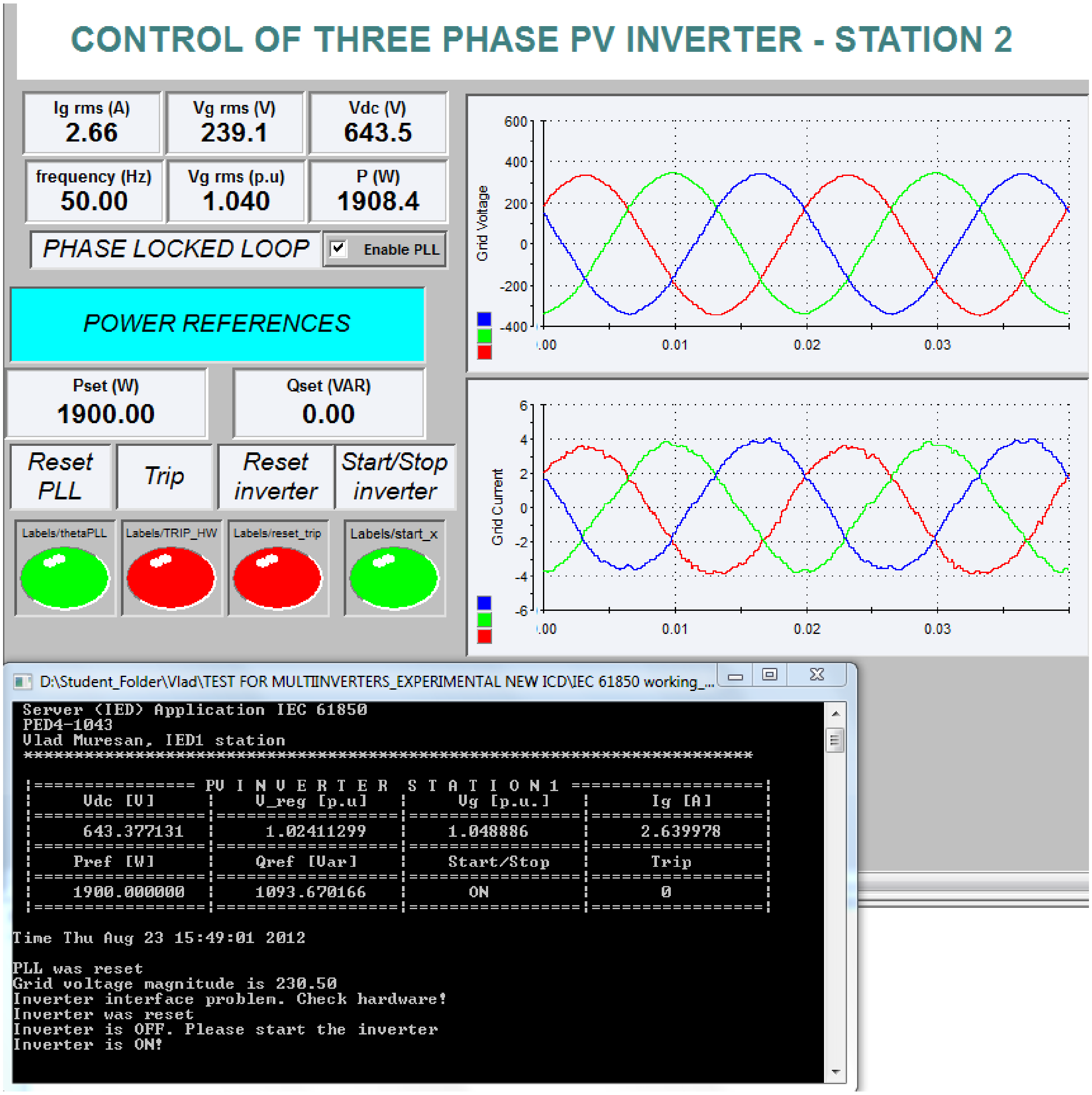

Figure H-10 Iteration 3, Station 2 server console application and Control Desk

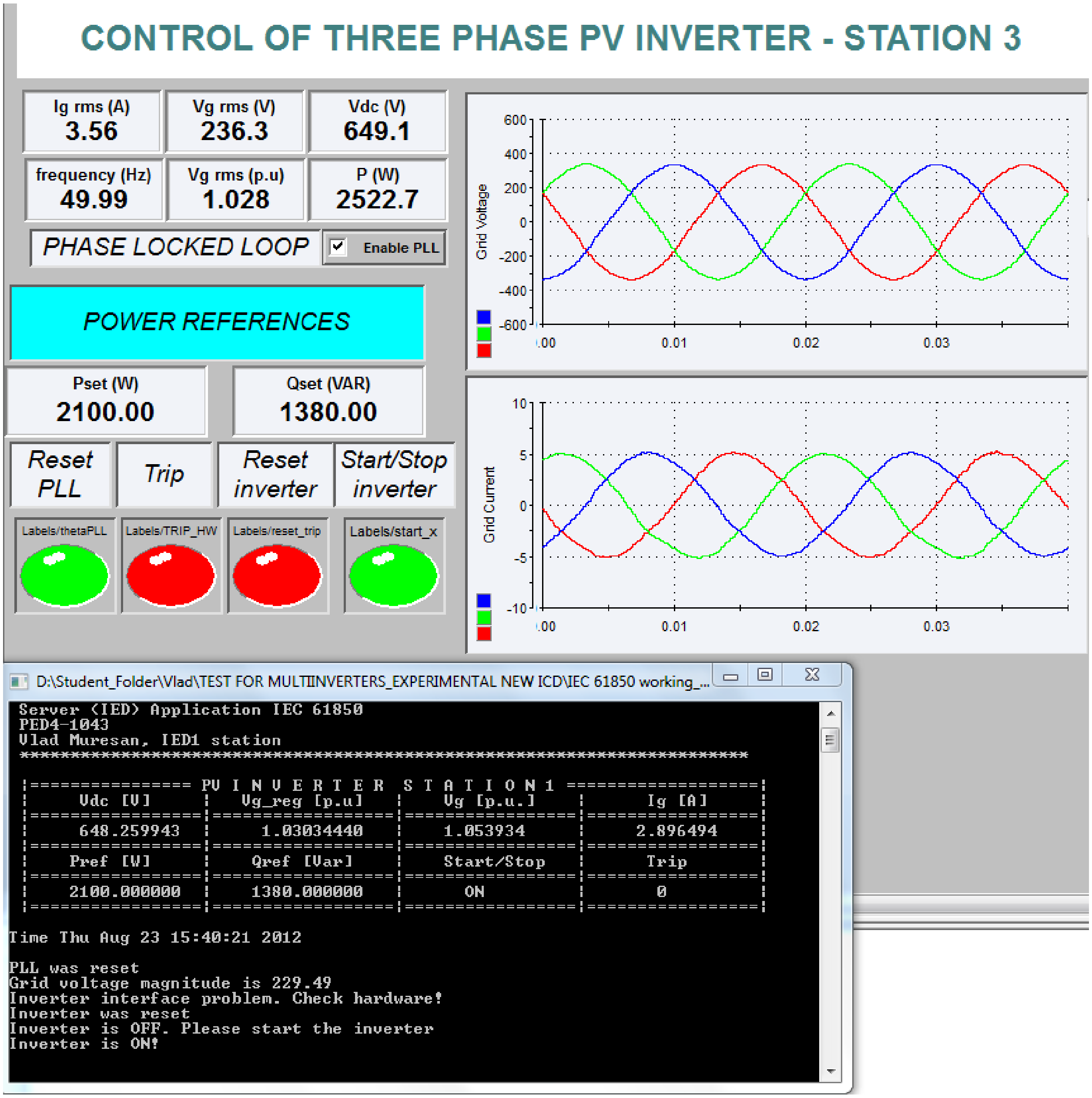

Figure H-11 Iteration 3, Station 3 server console application and Control Desk

Figure H-12 Iteration 3, Client console applications

IV. Iteration 4

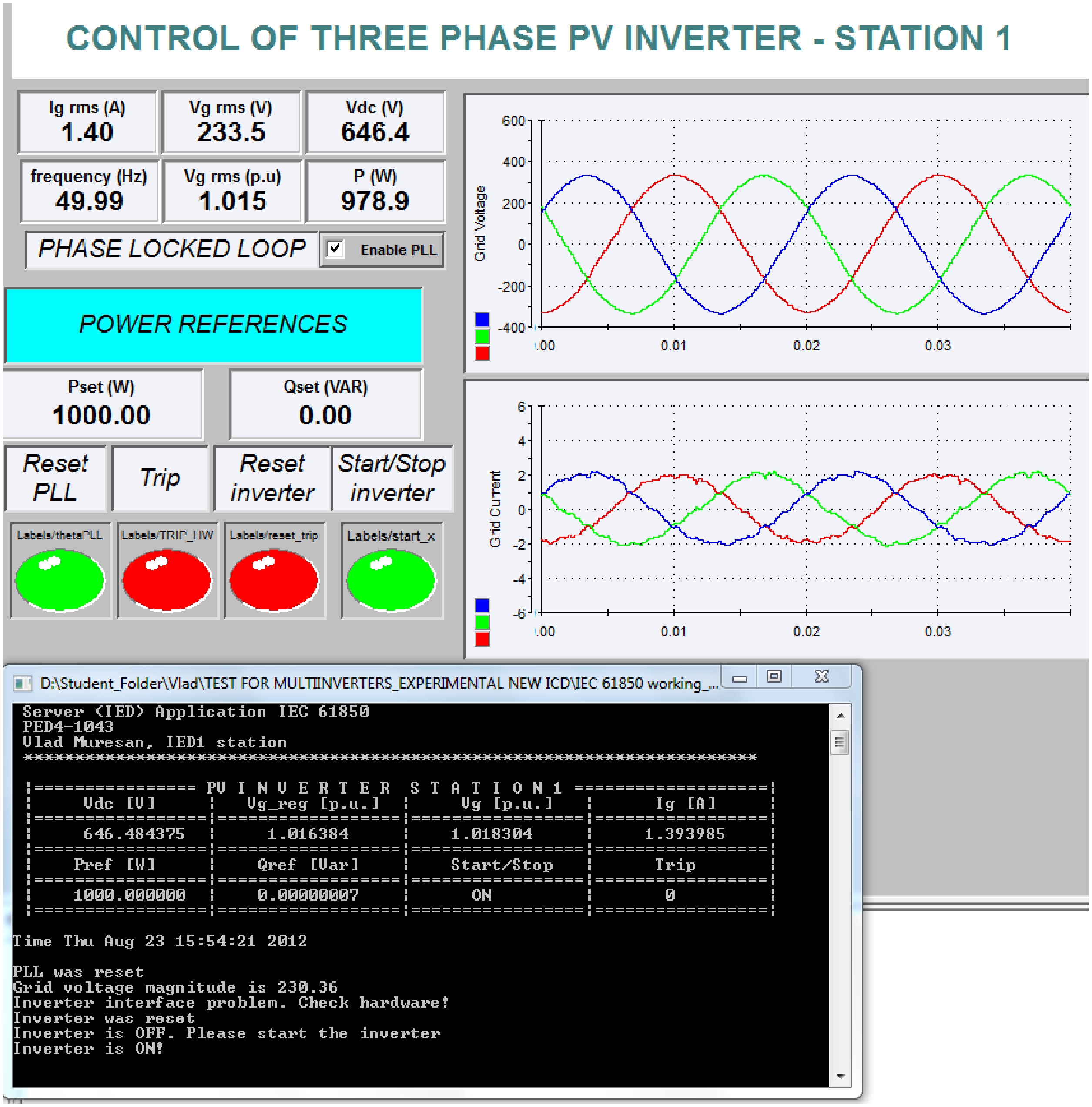

Figure H-13 Iteration 4, Station 1 server console application and Control Desk

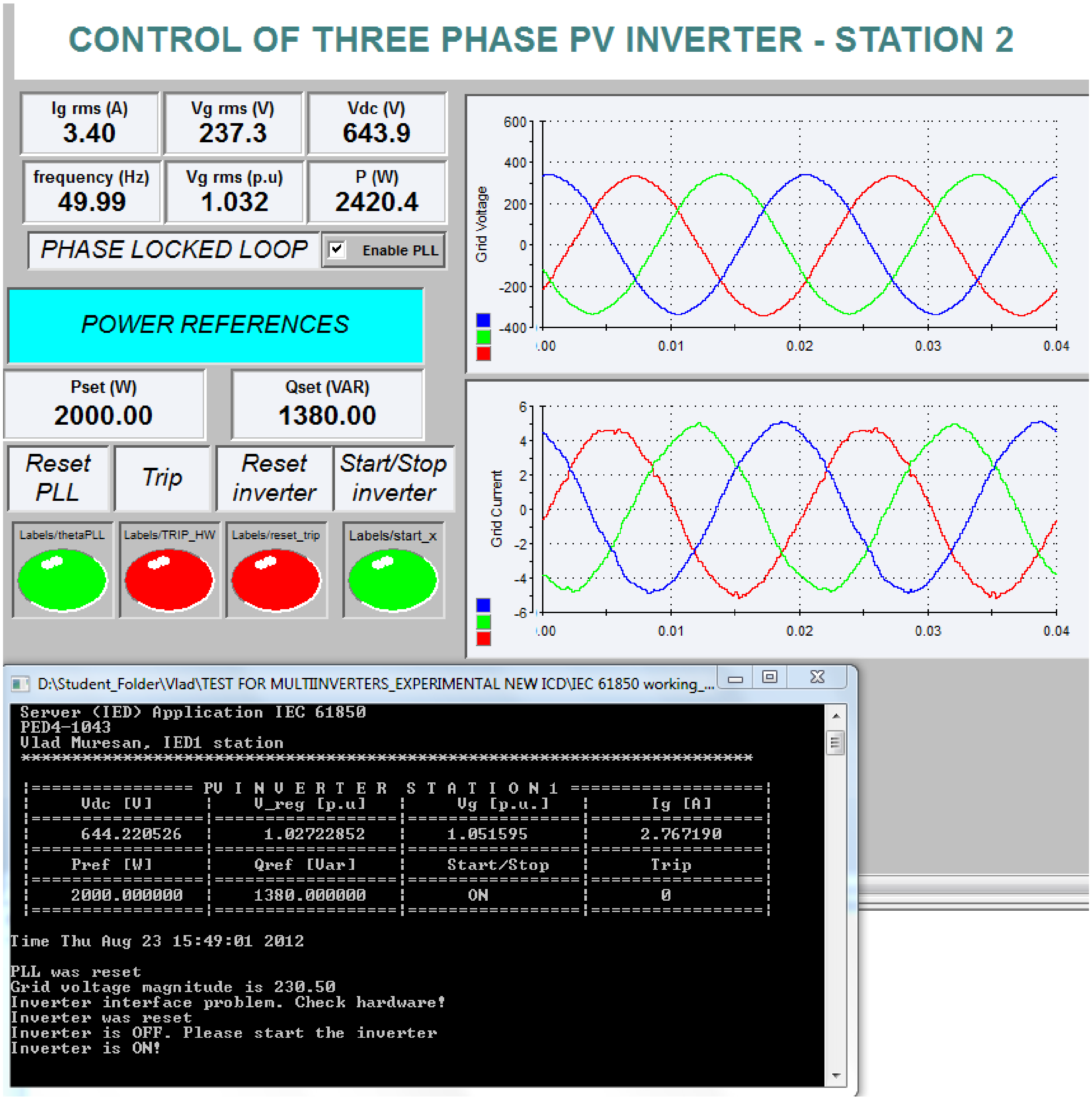

Figure H-14 Iteration 4, Station 2 server console application and Control Desk

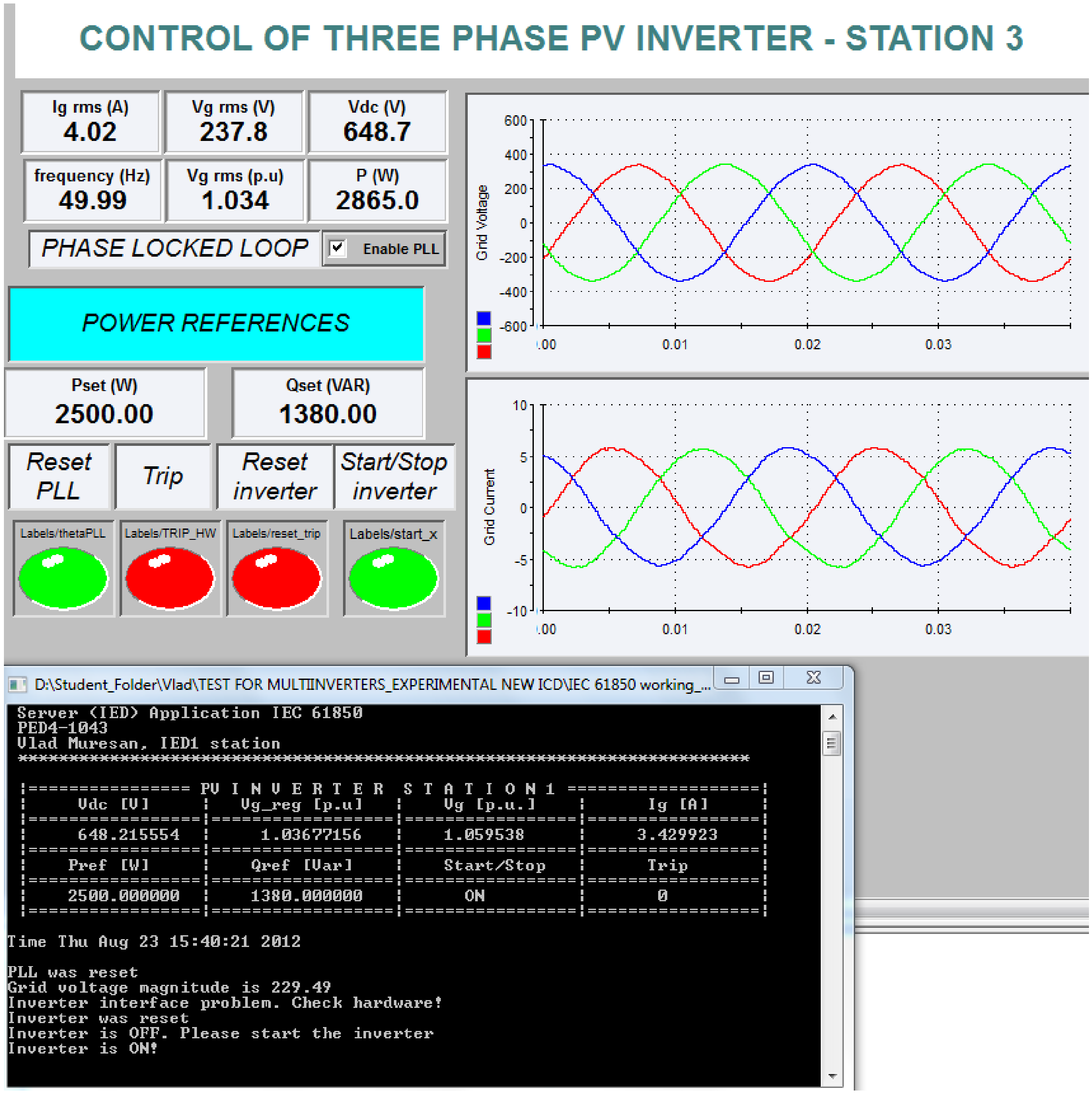

Figure H-15 Iteration 4, Station 3 server console application and Control Desk

Figure H-16 Iteration 4, Client console applications

Appendix I - Publication

B.I.Craciun, D.Sera, E.A.Man, V.Muresan, T. Kerekes, R.Teodorescu

Improved Voltage Regulation Strategies by PV Inverters in LV Rural Networks;

Power Electronics for Distributed Generation Systems (PEDG) 2012, Page(s) 775-781.

Improved Voltage Regulation Strategies by PV Inverters in LV Rural Networks

Bogdan-Ionut Craciun
Department of Energy Technology
Aalborg University
Pontoppidanstraede 101
9220 Aalborg, Denmark
bic@et.aau.dk

Elena Anamaria Man
Department of Energy Technology
Aalborg University
Pontoppidanstraede 101
9220 Aalborg, Denmark
eman10@student.aau.dk

Vlad Alexandru Muresan
Department of Energy Technology
Aalborg University
Pontoppidanstraede 101
9220 Aalborg, Denmark
vmures10@student.aau.dk

Dezso Sera
Department of Energy Technology
Aalborg University
Pontoppidanstraede 101
9220 Aalborg, Denmark
des@et.aau.dk

Tamas Kerekes
Department of Energy Technology
Aalborg University
Pontoppidanstraede 101
9220 Aalborg, Denmark
tak@et.aau.dk

Remus Teodorescu
Department of Energy Technology
Aalborg University
Pontoppidanstraede 101
9220 Aalborg, Denmark
ret@et.aau.dk

Abstract—**The growth of world energy demand and the environmental concerns lead to an increase of renewable energy production over the last decade. The increased number of grid-connected photovoltaic (PV) systems gave rise to problems concerning the stability and safety of the utility grid, as well as power quality issues. Lately, PV generators are required, according to the new German Grid Code (GC), to contribute to the grid stability and to provide grid classical functions during normal and abnormal operation. The purpose of this article is to investigate and optimize the standard voltage regulation methods for low voltage (LV) grid-connected PV systems. Reactive power supply strategy proposed by the German GC Q(U) is investigated and simulated performing load flow analysis on a European residential network benchmark. In order to improve the reactive power transfer in the system, an optimized algorithm of voltage regulation is designed with the aim of minimizing the losses in the system for a better integration of PV power generation into the grid.**

I. Introduction

Over the last decade various reasons have determined a continuous increase of the PV power systems. Some of them are the price drop of PV modules manufacturing, better social acceptance of PV parks or government support for renewable energy [1].

According to European Photovoltaic Industry Association (EPIA), at the end of 2011 the total installed PV capacity in the world has reached over 67.4 GW, with an increase of 68.5 % comparable to 2010. Europe still leads the market with over 50 GW of cumulative power installed with a 70 % increase in 2011. Italy became for the first time the top PV market in 2011 with 9 GW of newly connected capacity, with an impressive 290% increase from 2010 [2]. This increase was a consequence of advantageous tariffs if the systems were installed by the end of 2010 and connected until mid 2011. Germany was the second big player on the PV market in 2011 with 7.5 GW of new connected systems with a 44% increase from 2010 where more than 80% of the installed systems were located in the LV network [2, 3].

The fast expansion of PV system into the lower parts of the grid raised several concerns for grid reinforcement. In consequence, grid operators had to impose strict operational rules in order to keep the LV grid under control and to harmonize the behavior of all distributed generators connected to it in terms of reliability, efficiency and costs [4][5].

The first cost-effective measure, which brought a major improvement to the grid stability, was for the grid operators to suggest PV systems manufacturers to equip their products with grid support functions [6]. It is expected that until the end of 2015, the shipments of smart inverters in terms of MW will have a market share of 60 %, overtaking the standard inverter. Still, most of them will have only reactive power capabilities [7].

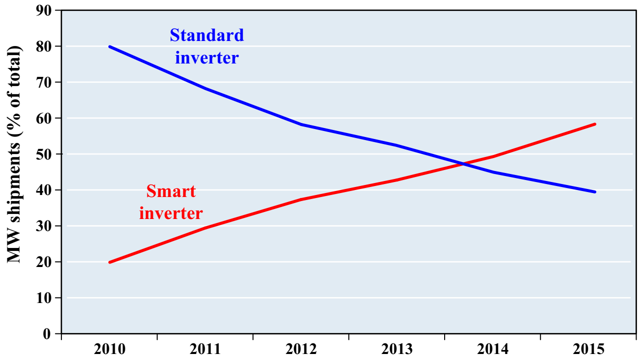

Fig. 1Total world market share for standard and smart PV inverters [7]

II. GRID INTERFACE REQUIREMENTS IN LV NETWORKS

The integration of large amounts of PV systems to the LV networks increases the generation of active power which leads to voltage rise along the feeder and can exceed the limits imposed by the GCs or can cause unexpected tripping of other grid-connected PV systems. Therefore, the PV capacity is limited and further investments of transformer and lines upgrade are needed [8-12].

According to the new German GC [13], the maximum voltage variation at the point of common coupling (PCC) after the connection of a distributed generator is maximum 3%. Therefore the PV capacity is limited by:

$$V_{pcc} \leq 1.03 \cdot V_n \tag{1}$$

$$\text{Transf.loading}_{max} = 100\% \tag{2}$$

Where: V_n is the voltage at the PCC before the connection of the PV system.

Besides the above mentioned limitations, rural LV networks are characterized by long distances between distribution transformer and consumers having large R/X ratios which are usually bigger than 1. This disadvantage results in limited reactive power flow along the cables [12, 14-16].

The network configuration chosen to be studied is a European LV benchmark and it can be seen in Fig. 2. [17].

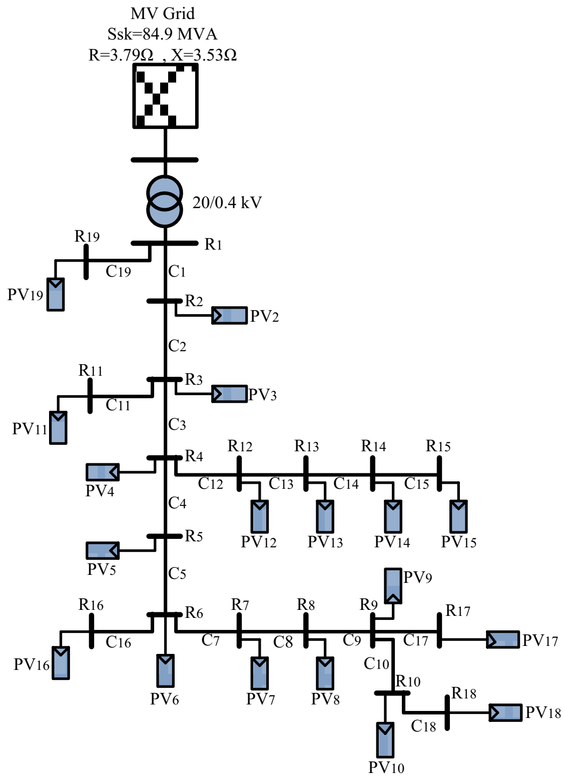

Fig. 2 European subnetwork benchmark [17]

The network is composed of a 100 kVA 20/0.4 kV transformer, one main feeder and two sub-feeders. For simplification purposes the impedances of the cables used to connect the PV system to the LV grid were assumed to be negligible, therefore, in the calculation process they were neglected. For simulation purposes, to observe the impact of PV generators over the LV network, 18 PV systems were analyzed, each having a peak installed power of 5 kW. The PV generators are three-phase connected and they operate with reactive power output corresponding to a minimum power factor of 0.9. The distance between the PV generators was chosen to be between 30m and 35m, depending on the LV topology. The complete data of the LV network can be found in Table I [17, 18].

TABLE I
Rural LV network specifications

External Grid	S_{SK}=84.9 MVA; R=3.79 Ω; X=3.53 Ω
Distribution transformer	S=100 kVA Dy5; 20/0.4 kV; ukr=4%; urr=2%;
LV Branch Feeder conductor (C11, C15, C16, C17, C18, C19)	NAYY 4x70 mm^2 AL OLH; R=0.413 Ω/km; X=0.3 Ω/km; length=0.3 km;
LV Branch Feeder conductor (C1, C2, C3, C4, C5, C7, C8, C9, C10, C12, C13, C14)	NAYY 4x70 mm^2 AL OLH; R=0.413 Ω/km; X=0.3 Ω/km; length=0.35 km;

The overhead cables between individual systems have impedance $Z = (0.413 + j0.300)$ Ω/km which resulted in an R/X ratio of 1.37. Therefore, the active power has greater impact over the grid voltage and causes voltage rise during high PV generation period. In this situation, the probability of voltage violation is higher than in the other typical networks such as urban and suburban given the fact that the character of those networks is more inductive.

In order to determine the maximum PV capacity which can be installed in residential LV networks and how PV systems are influencing the grid, test studies were performed using the simulation software Power Factory from DigSILENT and MATLAB.

The considered input data in terms of active power production was chosen from a real generation profile [19]. The measurements have a resolution of 15 min and they record the active power generation of a residential PV system during a day with high irradiance in June 2007. For the network presented in Fig. 2, 9 active power generation profiles were developed using the data from [19]. Each generation profile was assigned to 2 PV systems. In Fig. 3, the PV generation profile for PV8 and PV17 for one day in June 2007 is shown as an example.

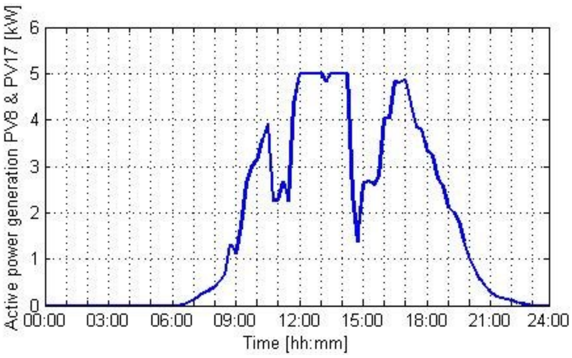

Fig. 3 PV8 & PV 17 power generation profile June 2007 [19]

In order to mitigate the voltage rise problem on the chosen LV network, successive load flow calculations are performed. The bus where the low-voltage side of the transformer is connected (R1) was chosen to be the slack bus and the PV generators are modeled as PQ sources. The initial conditions for the load flow calculation are: voltage magnitude $V_i^{pcc} = 1\,\text{p.u.}$ and angle $\delta_i = 0$. These conditions refer to all the buses in the network (slack and PQ buses).To emphasize the voltage increase due to PV power generation, a study case with zero load demand was considered.

First load flow analysis must be performed with the following conditions: maximum active power generation and no reactive power consumption. The purpose of this study is to examine the maximum voltage levels in the network and, based on these values, a reactive power compensation strategy can be proposed.

In this case, taking PV17 as an example, it can be observed from Fig. 4 the voltage rise at node R17 is violating the 3% threshold stated in the German standard.

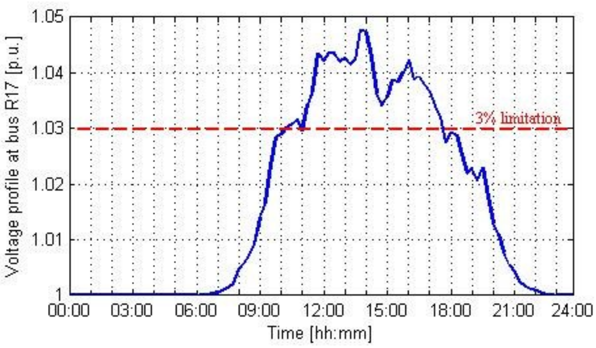

Fig. 4 Voltage profile for PV17 connected to node R17 when no voltage regulation methods are applied

In order for the whole system to be inbounded under the 3% voltage limit and to avoid power curtailment, PV generators have to adopt voltage regulation methods.

III. VOLTAGE REGULATION METHODS

To overcome the voltage variation problem with minimum reinforcement of the grid, the system operators recently adopted new GCs [13, 20] which require from PV generators to be more flexible and to provide voltage regulation techniques. For this purpose, different methods are proposed with the focus on static droop characteristics. The main voltage regulation methods are the following:

- Power factor characteristic: cosφ (P) method
- Fixed power factor: cosφ method
- Fixed reactive power: Q method
- Reactive power /voltage characteristic: Q(U)

The fixed cosφ and Q methods assign a corresponding power factor respectively reactive power reference for the PV generators based on the network power flow investigation. Load power profile information and PV power production are needed in order to assign a reasonable fixed reactive power set values to the inverters. Studies have shown that fixed cosφ and Q methods are not suitable for the LV networks due to their incapability of maintaining the voltage within limits and unnecessary reactive power consumption/absorption [9, 14, 18].

The cosφ (P) method is calculating the reactive power reference depending on the active power generation of the PVs. When the power generation value reaches half of the PV nominal power, the power factor decreases towards 0.9 and reactive power is absorbed based on a cosφ (P) droop characteristic. This method does not use the grid voltage information and is only assuming that high power generation matches the voltage increase [18].

The Q(U) strategy calculates the reactive power reference for each PV system depending on the voltage magnitude at the corresponding PCC. Therefore, the PV systems situated at the end of the feeder will start absorbing reactive power earlier than the PV systems located near the transformer. Moreover, the voltage magnitude at the buses near the transformer is likely to be within prescribed limits; hence they will not participate in the regulation process, making the task more difficult for the other PV systems.

The aim of this paper is to optimize the Q(U) regulation algorithm in terms of using the available capacity of all the PV inverters in the regulation process and avoid stressing the ones at the end of the feeder. This optimization strategy can be implemented on a centralized controller which could gather the information from all the PV systems and based on the voltage values it can calculate the optimal reactive power reference for each PV system.

The focus of the optimized Q(U) algorithm is to:

- Maintain the voltages at the PCCs below the specified limit
- Minimize the reactive power absorption of the overall network, hence minimize the losses in the line

A. Q(U) method

As stated in the German GC [13], the droop curve for the Q(U) method is provided by the network operator. Therefore, a droop characteristic specific for the network studied in this article must be designed. Based on the results of the first load flow analysis, for the maximum voltage value, the corresponding maximum reactive power absorption value can be assigned. As it can be seen from Fig. 4, this value can be taken as 1.05 p.u. because when there is no reactive power absorption in the network, the voltage magnitude does not exceed 1.05 p.u.. The start value for absorbing reactive power is chosen to be 1.02 p.u.. Using these values, the droop characteristic can be achieved and the Q(U) regulation method can be implemented (Fig. 5) [18].

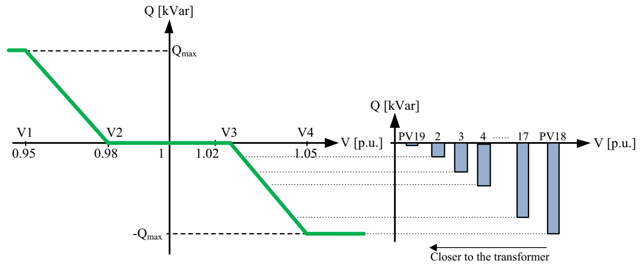

Fig. 5 Static droop curve for Q(U) method

Where V_1, V_2, V_3 and V_4 are the defined voltage values {0.95, 0.98, 1.02, 1.05}p.u. and V_{meas} is the measured voltage.

The flowchart presented in Fig. 6 the implementation of the Q(U) method. For this purpose the DigSilent Power Factory software was used and for each iteration, two load flow analysis are performed. First, the effect of active power generation on the voltage magnitude is investigated. Based on the measurement, an individual reactive power is assigned to each PV and a new load flow analysis is performed in order to check if the problem has been suppressed.

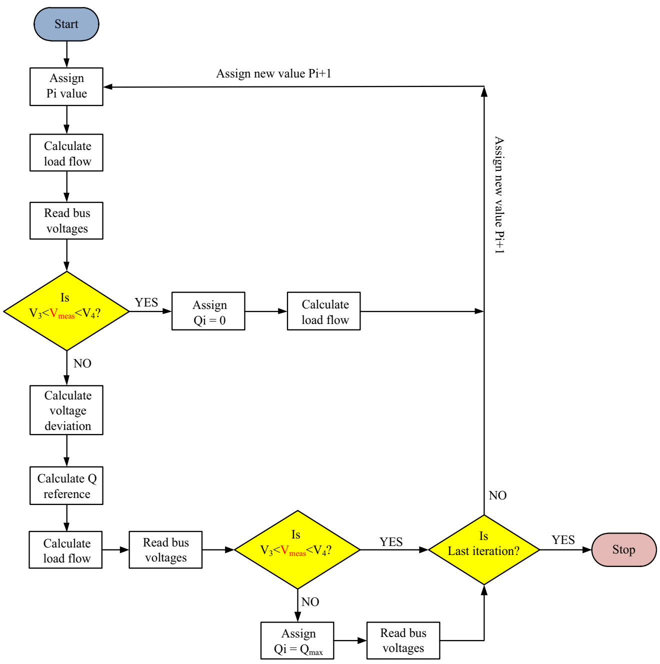

Fig. 6 Load flow simulation algorithm for Q(U) method

The algorithm for Q(U) method can be summarized by the script from (3). It can be mentioned that for the LV network studied in this article, the only concern is the voltage rise problem and PV systems are required only to absorb reactive power, therefore only the corresponding part from the Q(U) scrip was considered for implementation.

$$Q = \begin{cases} Q_{max}; & V_{meas} < V_1 \\ \dfrac{V_{meas} - V_1}{V_1} \cdot 100 \cdot Q_{max}; & V_1 < V_{meas} < V_2 \\ 0; & V_2 < V_{meas} < V_3 \\ \dfrac{V_{meas} - V_3}{V_3} \cdot 100 \cdot (-Q_{max}); & V_3 < V_{meas} < V_4 \\ -Q_{max}; & V_{meas} > V_4 \end{cases} \tag{3}$$

B. Optimized Q(U) algorithm

Nomenclature:

N_b - total number of buses in the system

N_{PQ} - number of PQ buses in the system

V_i - voltage magnitude at bus i

P_i^{ref}, Q_i^{ref} - active and reactive power injected at bus i

S_i - rated power of PV inverters

G_{ij}, B_{ij} - mutual conductance and susceptance between bus i and j

G_{ii}, B_{ii} - self conductance and susceptance of bus i

θ_{ij} - voltage angle difference between bus i and j

The optimization problem treated in this subchapter refers to the reactive power dispatch problem. The optimization algorithm has a specific objective function to be minimized while satisfying some predefined equality and inequality constraints.

The objective of this algorithm is to calculate an optimal value for the reactive power reference of each PV inverter. In this way, all the inverters will participate in the voltage regulation process with an optimized percent of their available reactive power capacity. [21]

In order to achieve this objective, it is necessary to properly adjust some variables like voltage magnitude and angle in each node. The equality constraints are formed by the power flow equations while the inequality constraints are the limits on voltage magnitude at PCCs and the inverter capacity.

The objective function of the algorithm can be expressed as the sum of all the reactive power references of the PV systems:

$$F = \sum_{i=2}^{N_b} \left(Q_i^{ref}\right)^2 \tag{4}$$

The equality constraints are represented by the power flow equations:

$$P_i^{ref} - V_i \sum_{j=1}^{N_b} V_j (G_{ij} \cdot \cos\theta_{ij} + B_{ij} \cdot \sin\theta_{ij}) = 0, i \in N_b - 1 \tag{5}$$

$$Q_i^{ref} - V_i \sum_{j=1}^{N_b} V_j (G_{ij} \cdot \cos\theta_{ij} + B_{ij} \cdot \sin\theta_{ij}) = 0, i \in N_{PQ} \tag{6}$$

The inequality constraints are the following:

- Voltage limit at PCC:

$$V_i^{pcc} < 1.03 V_n, i \in N_b \tag{7}$$

- Inverter capacity:

$$\left(P_i^{ref}\right)^2 + \left(Q_i^{ref}\right)^2 \le S_i^2, i \in N_b - 1 \tag{8}$$

The first step consists of performing a load flow analysis with the given initial conditions and afterwards, the optimized Q(U) algorithm takes the calculated values and performs the optimization. The variables in the system are the reactive power reference ($Q_i^{ref} = 0$) as control variable and two state variables: voltage magnitude (V_i^{pcc}) and angles (δ_i). Taking into consideration the equality and inequality constrains, a feasible solution will be obtained. The new values will be given as reference to the inverters and another load flow analysis will be performed in order to check if the voltage is kept between limits.

C. *Study case results*

The performance of the above described methods is investigated based on the reactive power flow and voltage level.

The main difference between the two strategies is the fact that while for the first one, each PV inverter absorbs a calculated value of reactive power corresponding to its local voltage magnitude, for the second strategy, the amount of reactive power values are computed based on all the PCC voltages of the network. In consequence, the optimized Q(U) algorithm makes the LV network more flexible in terms of connecting more PV systems.

In the first case, the behavior of the PV3 system was investigated. Knowing that the system is closer to the transformer, there was no overvoltage problem at the corresponding PCC, as seen from Fig. 7.

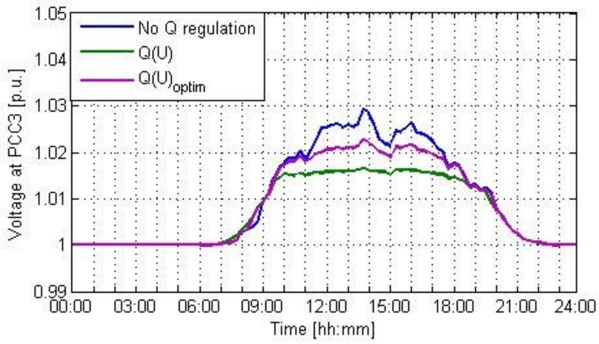

Fig. 7 Voltage profile at the PCC3 for the analyzed strategies

However, taking into consideration the droop characteristic of the Q(U) strategy, the PV3 inverter will start absorbing reactive power when the voltage at PCC3 exceeds the value 1.02 p.u.. As seen from Fig. 8**,** the value of the reactive power absorbed using the optimized Q(U) method is lower.

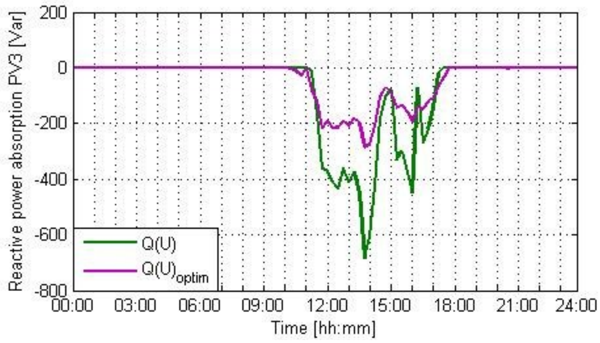

Fig. 8 Reactive power consumption of PV generator at the PCC3

Even though the voltage level using the optimized Q(U) method are higher compared to the voltage using the Q(U) algorithm, the benefit of the optimized method is the minimization of the reactive power absorption while the PV generators maintain their operation in maximum power point tracking.

Taking PV17 as a second example, from Fig. 9 it can be noticed that the voltage at PCC17 exceeds the 1.03 limit if no reactive power compensation methods are available.

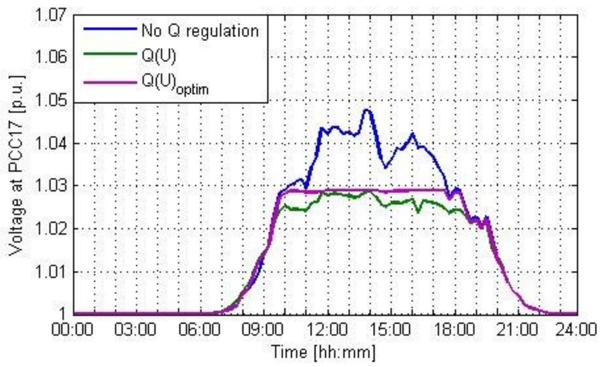

Fig. 9 Voltage profile at the PCC17 for the analyzed strategies

In Fig. 10, the reactive power absorption of PV17 inverter is shown and, as expected, when using the Q(U) method, higher values of reactive power are necessary to be absorbed compared to the values when using the optimized Q(U) strategy.

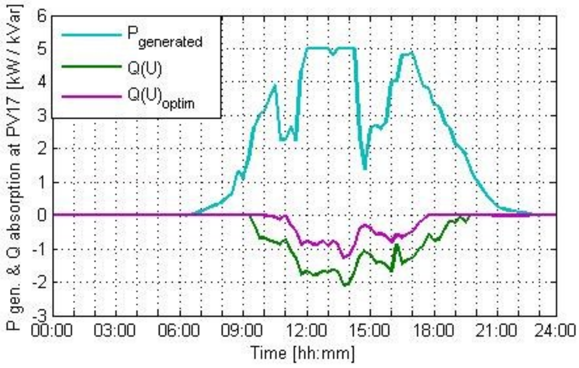

Fig. 10 Reactive power consumption of PV generator at the PCC17

Fig. 11 and Fig. 12 presents the total active and reactive power losses before and after performing the Q(U) optimized algorithm.

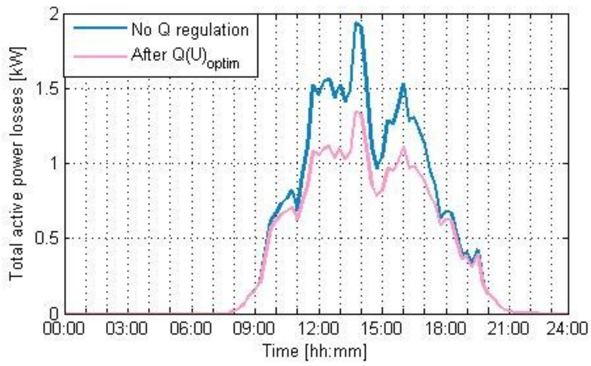

Fig. 11 Total active power losses in the network

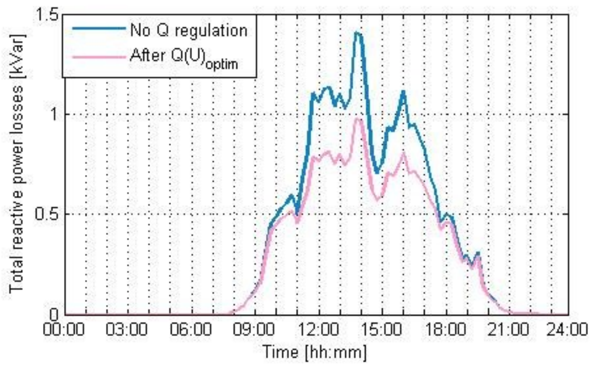

Fig. 12 Total reactive power losses in the network

Besides the optimization of the reactive power reference, the proposed algorithm presents the benefit of minimizing the active and reactive power line losses. This is achieved because the load flow equations are taken as equality constraints and the optimization algorithm performs the balancing of the power transfer in the network.

In Fig. 13, the transformer loading for the Q(U) method is presented. As it can be seen, the transformer does not exceed 100% loading.

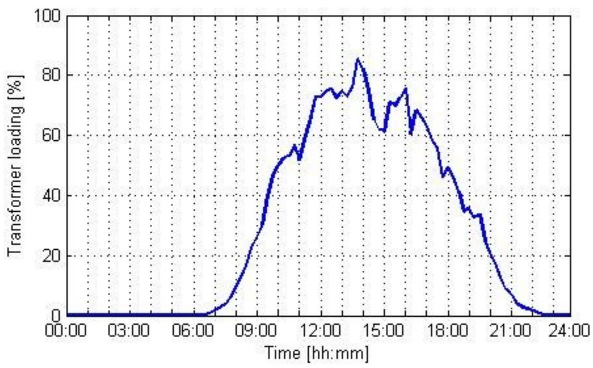

Fig. 13 Transformer loading for Q(U) method

Due to the fact that the optimized Q(U) method is absorbing less reactive power than the Q(U) method, it can be stated that the transformer does not exceed the 100% loading in this case also. In addition, the optimized Q(U) method presents the advantage of less stressing the transformer.

IV. CONCLUSIONS

This paper focuses on voltage regulation methods for PV systems with ancillary services. One of the strategies encouraged in the German GC for LV, the Q(U) strategy, was implemented and simulated on an European LV benchmark grid. Results showed that this regulation method can keep the voltages at PCCs below the 3% limit but with the drawback of absorbing more reactive power than needed. This is because each PV inverter calculates the necessary compensatory reactive power depending on the voltage at the corresponding PCC and based on a Q-U droop characteristic.

An optimized Q(U) algorithm using a centralized controller which is able to dispatch the minimum amount of reactive power to each PV inverter has the purpose to improve the existent solution encouraged by the system operators. The method considers all the voltages at the PCC of each grid-connected PV system in the network and calculates the minimum absorption of reactive power. To develop such optimized control strategy, communication infrastructure is needed in order for the central controller to transmit the calculated values of reactive power for each PV inverter which participates in the voltage regulation process.

The benefits of implementing the optimized Q(U) algorithm are: a better usage of the PV inverter capacity which leads to increased PV capacity in the network, lower transformer loading and lower network losses.

ACKNOWLEDGMENT

The authors would like to express their appreciation for PhD fellow Erhan Demirok and Ass.Prof. Henrik C. Pedersen for their cooperation and professional support.

REFERENCES

[1] European Photovoltaic Industry Association, "Market Outlook 2010," 2011.

[2] European Photovoltaic Industry Association, "Market Report 2011," 2012.

[3] European Photovoltaic Industry Association, "Solar generation 6. solar photovoltaic electricity empowering the world," 2011.

[4] K. Budenbender, M. Braun, T. Stetz and P. Strauss, "Multifunctional PV systems offering additional functionalities and improving grid integration," vol. Volume 7, Number 2 (2011) Pages 109-128, 2011.

[5] ABB, "IEC 61850: Special report," 2010.

[6] A. Mohd, E. Ortjohann, A. Schmelter, N. Hamsic and D. Morton, "Challenges in integrating distributed energy storage systems into future smart grid," in *Industrial Electronics, 2008. ISIE 2008. IEEE International Symposium on,* 2008, pp. 1627-1632.

[7] IMS Research Organization, "The World Market for PV Inverters 2011 Report," 2011.

[8] G. Kerber, R. Witzmann and H. Sappl, "Voltage limitation by autonomous reactive power control of grid connected photovoltaic inverters," in *Compatibility and Power Electronics, 2009. CPE '09.* 2009, pp. 129-133.

[9] E. Demirok, P. Casado González, K. H. B. Frederiksen, D. Sera, P. Rodriguez and R. Teodorescu, "Local Reactive Power Control Methods for Overvoltage Prevention of Distributed Solar Inverters in Low-Voltage Grids," *Photovoltaics, IEEE Journal of,* vol. 1, pp. 174-182, 2011.

[10] A. Canova, L. Giaccone, F. Spertino and M. Tartaglia, "Electrical impact of photovoltaic plant in distributed network," in *Industry Applications Conference, 2007. 42nd IAS Annual Meeting. Conference Record of the 2007 IEEE,* 2007, pp. 1450-1455.

[11] N. Grass, G. Kerber, R. Witzmann, M. Sebeck and R. Keck, "Increasing Grid Transmission Capacity and Power Quality by new Solar Inverter Concept and Inbuilt Data Communication," *Telecommunication - Energy Special Conference (TELESCON), 2009 4th International Conference on,* pp. 1-5, 2009.

[12] L. Herman, B. Blazic and I. Papic, "Voltage profile support in LV distribution networks with distributed generation," in *Universities Power Engineering Conference (UPEC), 2009 Proceedings of the 44th International,* 2009, pp. 1-5.

[13] VDE, "Generators connected to the low-voltage distribution network- Technical requirements for the connection to and parallel operation with low-voltage distribution networks (VDE-AR-N 4105)," 2011.

[14] T. Stetz, W. Yan and W. Braun, "Voltage Control in distribution systems with high level PV penetration (Improving absorption capacity for PV systems by reactive power supply);" vol. 25th European PV Solar Energy Con-ference and Exhibition, 6th - 10th September 2010, Valencia, Spain, 2010.

[15] E. Demirok, D. Sera, R. Teodorescu, P. Rodriguez and U. Borup, "Clustered PV inverters in LV networks: An overview of impacts and comparison of voltage control strategies," in *Electrical Power & Energy Conference (EPEC), 2009 IEEE,* 2009, pp. 1-6.

[16] G. Kerber, "Statistiche analyse von NS-VErteilungsnetzen und modellierung von referenznetzen," 2208.

[17] Cigre Task Force C6.04.02, "Benchmark Systems for Network Integration of Renewable and Distributed Energy Resources," 2011.

[18] M. Braun, T. Stetz, T. Reimann, B. Valov and G. Arnold, "Optimal reactive power supply in distribution networks; Technological and economic assessment for PV systems," vol. 24th European Photovoltaic Solar Energy Conference and Exhibition, Hamburg, 2009.

[19] D. EnergiMidt Entreprise A/S, "The SOL-300 project – A 300 roof-top project," 1998-2001.

[20] BDEW - Bundesverband der Energie- und Wasserwirtschaft, "Generating Plants Connected to the Medium-Voltage Network, Technical Guideline," 2008.

[21] L. Soder, "Load flow study and sensitivity analysis of power systems,"EG2030 Power System - advanced course, Sweden